DYNAMIC COUPLING OF THE STRATOSPHERE WITH THE

TROPOSPHERE AND SUDDEN STRATOSPHERIC WARMINGS

by

KEVIN EDWARD TRENBERTH

B.Sc (Hons), University of Canterbury (1966)

SUBMITTED IN PARTIAL FULFILLMENT

OF THE REQUIREMENTS FOR THE

DEGREE OF DOCTOR OF SCIENCE

at the

MASSACHUSETTS INSTITUTE OF TECHNOLOGY

January 1972

Signature of Author ....
Department of Meteorology, January 14, 1972

Certified by ....
Thesis Advisor

Accepted by ....
Chairman, Departmental Committee on Graduate Students

DYNAMIC COUPLING OF THE STRATOSPHERE WITH THE

TROPOSPHERE AND SUDDEN STRATOSPHERIC WARMINGS

KEVIN EDWARD TRENBERTH

Submitted to the Department of Meteorology on January 14, 1972 in partial fulfillment of the requirements for the degree of Doctor of Science.

ABSTRACT

Numerical time integrations of a 9-layer quasigeostrophic highly truncated spectral model of the atmosphere are used to study tropospheric-stratospheric interaction with particular regard to sudden stratospheric warmings. The model is global and extends to 0.05 mb (71 km) with roughly 10 km resolution in the stratosphere, and includes an annual heating cycle. A linear baroclinic analysis of a similar model shows that the inclusion of spherical geometry allows significant growth rates in the long wave region of instability. Preliminary integrations without eddies reveal the seasonal variation of a thermally driven circulation.

Model integrations simulating the months of December and January were made (i) without nonzonal forcing, and (ii) with nonzonal heating and orography included, to represent southern and northern hemisphere winters. The overall features of the atmosphere were very well simulated. With the inclusion of the annual heating cycle, the model successfully reproduced a more intense circulation in January than existed in December. This caused a maximum tropospheric meridional temperature gradient in the winter hemisphere to occur some weeks prior to the maximum in the external heating field.

The presence of nonzonal heating in the winter hemisphere brought about an increase in circulation intensity and produced a stationary perturbation with a strong westward slope with height extending high into the stratosphere. These are features somewhat similar to those of the Aleutian system. Associated with this were considerably warmer temperatures in the polar night stratosphere and a weaker stratospheric westerly jet. The winter mesosphere of the model was driven in the manner of the lower stratosphere and a temperature maximum was produced in mid latitudes.

Sudden stratospheric warmings occurred as a result of large increases in the intensity of planetary scale waves in the troposphere, which in turn produced surges of upwards propagating energy. The energetics of the warming occurred in two phases. A change from a baroclinically direct to a driven circulation occurred as the stratospheric temperature gradient reversed. This coincided with a change from enhancement to absorption of the vertical flux of energy. The mechanism of the warming was much as described by Matsuno (1971).

Nonlinear interactions between the progressive long wave and the nonzonal heating were primarily responsible for the tropospheric events that produced the upward flux of energy, which in turn caused the stratospheric warmings. A seasonal index cycle in the very long waves was also of significance in producing transient upward energy propagation. Interactions with other waves, and orographic forcing were of secondary importance in the long wave energetics of the sudden warmings.

Thesis Supervisor: Edward N. Lorenz

Title: Professor of Meteorology

To my parents,

Mr. & Mrs. Edward M. Trenberth

ACKNOWLEDGEMENTS

TABLE OF CONTENTS

LIST OF FIGURES

LIST OF TABLES

NOTATION

R   gas constant for dry air

C_p specific heat at constant pressure

χ R/C_p

g   acceleration due to gravity

p   pressure

P_{oo} 1000 mb

θ potential temperature

ω dp/dt

Z   height in geopotential units

ρ density

t   time

λ longitude, measured eastward

ϕ latitude, measured northward

a   radius of earth

T   temperature

Ω angular velocity of earth

f $2\Omega \sin\phi$, coriolis parameter

u,v   eastward and northward velocity components

σ $-\dfrac{\partial\theta}{\partial p}$, static stability

Q   diabatic heating per unit mass

F   frictional force per unit mass

c   phase speed of wave

Other parameters are defined as they are used.

CHAPTER   I

INTRODUCTION

The changeover in the stratospheric circulation from the winter

regime of polar night westerlies to the summer easterly regime during

spring is frequently preceded by a breakdown in the circulation of a

similar nature during the winter months. This breakdown is accompanied

by rapid warming of considerable magnitude at high latitudes in the

stratosphere and is known as a sudden stratospheric warming. Although

its discovery aroused much interest and it has been the subject of many

investigations, the cause and mechanisms of the event are still not

fully understood.

These sudden stratospheric warmings have at times been considered

to be caused by solar radiation, direct or indirect, or to be a manifes-

tation of baroclinic, barotropic or inertial instability or a combination

of these, and more recently to be a result of forcing from below. Radia-

tion effects are small at the time of many major midwinter warmings, and

hydrodynamic instability studies have been unsuccessful in explaining

the large scale changes in such short times as observed. These explana-

tions are also unable to explain the observed differences between the

events in each hemisphere as midwinter warmings are infrequently

observed in the southern hemisphere. However, energetics studies have

indicated the importance of very long waves propagating energy upwards
into the stratosphere at high latitudes just prior to the occurrence of
sudden warmings. The observed dominance of planetary scale quasi-
stationary waves in winter in the northern hemisphere tropospheric cir-
culation, while no such waves exist in the southern hemisphere, further
indicates a possible reason for the observed differences.

It appears from observed seasonal trends that the stratosphere
can adjust to gradual changes in forcing by increased quasihorizontal
transports of heat and momentum. However, we shall attempt to show that
an abrupt change in the vertical propagation of energy into the region
can cause sudden changes in the transports and induce vertical motions
which result in a sudden warming and a major modification of the flow.
Therefore the transient component of the very long waves, and dynamic
coupling between the stratosphere and troposphere, may be of great
importance.

Aside from the frequency of occurrence of sudden warmings, a
number of other substantial differences exist in the winter stratospheres
of the two hemispheres. The chief of these are the considerably warmer
polar night temperatures and the existence of a marked quasistationary
perturbation in the northern hemispheric stratosphere.

The purpose of this thesis is to attempt to explain these observed
differences and to consider all aspects of the sudden stratospheric
warming. The latter problem may be considered in three stages:

(i) the mechanism of the production of the very long wave energy which is propagated vertically and ultimately produces the sudden warming;

(ii) the mechanisms of the vertical propagation of the energy; and

(iii) the absorption of this energy and the mechanism of the warming itself.

There are many studies which prove relevant to these three stages of the warming. Descriptions of the sudden stratospheric warming and the observed differences between the hemispheres provided the basic stimulus for the investigation, with the realization that a full knowledge of the mechanisms involved may eventually allow these events to be predicted. Many studies used the energetics as tools to describe the events. A wide range of literature now exists on the stationary and transient very long waves in the atmosphere. However none appears directed at explaining stage I of the warming although closely related problems have been considered. The theory of the vertical propagation of energy, (stage II), has made great strides in the past decade and can now describe at least qualitatively the processes involved and the reasons for the dominant role of the very long waves. Very recently a few studies have considered how the vertically propagating energy may modify the zonal flow, (stage III). Previous attempts to simulate the phenomenon have met with limited success and suffer from a considerable amount of artificiality.

These background studies are critically reviewed in chapter 2 and provide the basis for setting up this investigation. A numerical model of the atmosphere is used as the basic tool. It is a nine-layer quasigeostrophic model formulated on a sphere with a highly truncated spectral representation of the variables. The model is global; includes an annual heating cycle and extends to .05 mb (near 71 km) with roughly 10 km resolution in the stratosphere. As such we aim to remove some restrictions and artificiality of former simulation attempts. To this end, hypotheses were established at the inception of this study so that a number of experiments were designed with a specific aim in mind. These are discussed in chapter 3.

CHAPTER II

BACKGROUND

2.1 The Stratospheric Circulation

The stratosphere in summer is characterized by a large anti-
cyclone centered on the pole in a fairly flat pole to equator tempera-
ture gradient. Winds are easterly with little variability. In
autumn, the polar regions begin to radiate and cool, and the tempera-
ture gradient and the winds become reversed. The stratospheric polar
night circulation is characterized by day to day fluctuations in winds
and temperatures, with gradual changes of greater extent also present.
The southern hemisphere (S.H.) winter vortex is more intense, with
lower polar temperatures and stronger westerlies, and much greater
zonal symmetry than its Arctic counterpart.

A representative mean zonal temperature field (^{O}K), and wind
field (m sec^{-1}) for the solstices are presented in Fig. 1(a) and (b),
(from Murgatroyd, 1970).

The reversal of easterlies to westerlies in the fall with the
onset of winter is fairly rapid, and variations from year to year are
small. In contrast, the timing and intensity of the winter circula-
tion breakdown is extremely variable, owing largely to the phenomenon
known as the sudden stratospheric warming. First noted by Scherhag
(1952), the warmings have been extensively studied, but the mechanism
is not fully understood. It involves a large warming at some long-
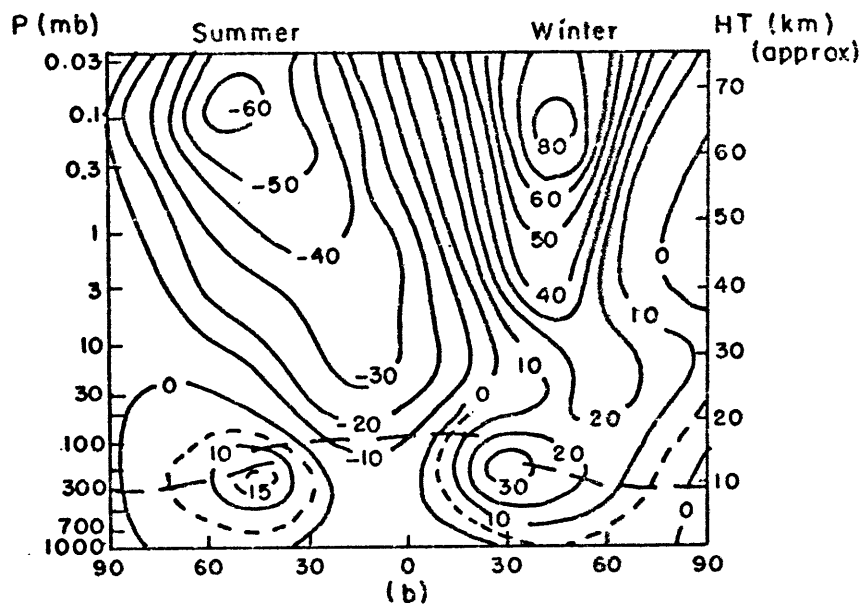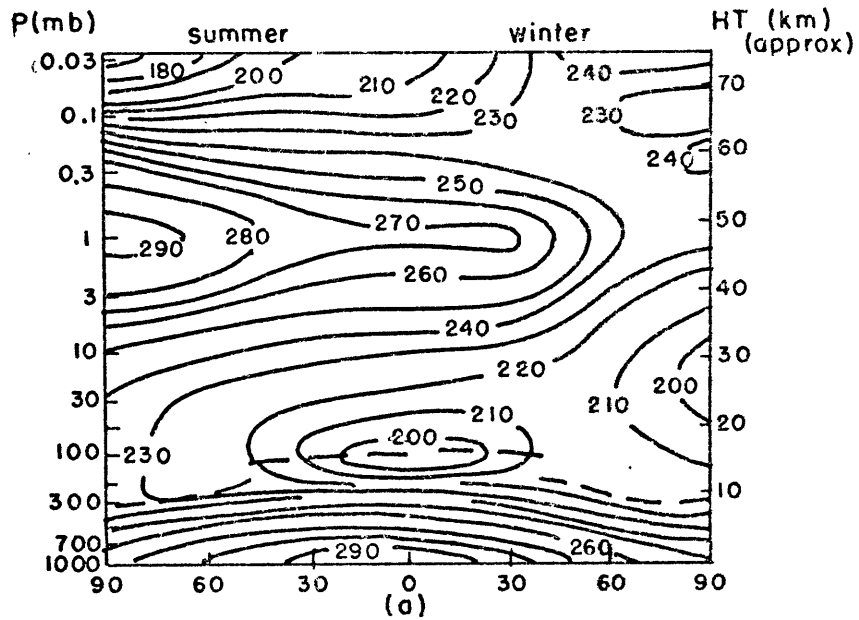
Fig. 1(a). Representative latitudinal mean cross-section of temper-
atures °K for the solstices. Heavy dashed lines repre-
sent the tropopause. (b) Representative latitudinal
mean cross-section of zonal wind speeds m sec⁻¹ at the
solstices. West to east components are positive.

itudes with cooling at others, and ultimately results in a decrease in the meridional temperature gradient as the entire high latitude region becomes warmer. In a major warming, the temperature gradient temporarily reverses and a breakdown and reversal of the polar night westerlies ensues.

Individual warmings have been illustrated and described by Teweles (1958), Teweles and Finger (1958), Craig and Hering (1959), Hare (1960), Finger and Teweles (1964), Quiroz (1969), Johnson (1969), and others for the N.H.; and Wexler (1959), Palmer (1959), Palmer and Taylor (1960) and Phillpot (1969) for the S.H.

The Antarctic stratosphere cools well into winter often relaxing slightly before the breakdown, which occurs in spring with some regularity. However sudden warmings in the N.H. often take place some weeks before the sun returns, after which slow radiative cooling may again set in. Several warmings may take place in one winter, but there is usually only one major event which eliminates the strong meridional temperature gradient. A final spring warming occurs with the differential heating reversed and the summer regime of steadier easterlies begins to dominate.

Major breakdowns have not been observed till spring in the S.H. although smaller mid-winter warmings have been detected (Julian, 1967; Shen et al., 1968). This situation may to some extent be caused by a lack of high level observations in the Antarctic. However recent developments in satellite radiometry should provide increased coverage on a global basis, and it is quite likely that our view of the occurrence,

altitude and intensity of these events will need to be revised, see for example Quiroz (1969) and Barnett et al. (1971a).

The stratospheric warmings are of greatest intensity above 10 mb and were thought to originate at these levels and propagate downwards. Hirota (1967a) has explained this as the westward movement of a westward tilted trough, so that a single station analysis would find the warming first at high levels. He finds the warming center first detectible near 50 mb, but of low intensity and propagating upwards at about 10 mb day^{-1}. When it is above 10 mb, intensification takes place and the warming then progresses downwards.

Many authors have associated blocking or low index type of situations with sudden warmings. Craig and Hering (1959), Julian (1961), Teweles (1963), Miyakoda (1963), Labitzke (1965), Julian (1965), and Murakami (1965) have commented on various aspects of this, usually on the presence of anticyclonic blocking upstream from the region of initial stratosphere warming.

2.2 Energetics

Fields of mass, motion and temperature may be resolved into amounts associated with the zonal average, and with the eddies. Thus use is made of zonal and eddy components of kinetic energy (K) and available potential energy (A), as described by Lorenz (1955).

$$K = KZ + KE \quad ; \quad A = AZ + AE.$$

In considering the energetics of a separate layer of the atmosphere, such as the stratosphere, vertical and horizontal advection of energy through the boundaries, and pressure work on the mass within the layer, must be considered. Of these, only the vertical flux of geopotential (commonly referred to as the '$\omega\phi$' or 'pw' term) is of major importance, and it is now widely accepted that it plays an important role in maintaining the motions of the lower stratosphere.

The dominant energy cycle in the troposphere in the mean is

$$GZ \longrightarrow AZ \longrightarrow AE \longrightarrow KE \longrightarrow KZ$$
$$\searrow \qquad \searrow$$
$$DE \qquad DZ$$
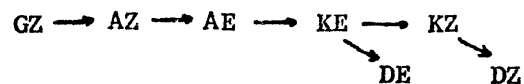
where GZ is the generation of AZ by diabatic heating and D is the dissipation by friction.

The mean lower stratosphere is maintained by quite different processes. Owing largely to the increasing static stability, baroclinic eddies are damped and drive countergradient heat transports (KE $\longrightarrow$ AE $\longrightarrow$ AZ) with AZ and AE destroyed by radiative processes. Barotropic damping of the eddies (KE $\longrightarrow$ KZ) continues to maintain the mean flow, and a source of KE is required. Observational studies show this source to be a convergence of the vertical flux of eddy geopotential energy ($V\phi E$) from the troposphere into the layer.

$$K? \longleftarrow KE \longrightarrow AE \longrightarrow AZ \longrightarrow GZ$$
$$\searrow \quad \uparrow \searrow \qquad \searrow$$
$$DZ \quad | \quad DE \qquad GE$$
$$V\phi E$$
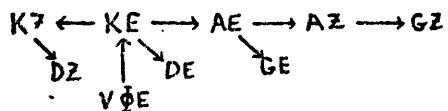
$V\phi E$ forms a small loss of energy to the troposphere, but is a major part of the stratosphere energetics. Thus the lower stratosphere

is driven from below by large scale quasi-horizontal eddies, which

maintain a pole-equator temperature gradient with up-gradient heat

transports. This is the long period average situation as depicted

by Oort (1964a) and Richards (1967). Recent results by Dopplick (1971)

also show the zonal flux of geopotential energy to be upwards, and

to maintain a conversion KZ $\longrightarrow$ AZ.

It is evident that very large changes in this mean cycle may

occur from day to day, particularly during winter. In the winter

hemisphere, high latitude cooling maintains a poleward temperature

decrease at high latitudes in the lower stratosphere. As Fig. 1

shows, this temperature gradient exists at high latitudes throughout

the atmosphere to at least 60 km. Hence AZ is being generated and

a source of energy for baroclinic eddies exists in situ. The resulting

atmosphere structure is favorable for energy to propagate vertically,

(see Section 2.4).

Energetics studies of individual sudden warmings (Reed et al.,

1963; Miyakoda, 1963; Muench, 1965; Julian and Labitzke, 1965; Perry,

1967; and others) generally find the winter lower stratosphere to be

dominated by this baroclinic region, and that a strong and sustained

upward flux of geopotential energy from the troposphere seems to pre-

cede a sudden warming, (see also Quiroz, 1969).

Millar (1966) further shows this flux to take place chiefly at

high latitudes. Miyakoda et al. (1970) using the G.F.D.L. 9-level

general circulation model, attempted to simulate a sudden warming using

real data, and while only partially successful, found a narrow belt of

strong upward flux of energy at high latitudes.

Dopplick (1971) confirmed the pattern which has emerged from these studies. By including diabatic heating in computing 24-hour average large scale vertical motions for 1964, he obtained greater accuracy in the conversion terms and vertical fluxes than formerly available. Energy which had its source in the troposphere was shown to propagate vertically through 100 mb and 10 mb in winter. The character of the changes in the flux through 10 mb was similar to that at 100 mb and the magnitude was slightly reduced. However, owing to the baroclinic nature at the lower stratosphere, periods of divergence of this flux in the layer resulted. A notable exception occurred at the time of the spring warming of that year (March), when a sustained upward flux of geopotential energy through 100 mb was trapped below 10 mb thereby causing the observed warming.

The warming resulted from increased conversions $CK(KE \longrightarrow KZ)$, $CE(KE \longrightarrow AE)$, and $CA(AE \longrightarrow AZ)$, which caused decreased westerlies or increased easterlies to result. Dopplick found this process to lower the trapping level, thus causing the warming and vortex breakdown to progress downwards.

The energetics studies already cited, further show the energy transport to be brought about by the longer waves, chiefly waves 1, 2 and 3. Observations also show the major troughs and ridges in the stratosphere to conform generally with those in the troposphere, but they are little influenced by baroclinic waves, e.g. Muench, (1965); Finger et al. (1966). In the event of a sudden warming occurring,

it is usually characterized by a dominance of a single wave, either wave 1 or 2. Thus it may be referred to as asymmetric or bipolar.

Another feature of the warming is the appearance of very strong winds preceding the event, Quiroz, (1969); Johnson, (1969). These produce strong horizontal advection of temperature and result in large upward vertical motions at the time of the warming, Mahlman, (1969); Quiroz, (1969). The upwards motion at high latitudes and subsidence at low latitudes act to decrease the magnitude of the warming.

These observationally based studies demonstrate the importance of the structure of the atmosphere to the energetics of the region, and whether waves can propagate or will be trapped. Only the long waves are capable of propagating energy into the stratosphere, and the question arises as to the source of this long wave energy. Very long forced waves in the troposphere are present in the N.H. winter, but are largely absent in the S.H. winter. How this accounts for the large differences observed between the winter stratospheric temperatures and wind fields in each hemisphere, will be considered in this thesis.

In the following section, sources of the planetary scale waves in the troposphere are therefore reviewed.

2.3 Origin and Growth of Waves

Motions in the atmosphere may be considered in the form of waves, which originate and evolve in many ways and have widely varying structures. In this section, current knowledge of the sources and existence of the very long waves as it has emerged from previous studies will be considered.

Because of the transparency of the atmosphere to solar radiation, the surface of the earth acts as the primary heat source. Topographical features thus realize a variable heat source, particularly in land-sea contrasts. Frictional drag and mountain torque act as spatially varying momentum sinks or sources. Water vapor, which condenses to release latent heat, and other atmospheric constituents such as dust, are also not evenly distributed longitudinally, largely because of the location of land masses.

Monthly mean upper air charts reveal disturbances of considerable magnitude to be present, and demonstrate the quasi-stationary nature of the waves, and hence presumably their source. Monthly changes are then attributable to the seasonal progression of the above factors. General circulation studies (Starr and White, 1954; Obasi, 1963) show these standing waves to be of great significance in the N.H. but of little importance in the S.H.

However many treatments of the large scale dynamics of the atmosphere assume zonally symmetric heating. The effects of non zonal forcing are often neglected in short term integrations of the equations

of motion, or in instability analyses, by relegating them to second order (Phillips, 1963). Since the growth of self excited waves is on a time scale of one to three days, heating, friction and orography only slightly modify the results, and the unstable waves derive their energy from the larger scales. Accordingly, depending upon whether the source is potential or kinetic energy of the zonal flow, the problem is usually further broken down, for ease of treatment, into baroclinic and barotropic instability. A neutral wave also forms part of the solution to perturbation analyses. The latter is the free mode of oscillation of the atmosphere.

2.3.1 Stationary very long waves

In the following discussion the very long (or planetary scale) waves are considered as distinct from the cyclone scale waves. This includes waves referred to elsewhere as ultralong waves.

The relatively simple models of Charney and Eliassen (1949) and Smagorinsky (1953) were able to reproduce at least the gross aspects of the zonally asymmetric stationary flows. Orography and nonzonal heating were both shown to be important when considering longer periods of time. Both investigations showed the introduction of friction to be necessary in order to eliminate the possibility of infinite amplitude resonant waves. Smagorinsky pointed out that even with friction included, disturbances are still enhanced in the neighborhood of this free mode.

Since these pioneering works, many such steady state models have
been produced. Saltzman (1968) summarized the results of the early
studies of this nature. The most comprehensive results are given by
Sankar-Rao (1965) and Sankar-Rao and Saltzman (1969) who computed the
spectral components of the earth's topography and heating, and made up
composite maps of the response. They conclude that nonzonal heating
has greater effects in causing the stationary disturbances throughout
the troposphere.

However Derome and Wiin-Nielsen (1971) found orographical effects
to be larger in their two layer model.

Results from the steady state approach show great sensitivity to
the assumed vertical structure of the basic state of the atmosphere,
the parameters chosen, and the vertical structure of the forcing, espe-
cially when resonant modes are approached. Thus investigations may
reach opposite conclusions while resembling the observed state of the
atmosphere.

The alternative approach is to consider the time dependent
equations of motion for the atmosphere, subject to the lower boundary
condition and nonzonal heating, and allow all scales of motion to
develop naturally. The time average of the resulting circulation
reveals the stationary features of the flow, which may then be compared
to the observed circulation.

Mintz (1968) used this approach and found orography to have vir-
tually no effect on the energetics of his model. Mountains were impor-

tant in maintaining the Siberian high pressure system in winter by preventing baroclinic waves from mixing the radiating cooled air over Siberia with the warm heated air over the Indian ocean. Kasahara and Washington (1969, 1971) confirmed these impressions with the 2-layer and 6-layer NCAR models. Major stationary features of the M.S.L. pressure field were present with mountains excluded. Orography played a minor role mainly serving to alter slightly the location and strength of the stationary features. As noted by Mintz, the Himalayas produced greatest change in this respect. The patterns in the upper atmosphere (Kasahara and Washington, 1971) were also well reproduced, and the differences made by introducing orography were small.

The energetics of the stationary planetary waves in the troposphere have been computed from observed data by Holopainen (1970). The mountain effect was very small. Winter waves were baroclinically maintained and their stationarity was maintained through a balance between the advection and retardation by the heating field. Thus heating continually acts to deplete the eddy available potential energy. These waves sloped strongly westward with height. Saltzman (1965) and Murakami (1967) found similar energetics in the steady state models.

In summer, Holopainen found that nonzonal heating caused the generation of eddy available potential energy resulting in a thermally direct system. Such waves slope eastward with height and were also produced by Saltzman (1965).

A further source of energy of long waves appears to be from the exchange of kinetic energy with cyclone scale waves through non-linear interactions (Saltzman and Fleischer, 196C; Saltzman and Teweles, 1964). The latter study, which was based on considerably more data and divided into summer and winter, showed wave number 0 and 1 to have the greatest gain by this method, with a second peak at wave 4. In great contrast, wave 2 showed a substantial loss, and apparently has its source from the baroclinically derived energy as described above.

2.3.2 Transient Very Long Waves

Very long transient waves in the atmosphere have been analysed in several studies using atmospheric data. Deland (1964, 1965), Eliasen and Machenhauer (1965, 1969) and Deland and Lin (1967) described waves at 500 mb which move with a speed near that determined from a divergent barotropic model formulated as a homogeneous fluid with a free surface.

Deland and Johnson (1968) and Bradley and Wiin-Nielsen (1968) considered the vertical structure of the transient modes and found a considerable westward slope with height, so that the waves are of a baroclinic nature. In particular, the latter study found three vertical pressure modes to be present. One mode was identified with the waves found by the studies using 500 mb only. Another was divergent and had small amplitude at that level. It progressed eastward at about 15° day^{-1}.

Wiin-Nielsen (1971a and b) used linearized analyses to consider these transient waves theoretically with a β-plane and spherical geometry. He identified the observed modes of Bradley and Wiin-Nielsen

(1968) with solutions in the model, and showed them to be quasigeos-
trophic.

Transient planetary scale waves have also been identified in the lower stratosphere by Hirota (1968) and have a strong westward slope with height. Hirota and Sato (1969) found a correlation between the transient waves and the variations in the zonal flow. Hirota (1971) was able to excite planetary scale Rossby waves in his model of the winter stratosphere by periodically forcing the mean zonal wind to vary in strength.

Phillpot (1969) found a marked wave 2 at 30 mb in the S.H. circulation which advanced eastward with a period of 17 to 32 days. This case was notable since the wave was primarily transient, whereas in the N.H. studies, the waves are quasi-stationary and the transient component has to be extracted. A stratosphere warming later grew from this perturbation.

Thus observational evidence reveals the importance of the transient waves in causing fluctuations in the zonal flow, and they are found to be quasigeostrophic and baroclinic in nature.

2.4 Vertical Energy Propagation

Observations above the tropopause reveal a predominance of longer wavelengths with increasing height in the stratosphere in winter, while short waves vanish. In summer the easterlies are virtually undisturbed. A number of theoretical studies aimed at explaining these characteristics now exist.

Eliassen and Palm (1961) showed the energy flux would be upwards in a stationary planetary wave provided the wave sloped westward with height, realizing a polewards transport of heat. They also showed that the energy flux could not cross the singularity at the zero velocity zonal wind.

Using a quasigeostrophic baroclinic model, Charney and Drazin (1961) showed unstable short waves would be external and thus could not penetrate far into the atmosphere. They found that forced stationary waves could propagate provided $c < u < u_c$; where c is the phase speed of the wave, and Uc is a critical value of U which increases with the wavelength of the disturbance. Thus the longer waves were shown to be more likely to propagate vertically while short waves would be trapped, provided the wind is westerly relative to the phase speed.

Charney and Pedlosky (1963) showed that the vertical energy flux from unstable planetary scale waves would decrease exponentially in a layer containing no vertical or horizontal wind shear. Lindzen (1967) found planetary waves could propagate in equatorial regions through westerlies of any strength. However, as he has since pointed out, the small vertical wavelength of these waves may make them particularly subject to dissipation.

A simple baroclinic model was used by Murakami (1967) to consider steady state forcing by orography and nonzonal heating. Orography produced upward propagation of energy with a maximum in middle and low latitudes, but nonzonal heating was able to produce an upward flux of energy only at high latitudes.

In expanding Charney and Drazin's treatment to consider the
effects of the lack of N-S wind shear, Dickinson (1968a) established
that planetary waves were absorbed by the mean flow at the critical
level rather than reflected. Vertically propagating waves are
refracted by strong westerlies and channeled into ducts in the atmos-
phere. The ducting allows waves to propagate at high latitudes, but
because of absorption at the easterlies in low latitudes, propagation
is unlikely there. Dickinson (1968b) also considered the limitations
of the β-plane used by Charney and Drazin and found similar criteria
for propagation, but with greatly differing quantitative requirements.
Thus two or more planetary wave modes were found to be always able to
propagate through any observed westerlies in the troposphere or stra-
tosphere.

Photochemical relaxation was found to attenuate planetary wave
propagation (Dickinson, 1969a), thus perhaps explaining the observed
absence of such large fluxes of energy implied by the (1968b) paper.
Matsuno (1970) considered the observed basic state and found waves
1 and 2 may propagate into the stratosphere. He was able to duplicate
certain features of the observed winter stratospheric flow and found
a major sink of the upward flux of energy to be at the line of zero
zonal wind in low latitudes.

Charney and Drazin (1961) also found the second order changes
in the zonal flow due to vertically propagating waves should vanish.
More recently, Dickinson (1969b) found the presence of photochemical
relaxation or singular lines would enable a net forcing of the mean

flow. Thus there is a tendency for the effects of eddy fluxes to be balanced by the mean meridional circulation for a steady state in the absence of critical levels. Matsuno (1971) has considered instances when this does not hold, so that changes in the zonal flow may ensue (see Section 2.5.2).

Thus waves in the midlatitude westerlies may propagate vertically and transport energy upwards. Wave energy is absorbed in easterlies, and is reflected and refracted by the tropospheric jet so that energy transmission occurs chiefly at middle to high latitudes. The waves are damped by frictional and radiative effects and baroclinic waves tend to be trapped. Little penetration of waves into the stratosphere occurs in summer, or at low latitudes in winter. Only quasi-stationary planetary scale waves can propagate at high latitudes in winter to any extent.

The theory, although based on greatly simplified atmospheric models which largely ignore nonlinear effects, shows good agreement with observations.

2.5 Sudden Stratospheric Warming Explanations

2.5.1 Early Theories

Early explanations of this phenomenon considered the source of energy to be external to the earth, as direct radiation, or solar corpuscular radiation and related auroral heating. However these effects

are generally too small to bring about the observed changes.

The importance of ozone and its photochemical reactions in determining the thermal structure of the stratosphere has been recognized. But although ozone concentrations are observed to be very high at or shortly after a sudden warming, it seems to be an effect rather than a cause. Large scale quasihorizontal eddies are primarily responsible for the observed distribution in the lower stratosphere, Newell (1961), Byron-Scott (1967).

Investigations have been carried out on the stability of the polar night vortex. Nevertheless the application of baroclinic, barotropic and other instability theories which concentrate on the release of energy of the basic flow, but which exclude energy propagation from the troposphere, has not been very successful.

Fleagle (1957, 1958) developed a simple instability criterion which indicated that baroclinic instability is present in the stratosphere in winter, but is limited to polar regions and has a slow growth rate for large disturbances. Murray (1960) found inertial instability to be unlikely. He also made use of a four level numerical model to conclude that the large static stability of the stratosphere made the region strongly baroclinically stable. McIntyre (1970) expanded Murray's analysis and found instability could occur but would be very shallow and have a slow growth rate. Charney and Stern (1962) established a more general necessary condition for the instability of an internal jet, and found it to be satisfied by the conditions

in the polar night jet. Sufficient conditions for such instability have not been found. An investigation of the boundary conditions showed the meridional temperature gradient at the earth's surface to be a destabilizing factor. Ozone photochemistry and radiative processes were shown to have a destabilizing effect (Lindzen, 1966), but produced very small baroclinic growth rates.

A barotropic problem was considered by Matsuno and Hirota (1966) and Hirota (1967b). A basic elongated current, maintained by unspecified external forces, was found to be barotropically unstable. The source of the growing wave energy was the basic current and thus from the unspecified external forces.

The lack of success in explaining the phenomenon, plus the observational evidence in the energetics studies, has led to the conclusion that the energy propagating into the region from below is not only not negligible, but forms the primary source of energy for the large scale warming.

Furthermore, an instability theory of the breakdown would not account for the observed greater stability of the more intense southern hemispheric polar night jet. However in-situ sources of energy may serve to enhance such events.

2.5.2 Simulation

In a study of the stratosphere with a simple 3-layer model, Byron-Scott (1967) attempted to simulate a polar night vortex breakdown by forcing the circulation from below. The Burger (1958)

diagnostic quasigeostrophic equations were used and ozone was treated explicitly. By continually specifying the lower boundary fields of temperature and geopotential, surges of vertically propagating energy were triggered, but trapped by the upper boundary condition. Thus a sudden warming type of breakdown was induced. Although not realized by the author, the experiment indicated the importance of abrupt changes in forcing the stratosphere, and its effects.

Miyakoda et al. (1970) attempted to simulate a breakdown of the polar night vortex using the G.F.D.L. 9-level general circulation model. The model was initialized with real data and a computation made to compare the evolution of the model with the observed atmosphere. The simulation was able to reproduce a split of the polar vortex into two vortices, but these subsequently reunited without producing a warming, whereas in the real atmosphere the vortices remained separate and a warming ensued. The model failed to predict the intensity of the Aleutian low in the troposphere and the vertical structure of this feature was very poorly reproduced. In the stratosphere, the Aleutian high was poorly predicted as a result. A blocking type ridge over the Eastern Pacific was also not predicted.

More recently, Clark (1969, 1970) used a hemispheric quasigeostrophic spectral model and further demonstrated the importance of tropospheric forcing on the stratosphere. However the model had a serious deficiency since it did not conserve momentum owing to an incorrect formulation of frictional dissipation. This probably

affected the spontaneous minor warmings which he found to occur, as non-linear exchanges of kinetic energy played a vital role. A major warming was triggered by causing an abrupt change in the N-S lower tropospheric temperature gradient.

Matsuno (1971) treated the interaction of vertically propagating planetary waves with the zonal flow.

He suggested a means whereby the effects of eddy fluxes induced by vertically propagating waves would not be balanced by the mean meridional cell, as usually appears to be the case, see Section 2.4. The presence of transient planetary wave upward propagation, or the existence of a critical layer (where c = U) intercepting the vertical flux, violates the balance. The former produces a vertical gradient of the poleward heat transport accompanying the upward propagating waves, which induces a meridional circulation and weakens the westerlies. If this process continues, a critical layer may be formed which would produce similar effects, but concentrated in a shallow layer. Matsuno demonstrated the mechanism with a simple model which assumed a lower boundary condition of planetary scale waves growing in time to reach a very large amplitude and persisting for a long time.

Matsuno's model produces many observed features present in sudden warmings. This mechanism of the warming will be considered in this thesis. However the cause of the increasing and sustained vertical propagation of energy remains unexplained.

CHAPTER III

PURPOSE OF THESIS

Although all aspects of the sudden stratosphere warming will be examined, the source of the long wave energy which produces the warming has not been formerly considered. This chapter discusses possible sources in the troposphere.

3.1 Sudden Warming Hypothesis

The variability of heating between the equator and the pole with the seasons indicates that a change in the forcing of the atmosphere produces corresponding changes in the quasihorizontal transports of heat and momentum. However a sudden change in the forcing will upset this quasisteady state causing a change in the vertical motions and the horizontal transports, and a corresponding adjustment in the temperature and wind fields. The stratosphere, when subjected to abrupt changes in forcing through increased vertical propagation of energy, responds in this way. This was demonstrated in the numerical models of Byron-Scott (1967), Clark (1970) and very recently by Matsuno (1971). We shall consider this point further in a more quantitative fashion by considering realistic mechanisms which may produce such changes in forcing.

Indications of the sudden nature of the change are provided in most major warmings which show evidence of over compensation in the temperature field, and relaxation to lower values following. The intensity of the warming or breakdown of the polar vortex may then be

expected to be proportional to the magnitude of the sudden increase in upwards propagation of energy, and to how long it is maintained. The energetics studies already cited illustrate these points.

Clearly the phenomenon is not instantaneous, but takes place over a series of days. Hirota (1967a) measured the speed of propagation of energy upwards to be about 10 mb day^{-1} above 50 mb. Charney (1949) found a maximum value in the midlatitude troposphere to be about 5 km day^{-1}. This value was also deduced from data by Hirota and Sato (1969). Thus events which affect the upper levels may occur a few days earlier.

We now pose the question: 'What are the mechanisms which produce such an increase in the vertical flux of geopotential?' A closely related question is 'How and why is energy put into the longer waves?' It is clear that we are considering non steady state situations and that transient forcing or transient waves themselves are of major importance.

Some answers which we shall consider as hypotheses are:

H(1)   The zonal westerlies become stronger with the onset of winter thereby enhancing the effects of boundary forcing due to orography. Latitudinal shifts in this current may serve to change the magnitude of this forcing and produce an effect at higher levels. Such a short term shift in westerlies may be associated with an index cycle.

H(2)   A likely greater effect is that due to the gradual establishment of the land-sea contrast causing a large perturbation in

the tropospheric zonal flow. The phase and amplitude of the

heating is a function of the time of year, but short term

fluctuations are very likely present, perhaps associated with

the concept of an index cycle. If variations in the degree

of activity of small scale cyclones are present, then since

the latent heat release on this scale is in a pattern deter-

mined by the large scale steering flow, it is likely that the

pattern of latent heat release affects the larger scale

directly, perhaps with repercussions at high levels of the

atmosphere.

H(3)   A further source of variation may be the concept of the

index cycle itself, acting on the scale of the long wave.

This is interpreted to be fluctuations in the baroclinic

rate of generation of eddy kinetic eddy, see the discussion

which follows.

H(4)   A similar source of variation in the gain of long wave

energy is in the rate at which energy is gained from non-

linear interactions from cyclone scale waves. Variations

may thus be caused through an index cycle operating on the

scale of the short waves.

To summarize these hypotheses in terms of an energetics diagram,

we have (L.W. = long wave, S.W. = short wave).

H(1)   KZ $\longrightarrow$ KE$_{L.W.}$ by topographical distortion of the zonal flow.

H(2)   GE $\longrightarrow$ AE$_{L.W.}\longrightarrow$ KE$_{L.W.}$ by nonzonal heating.

H(3) $AZ \longrightarrow AE_{L.W.} \longrightarrow KE_{L.W.}$ baroclinic process.

H(4) $AZ \longrightarrow AE_{S.W.} \longrightarrow KE_{S.W.} \longrightarrow KE_{L.W.}$ baroclinic cyclone scale waves

and $KZ \longrightarrow KE_{S.W.}$ plus non-linear interactions.
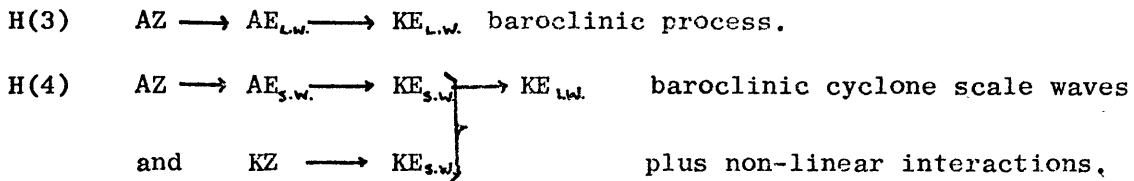
All these mechanisms include some mention of an index cycle, a term which has been used loosely here, but which we shall now qualify.

The meridional temperature gradient increases as winter progresses to some time after the solstice. Miyakoda (1963) found the peak gradient in the troposphere and lower stratosphere to occur just before the sudden warming.

Annular dish pan experiments (Lorenz, 1963) have demonstrated that the wave number of the flow is determined by a thermal Rossby number, which depends on the meridional temperature gradient. As the temperature gradient increases the wave number of the flow decreases. This is explained by the following mechanism. As the meridional temperature gradient increases, the baroclinicity and hence the intensity of the circulation increases. A greater vertical transport of heat and energy by baroclinic eddies results, which is not offset by radiational cooling thereby causing an increase in static stability. This in turn causes the wavelength and shear required for baroclinic instability to increase. Bryan (1959) found this process to exist in the atmosphere and to affect the wavenumber which dominates the flow. This kind of vacillation type process has been likened to the atmospheric index cycle. Both are processes which act to reduce the meridional temperature gradient.

Whereas the index cycle strictly refers to variations in the strength or latitude of the zonal westerlies, in terms of energetics it may be interpreted as a cycle in the strengths of zonal and eddy kinetic energy. As such it appears to be a two stage process. Initially there is strong baroclinic development (AZ $\longrightarrow$ AE $\longrightarrow$ KE) with barotropic damping (KE $\longrightarrow$ KZ) and a forced indirect cell (KZ $\longrightarrow$ AZ). This serves to decrease the zonal index. At some stage, a critical point may be reached in the amplitude of the eddies where barotropic instability arises (KZ $\longrightarrow$ KE). A splitting of the westerly jet results and a blocking pattern develops, producing the extreme low index situation.

Charney (1959) discusses the first stage of this kind of process and Lorenz (1960a) considers the entire cycle, suggesting the above mechanism for barotropic instability on the basis of his model.

Thus the index cycle may correspond to a cycle in the intensity of the energy conversions and energy amplitudes. In the extreme case of blocking, some conversions may even reverse direction.

In this way, the long waves are subject to an index cycle (hypothesis 3), although whether the length of such a cycle is less than one season is not clear.

The long waves provide a basic current for cyclone scale waves, and further cause some areas to be more favorable for cyclogenesis than others. For example, baroclinic waves may be seen to develop off the East Asian coast, moving generally around the Aleutian low. They typically deepen in mid-Pacific and occlude in the north-east Pacific Ocean.

Barotropic mechanisms become important at this stage and redistribute the eddy energy as the smaller system merges into the larger. As this process occurs in the troposphere, the Aleutian high in the stratosphere seems to respond by intensifying. Boville (1960) associated strong cyclogenesis in the troposphere with the Aleutian high, but did not elaborate on mechanisms such as that suggested here, which we shall consider as hypothesis (4).

Alternatively, the release of latent heat by this process may affect the larger scale directly (hypothesis 2).

As mentioned in Section 2.3.1 Saltzman and Fleischer (1960) and Saltzman and Teweles (1964) show such non-linear exchanges to be an important source of long wave energy. Teweles (1958), Finger and Teweles (1964), and Labitzke (1965) have mentioned that warmings commence above a region of intense cyclonic activity.

The index cycle, as it is usually discussed, is an irregular quasicyclic change in the basic zonal circulation with a period which may vary from 3 to 8 weeks, (Willett and Sanders, 1959). The length and intensity are subject to appreciable variations and quantitative searches for such a cycle have been unsuccessful (e.g. Julian, 1966). Thus the index cycle is of a somewhat tenuous nature. In the discussion above, this definition has been qualified in terms of energetics, and as such, individual waves may be subject to an 'index cycle' relative to their own basic current.

We have discussed four mechanisms which may be responsible for changes in the circulation of the troposphere, and hence the stratosphere. The concepts have been simplified for the purposes of discussion, and the mechanisms were considered separately. Further interesting possibilities may exist if some sort of reinforcement of these effects is established at any given time.

3.2 Reinforcement and Quasi-resonance

The steady state model approach to forced waves (Section 2.3.1) revealed difficulty in finding the response near resonant modes. The trend for the winter atmospheric structure to form ducts (Dickinson, 1968a) for propagating waves, allows for the possibility of quasi-resonance to exist in the atmosphere. Matsuno (1970) has considered this and suggests that small changes in the atmospheric structure may produce quite different responses.

An alternate form of resonance may occur if the forcing field is structured in a manner to reinforce self-excited baroclinic waves. Nonzonal heating may produce this kind of response as found by Sankar-Rao and Saltzman (1969). Thus further hypotheses for producing a large change in the tropospheric long waves may be formulated. We note that, in effect, this is the same as considering our former hypotheses as reinforcing one another. Thus we may consider H(2) and H(3), or perhaps H(1) and H(3) together.

In a similar way, since the phase of the non-zonal heating changes with time, it may serve to reinforce the topographical effect.

Thus we may consider H(1) and H(2) together, or even a combination of H(1), H(2) and H(3).

Presumably each of these factors plays a role of varying import each year and thus we may account for the year to year changes in sudden warmings observed.

3.3 The Southern Hemisphere

As large scale perturbations are virtually non-existent in the southern hemisphere, the mechanisms discussed above will be largely absent.

The greater symmetry of the Antartic vortex could be expected to give smaller changes in forcing and hence produce effects only at high levels or of small amplitude. Such smaller mid-winter warmings have been observed (Julian (1967), Shen et al. (1968a, b). Murgatroyd et al. (1965) suggested that the contraction of the Antarctic vortex as the sun returns, may cause the asymmetry of the Antarctic continent to have a greater effect on the flow, thereby stimulating the major spring breakdown.

3.4 The Relation with Tropospheric Blocking

The association of sudden warmings with anticyclonic blocking upstream was mentioned in Section 2.1. It seems that the observations of intense cyclonic activity at the time of the warming and the ensuing blocking are consistent with the hypotheses involving an index cycle.

In this way blocking and the breakdown may be regarded as being a result of the same process, and not that the blocking is somehow caused by the warming.

3.5 The Experiments

In order to gain some insight into the mechanisms proposed, and how they affect the vertical flux of geopotential into the stratosphere a number of experiments have been devised. The method chosen is to incorporate the basic physics into a numerical model and perform a number of controlled experiments with realistic external forcing. The following experiments will be considered.

(a) Set up an atmospheric general circulation model, the requirements of which are discussed in the next section. Include an annual heating cycle and make a test run without eddies for a year's duration as a reference for evaluating the effects of eddies.

(b) Introduce eddies into the model. A run without non-zonal forcing of any kind at the time of the onset of winter will serve to simulate a S.H. situation.

(c)&(d) From the same initial state, introduce (c) lower boundary forcing to simulate orography, and (d) non-zonal heating to simulate land-sea contrast. Thus an assessment may be made of the effect of each kind of forcing.

(e)   Combine both nonzonal effects, and again make a run from
the same initial state. This run will serve to simulate a
N.H. winter.

(f)   Consider the effects of changing the phase of the heating
relative to orography, and perhaps reinforce the two effects.

CHAPTER   IV

MODEL FORMULATION

4.1   Governing Equations

It is desirable to work with as simple a model as possible in
order to obtain mathematical tractibility, but still include all the
important features of the atmospheric phenomenon we wish to investigate.
If we were to choose a full scale primitive equation general circula-
tion model, reasons for the success or lack of success in attaining our
goals might be difficult to determine, e.g. Miyakoda et al. (1970).
Instead, using the ideas already formulated, a more limited model is
chosen.

Since we have no interest in inertia or gravity waves the filter-
ing approximations are invoked. Lorenz (1960b) and Charney (1962) per-
formed systematic derivations of sets of equations from the primitive
equations. Hence consistent assumptions are required so that the
simplified equations conserve total energy under reversible adiabatic
processes, and include terms of the same order of magnitude. Charney
showed these requirements to be compatible.

The equations of balance, although more accurate, are difficult
to use. Proceeding to the quasigeostrophic approximation omits the
transport of momentum by the vertical motions and by the divergent
part of the wind. Hence it omits the net transport of momentum by the
mean meridional cell. However these terms may reasonably be neglected

in the present investigation. The quasigeostrophic assumption is also valid, only provided tidal motions have amplitudes less than that of the mean zonal wind, i.e. below about 80 km, (Hines, 1963).

The thermodynamic equation may be simplified by allowing the static stability (σ), to vary as a function of pressure alone, or by describing the detailed horizontal and time dependence as well, Lorenz (1960b, 1962). Furthermore, we may suppress the spatial dependence but allow temporal variations, e.g. Bryan, (1959). However the additional non-linear terms introduced in a multilevel model would increase computation time by roughly a factor of two. This feature ($\sigma = \sigma(p,t)$) proved to be of importance in the motions of Bryan's experiments, but the effects are most likely less important here since energy may propagate into the stratosphere, whereas the two level model traps energy in the troposphere.

Therefore we use $\sigma = \sigma(p)$, but with the knowledge that we shall be unable to simulate the increasing static stability of winter and thus perhaps changes in the dominant wave number of the flow.

The p-dependence will be removed by taking finite differences in the vertical. However, rather than representing the variables as discrete functions on a mesh, thereby including many scales of motion, there are certain advantages in further simplifying the model with variables represented as highly truncated spectral functions.

Lorenz (1960a) proposed the use of orthogonal function series expansions for each dependent variable after omitting certain physical

features or processes believed to be of secondary importance. The series are then truncated and all but a small number of functions discarded. The coefficients of the retained orthogonal functions become the new dependent variables, and the new equations are ordinary differential equations. The method is illustrated by Lorenz (1960a, 1962, 1963), Bryan (1959), Baer and Platzman (1961), Peng (1965), Ellsaesser (1966), Clark (1970) and others.

Advantages of using this method are: (i) the mapping on a sphere is not necessary, thereby eliminating finite difference difficulties at the pole; (ii) the interaction coefficients between retained modes are treated exactly so that energy is conserved in non-linear interactions, and no instability due to aliasing errors can exist; and (iii) each wave number may be easily isolated.

The energetically consistent set of equations may be written as follows:

$$p = \rho RT \qquad (4.1)$$

$$\theta = (P_{oo}/p)^{x} T \qquad (4.2)$$

$$\partial p/\partial z = -\rho g \qquad (4.3)$$

which are the equation of state, potential temperature definition and the hydrostatic relation. Symbols have their usual meaning and are tabulated elsewhere. We put

$\underline{V} = \underline{V}_r + \underline{V}_d$, where $\underline{V}_r = \underline{k} \times \nabla \psi$ is the nondivergent velocity, and $V_d = -\nabla \chi$ is the divergent part of the velocity. Then the vorticity $\zeta = \nabla^2 \psi$. We have

$$\frac{\partial}{\partial t} \nabla^2 \psi = -\nabla \psi \cdot \nabla (\nabla^2 \psi + f) \times \underline{k} + \nabla \cdot (f \nabla \chi) + \nabla \cdot \underline{F} \times \underline{k} \tag{4.4}$$

$$\frac{\partial \theta}{\partial t} = -\nabla \psi \cdot \nabla \theta \times k + \sigma \omega + Q/c_p \tag{4.5}$$

$$\nabla \cdot (f \nabla \psi) = g \nabla^2 z \tag{4.6}$$

$$\nabla^2 \chi = \partial \omega / \partial p \tag{4.7}$$

where $\sigma = -\frac{\partial \theta_s}{\partial p}$, and these are the vorticity equation, the thermodynamic equation, the quasigeostrophic equation and the equation of continuity.

By differentiating (4.6) with respect to p we obtain the thermal wind equation,

$$\nabla \cdot (f \nabla \frac{\partial \psi}{\partial p}) = -R \rho^{\kappa - 1} p_{\infty}^{-\kappa} \nabla^2 \theta \tag{4.8}$$

and by differentiating this with respect to t and substituting from (4.4) and (4.5) we may derive the ω-equation for this system.

4.2 Energy Source and Sink Representation

For long term integrations of the equations, friction and heating must be included. We are not here interested in these processes themselves, only in the effects they have on the motion, and therefore a crude parameterization of the mechanisms may suffice. Also, the exact mechanisms are extremely complicated and not known, and simple parameterization provides for greater control and knowledge of the actual forcing of the model atmosphere.

Following Charney (1959) we take

$$\underline{F} = -g \, \underline{k} \cdot \frac{\partial \underline{\tau}}{\partial p} \qquad \text{where} \qquad \underline{\tau} = -\mu \rho g \frac{\partial \underline{v}}{\partial p} \quad ;$$

that is we assume stress proportional to the vertical wind shear, where μ is the eddy viscosity. Thus

$$\nabla \cdot \underline{F} \times \underline{k} = g^2 \frac{\partial}{\partial p} \left(\rho \mu \frac{\partial}{\partial p} \nabla^2 \psi \right) \qquad (4.9)$$

Thermal forcing is complicated by the fact that heating and cooling are both operating with quite different time constants in the stratosphere. Methods have been devised for treating ozone as an extra variable (Byron-Scott, 1967; Clark, 1970) but will not be so represented here. In this way, the computation will be somewhat simplified and complementary effects of ozone on the sudden warming will be eliminated. Thus we may be able to throw some light on the speculation that ozone plays an important role in the sudden warmings.

Above 10 mb photochemical effects become of major importance and the treatment of Leovy (1964) is used. The net heating q_n is given by

$$q_n = q_r(T) + q_s(T) \qquad (4.10)$$

where q_r is the total infrared heating, principally in the 15μ CO_2 band, and q_s is the absorption of solar energy principally by ozone. Newtonian cooling is commonly used to approximate q_r (Murgatroyd and Goody, 1958; Leovy, 1964). Thus

$$q_r = k_o - k_r T \qquad (4.11)$$

If T_e is an equilibrium temperature such that

$$q_r(T_e) + q_s(T_e) = 0 \qquad (4.12)$$

and T_o is the latitudinal mean of T_e, we define δT and T' by

$$\left.\begin{array}{l} T = T_e + \delta T = T_o + T' \\ \delta T = (T_o - T_e) + T' \end{array}\right\} \qquad (4.13)$$

We expand

$$q_s(T) = q_s(T_e) + \left(\frac{\partial q_s}{\partial T}\right)_e \delta T$$

$$= q_s(T_e) + (T_o - T_e)\left(\frac{\partial q_s}{\partial T}\right)_e + \left(\frac{\partial q_s}{\partial T}\right)_e T' \qquad (4.14)$$

Leovy found this linearization could have an error as large as 50% of the second term for large δT.

Substituting (4.10) using (4.11), (4.12), (4.13), we have

$$q_n = q_e + q_i \qquad (4.15a)$$

where $\qquad q_e = \left(\frac{\partial q_s}{\partial T}\right)_e (T_o - T_e) - k_r(T_o - T_e) \qquad (4.15b)$

$$q_i = \left(\frac{\partial q_s}{\partial T}\right)_e T' - k_r T' \qquad (4.15c)$$

q_e is externally determined by physical properties of the atmospheric gases, the solar spectrum, the earth-sun geometry and the temperature above and below the region of interest. Hence we may put

$q_e = h(T^* - T_o)$, where h, defined as $h = k_r - \left(\frac{\partial q_s}{\partial T}\right)_e$, is a function of pressure alone, and T^* is also a function of latitude and longitude.

The first term in (4.15c) results from the dependence of ozone photochemistry on temperature in the reaction

$$O + O_3 \rightarrow 2O_2 + \Delta Q \qquad , \text{ where } \Delta Q \text{ is the}$$

activation energy (given by Schniff (1969) as 4.06 Kcal mole^{-1}).
Leovy (1964) finds

$$\left(\frac{\partial q_s}{\partial T}\right)_e = -\frac{\Delta Q}{2 R^* T_e^2} q_s(T_e) \qquad (4.16)$$

to hold above about 40 km, where R^* is the universal gas constant. This term provides an important stabilizing effect on the external heating and acts to give enhanced Newtonian cooling.

We may now express (4.15a) as

$$q_n = h(T^* - T) \qquad (4.17)$$

This is the generalized form of Newtonian heating and cooling with a time constant h, and heating or cooling determined by the difference of the ambient temperature T from the equilibrium profile given by T^*.

This form of heating will be adequate for our purposes, but it is a gross oversimplification. The deficiency is probably greatest near the stratopause, where the time constant for polar night cooling should be quite different from that due to ozone heating at the summer pole in the opposite hemisphere.

At lower levels where photochemical effects may be ignored, a single time constant should serve well, but heating effects due to latent heat release and boundary layer heating, as well as radiation should be included.

We are interested in baroclinically unstable and forced waves and their interaction. They must be capable of transporting heat and momentum and must include barotropic effects. Waves will be introduced to provide these mechanisms, but severe truncation will eliminate the effects of very short waves. To allow for this lateral diffusion eddy viscosity and eddy diffusion of heat will be included, as used by Phillips (1956). Charney (1959) found this to be negligible for their problem, but we shall neglect waves which were dealt with explicitly

by Charney and Phillips.

Thus we put

$$Q = c_p E_T \nabla^2 \theta \tag{4.18}$$

$$\nabla \cdot \underline{F} \times \underline{k} = E_V (\nabla^2 + 2/a^2) \nabla^2 \psi \tag{4.19}$$

where ∇^2 is the spherical operator

E_V is the lateral kinetic eddy viscosity coefficient

E_T is the lateral eddy diffusion coefficient for heat.

The last term in (4.19) results from the effect of a spherical earth.

Now following Lorenz (1960b) we define

$$X = \int_0^P \mathcal{X}(p) \, dp \tag{4.20}$$

so that $\mathcal{X} = \dfrac{\partial X}{\partial p}$, $\omega = \nabla^2 X$.

Substituting for ω and $\mathcal{X}$ in (4.4), (4.5) and (4.8)

$$\frac{\partial}{\partial t} \nabla^2 \psi = -J(\psi, \nabla^2 \psi + f) + \nabla \cdot (f \nabla \frac{\partial X}{\partial p}) + g^2 \frac{\partial}{\partial p} (\rho^\mu \frac{\partial}{\partial p} \nabla^2 \psi)$$

$$+ E_V (\nabla^2 + 2/a^2) \nabla^2 \psi \tag{4.21}$$

$$\frac{\partial \theta}{\partial t} = -J(\psi, \theta) + \sigma \nabla^2 X + h(\theta^* - \theta) + E_T \nabla^2 \theta \tag{4.22}$$

$$\nabla \cdot \frac{\partial}{\partial p} (f \nabla \psi) = -R p^{k-1} p_\infty^{-k} \nabla^2 \theta \tag{4.23}$$

where $J(A,B) = \nabla A \cdot \nabla B \times \underline{k}$ is the Jacobian.

4.3 Boundary Conditions

The lower boundary condition will be $\omega = 0$ at $p = p_{oo}$ except when orography is introduced.

As we shall be using a limited number of spherical harmonics to represent the variables, we will be unable to include a realistic orography representation. Instead we shall attempt to represent only the very large scale orography in the N.H. as best we can, while allowing completely spurious but relatively small features in the S.H. Then, following Peng (1965) and Kikuchi (1969) the term $\nabla \cdot f \nabla \chi$ at the lower boundary will be approximated by

$$f_o \nabla^2 \chi_o \sim -f_o \rho_o g w = -f_o \rho_o g \underline{v} \cdot \nabla h$$

where f_o and ρ_o are constant values of the coriolis parameter and density, and h is the mountain height profile. Thus we put

$$\nabla \cdot f \nabla \chi_o \sim -f_o \rho_o g J(\psi, h) \qquad (4.24)$$

There is a considerable approximation involved in this expression since the coriolis parameter has opposite signs in each hemisphere and we shall choose a value of f_o for middle latitudes of the N.H. Hence the response in the S.H. will be completely erroneous, but the orography there is small and arbitrary in the model, and we are interested in the N.H. winter response which should not be greatly affected. The effect of this representation in the S.H. is to change the phase of the orography by one half wave length.

The advantage of this simple treatment is that it conserves energy while having the effect of distorting the flow to create eddy kinetic energy from the zonal kinetic energy or vice versa.

A more realistic formulation which includes a variable f is not energy conserving in this simple manner. In order to conserve energy it is necessary to consider a temperature field at the lower boundary which introduces available potential energy into the lowest layer (see Section 4.4) thereby changing the total for the atmosphere. This temperature field must be that which satisfies a variant of the thermal wind equation and adjusts in such a way that the change in available potential energy compensates the change in kinetic energy due to orography, so that A+K = constant.

Since the vertical motion in the zonal flow is induced by a wave interacting with orography of like wave length, the gain in AZ should be approximately offset by a loss in AE. Similarly KE and KZ may tend to balance, so that the result could be similar to that of the simpler formulation.

However the existence of a temperature field at the lower boundary, where a velocity field is inducing vertical motions, implies the need for a thermodynamic equation to be applied there.

This would make the methods of integration of the model with and without orography somewhat different as it effectively changes the number of levels in the model (see Section 6.1). Hence (4.24) is used.

The upper boundary condition could present a problem since we are particularly interested in vertically propagating energy. The condition usually used in numerical models is $\omega = 0$ at $p = 0$. However, owing to truncation errors and the like, this is equivalent to $\omega = 0$ at some small finite pressure and hence the atmosphere is bounded. Lindzen, Batten and Kim (1968) isolate this problem and show that bounded atmospheres do not respond properly to vertically propagating oscillations.

With many layers in the vertical, and by including frictional and radiational damping, the problem should be minimized. In the event of a sudden warming, there should be a trapping layer below the top level of the model or an artificial form of resonance may result.

There is some evidence to suggest that such a level may exist above the stratopause so we shall place our uppermost level in this region with $\omega = 0$ at $p = 0$ as the upper boundary condition.

We now have a set of equations in (4.21), (4.22) and (4.23) which, together with the appropriate boundary conditions, form a closed system in the three dependent variables x, ψ and θ .

$$18 \quad\text{———}\quad \omega_{18} \quad\text{———}\quad 0 \qquad \alpha$$
$$\text{———}\quad \psi_{17}\text{-—} \qquad 0.05 \qquad 71$$
$$16 \quad\text{———}\quad \omega_{16},\theta_{16}\text{———} \qquad 0.1 \qquad 66 \qquad \psi_{16}=1/3(2\psi_{17}+\psi_{15})$$
$$\text{———}\quad \psi_{15}\text{-—} \qquad 0.2 \qquad 61$$
$$14 \quad\text{———}\quad \omega_{14},\theta_{14}\text{———} \qquad 0.5 \qquad 54 \qquad \psi_{14}=1/8(5\psi_{15}+3\psi_{13})$$
$$\text{———}\quad \psi_{13}\text{——} \qquad 1 \qquad 48$$
$$12 \quad\text{———}\quad \omega_{12},\theta_{12}\text{———} \qquad 2 \qquad 43 \qquad \psi_{12}=1/4(3\psi_{13}+\psi_{11})$$
$$\text{———}\quad \psi_{11}\text{—} \qquad 5 \qquad 36$$
$$10 \quad\text{———}\quad \omega_{10},\theta_{10}\text{———} \qquad 10 \qquad 31 \qquad \psi_{10}=1/3(2\psi_{11}+\psi_{9})$$
$$\text{———}\quad \psi_{9}\text{—} \qquad 20 \qquad 26$$
$$8 \quad\text{———}\quad \omega_{8},\theta_{8}\text{———} \qquad 40 \qquad 22 \qquad \psi_{8}=1/5(3\psi_{9}+2\psi_{7})$$
$$\text{———}\quad \psi_{7}\text{—} \qquad 70 \qquad 18$$
$$6 \quad\text{———}\quad \omega_{6},\theta_{6}\text{———} \qquad 120 \qquad 15 \qquad \psi_{6}=1/13(8\psi_{7}+5\psi_{5})$$
$$\text{———}\quad \psi_{5}\text{—} \qquad 200 \qquad 12$$
$$4 \quad\text{———}\quad \omega_{4},\theta_{4}\text{———} \qquad 300 \qquad 9 \qquad \psi_{4}=1/5(3\psi_{5}+2\psi_{3})$$
$$\text{———}\quad \psi_{3}\text{—} \qquad 450 \qquad 6$$
$$2 \quad\text{———}\quad \omega_{2},\theta_{2}\text{———} \qquad 600 \qquad 4 \qquad \psi_{2}=1/7(4\psi_{3}+3\psi_{1})$$
$$\text{———}\quad \psi_{1}\text{—} \qquad 800 \qquad 2$$
$$j=0 \quad\text{———}\quad \omega_{0} \quad\text{———}\quad 1000 \qquad 0$$

			P(mb)	Approx Height (km)	Interpolated ψ

Fig. 2. Vertical Resolution.

4.4 Method of Solution

Following Lorenz (1960b) the model is now divided into n layers by the n+1 surfaces P_0, P_2 --- P_{2n} numbered from the ground upward. Unequal layers of P are chosen in order to emphasize the stratosphere, see Fig. 2. The system of differential equations is replaced by a system in which finite differences replace derivatives with respect to p , in such a way that reversible adiabatic processes have equal effects on kinetic and potential energies.

$$\frac{\partial}{\partial t} \nabla^2 \psi_j = -J(\psi_j, \nabla^2 \psi_j + f) + \frac{1}{(P_{j-1} - P_{j+1})} \nabla \cdot f v (x_{j-1} - x_{j+1})$$

$$-k_j \nabla^2 (\psi_j - \psi_{j-2}) - k'_j \nabla^2 (\psi_j - \psi_{j+2}) + E_v (\nabla^2 + 2/a^2) \nabla^2 \psi_j \quad \text{(4.25a)}$$

$$j = 1, 3, 5 \text{ --- } 17$$

where

$$k_j = \frac{\mu_{j-1} g^2 P_{j-1}}{R T_{j-1} (P_{j-2} - P_j)(P_{j-1} - P_{j+1})} \quad \text{(4.25b)}$$

$$k'_j = \frac{\mu_{j+1} g^2 P_{j+1}}{R T_{j+1} (P_j - P_{j+2})(P_{j-1} - P_{j+1})} \quad \text{(4.25c)}$$

and ψ_{-1}, ψ_{19}, k'_{19} are identically zero.

$$\frac{\partial \theta_j}{\partial t} = -J(\psi_j, \theta_j) + \sigma_j \nabla^2 x_j + h_j(\theta^*_j - \theta_j) + E_T \nabla^2 \theta_j \quad \text{(4.26)}$$

$$j = 2, 4, 6 \text{ --- } 16$$

$$R P_{oo}^{-\kappa} P_j^{\kappa-1} (P_{j-1} - P_{j+1}) \nabla^2 \theta_j = -\nabla \cdot f \nabla (\psi_{j-1} - \psi_{j+1}) \quad \text{(4.27)}$$

$$j = 2, 4, 6 \text{ --- } 16.$$

For the above set of equations, we may readily make use of the concept of available potential energy. Therefore in the absence of friction and diabatic heating A+K is conserved, where we have defined

$$A = \frac{1}{2} R P_{oo}^{-\kappa} \int P^{\kappa-1} \sigma^{-1} (\theta - \{\bar\theta\})^2 \, dM \quad \text{(4.28)}$$

$$K = \frac{1}{2} \int \nabla \psi \cdot \nabla \psi \, dM \quad \text{(4.29)}$$

$$dM = g^{-1} \sum_j (P_{j-1} - P_{j+1}) \int dH$$ and dH is an element

of horizontal area.

We assume that the method of specifying X_j (or ω_j) and Θ_j

for j odd, and ψ_j for j even is linear interpolation between

levels, see Fig. 2.

We now expand $\nabla^2 \psi_j$, Θ_j and $\nabla^2 X_j$ from the closed set of

equations (4.25), (4.26) and (4.27) in the complete set of surface

spherical harmonics

$$\left\{ Y^m_{|m|+\ell} \; ; \; m = 0, \pm 1, \pm 2, \cdots ; \; \ell = 0, 1, 2, \cdots \right\} \qquad (4.30)$$

where Y^m_n is the function of order   m   and   degree   n   (or mode

n-m). The order indicates the number of waves around a latitude circle

and the mode indicates the number of zeros between the poles.

When the complete set of expansions are obtained, we truncate to

retain a finite number of terms, namely the smallest subset capable of

representing the features and mechanisms of interest and importance.

Therefore we choose to include only wave numbers 0, 2, 4, and 6. We

expect waves 4 and 6 to play the role of baroclinically unstable waves

with greatest growth rates, while wave 2 belongs to the class of planet-

ary waves and will be subjected to nonzonal forcing. The inclusion of

all 3 waves will allow non trivial interactions between waves to occur.

It is necessary to include Y^0_6 to represent a 3-cell merid-

ional circulation in each hemisphere. Hence 6 modes are chosen to

represent the zonal flow, but only 3 modes will be used to represent

the eddies. We include asymmetric modes about the equator, which
requires careful handling of the heating field in order that an inflec-
tion point occurs at the equator, and temperature gradients are small
near there.

We choose

$$\left\{ Y_{|m|+\ell}^{m} \; ; \; m = 0, \; \ell = 1, 2, 3, 4, 5, 6; \; m = 2, 4, 6, \; \ell = 1, 2, 3 \right\} \quad \text{to represent}$$

$$\nabla^2 \psi_j \; ,$$

$$\left\{ Y_{|m|+\ell}^{m} \; ; \; m = 0, \; \ell = 1, 2, 3, 4, 5, 6; \; m = 2, 4, 6, \; \ell = 0, 1, 2 \right\} \quad \text{to represent}$$

$\nabla^2 X_j$ and Θ_j . We expand as follows

$$\nabla^2 \psi_j = \sum_{\substack{\ell = \\ 1,2,3,4,5,6}} S_{\ell j}^{0} \, Y_{\ell}^{0} + \sum_{\substack{m = \\ 2,4,6}} \sum_{\substack{\ell = \\ 1,2,3}} \left(S_{|m|+\ell j}^{m} \, Y_{|m|+\ell}^{m} + S_{|m|+\ell j}^{-m} \, Y_{|m|+\ell}^{-m} \right) \qquad (4.31)$$

$$j = 1, 3, \text{--} \; 17$$

$$\nabla^2 X_j = \sum_{\substack{\ell = \\ 1,2,3,4,5,6}} \omega_{\ell j}^{0} \, Y_{\ell}^{0} + \sum_{\substack{m = \\ 2,4,6}} \sum_{\substack{\ell = \\ 0,1,2}} \left(\omega_{|m|+\ell j}^{m} \, Y_{|m|+\ell}^{m} + \omega_{|m|+\ell j}^{-m} \, Y_{|m|+\ell}^{-m} \right) \qquad (4.32)$$

$$j = 2, 4, \text{----} \; 16$$

$$\Theta_j = \sum_{\substack{\ell = \\ 1,2,3,4,5,6}} \Theta_{\ell j}^{0} \, Y_{\ell}^{0} + \sum_{\substack{m = \\ 2,4,6}} \sum_{\substack{\ell = \\ 0,1,2}} \left(\Theta_{|m|+\ell j}^{m} \, Y_{|m|+\ell}^{m} + \Theta_{|m|+\ell j}^{-m} \, Y_{|m|+\ell}^{m} \right) \qquad (4.33)$$

$$j = 2, 4, \text{----} \; 16$$

The coefficients are complex for $m \neq 0$ and we set

$$S_{nj}^{-m} = (-1)^{m} \, \bar{S}_{nj}^{m} \qquad ; \qquad \omega_{nj}^{-m} = (-1)^{m} \, \bar{\omega}_{nj}^{m} \qquad ;$$

$$\Theta_{nj}^{-m} = (-1)^{m} \, \bar{\Theta}_{nj}^{m} \qquad ; \qquad \text{where a bar indicates}$$

the complex conjugate. Then the expansions are real valued.

Since non-linear interactions, as well as terrestrial local vorticity, always disperse the spectra, the harmonics produced outside the prescribed finite spectra, must be omitted in order to make the system of spectral equations closed and energetically self consistent. Therefore equations (4.4)-(4.8) will be only approximately satisfied.

We now make use of the general properties of spherical harmonics given in the appendix, and find the spectral equations as follows.

$$\frac{d\zeta^m_{m+nj}}{dt} = -i\sum_{\ell=0}^{\infty}\sum_{r=-\infty}^{\infty} \frac{\zeta^r_{r+sj}\,\zeta^{m-r}_{|m-r|+\ell j}\,L^m_{m+n}\,{}^r_{r+s}\,{}^{m-r}_{|m-r|+\ell}}{(|m-r|+\ell)(|m-r|+\ell+1)} + i\,b^m_n\,\zeta^m_{m+nj}$$

$$+(m+n+1)\,Q^m_{nj}\left(\omega^m_{m+n-1j-1} - \omega^m_{m+n-1j+1}\right)$$

$$+(m+n)\,Q^m_{m+1j}\left(\omega^m_{m+n+1j-1} - \omega^m_{m+n+1j+1}\right) - g^m_{nj}\,\zeta^m_{m+nj}$$

$$-k_j\left(\zeta^m_{m+nj} - \zeta^m_{m+nj-2}\right) - k'_j\left(\zeta^m_{m+nj} - \zeta^m_{m+nj+2}\right) \quad (4.34)$$

where $\zeta^m_{n-1} = 0$, $\zeta^m_{n\,1q} = 0$, $\omega^m_{n\,1s} = 0$; for $m = 0$, $n = 1,2,3,4,5,6$;

$$m = 2,4,6, \quad n = 1,2,3 \ ;$$

$$j = 1,3,\cdots 17$$

$$\frac{d\theta^m_{m+nj}}{dt} = -i\sum_{\ell=0}^{\infty}\sum_{r=-\infty}^{\infty} \frac{\theta^r_{r+sj}\,\zeta^{m-r}_{|m-r|+\ell j}\,L^m_{m+n}\,{}^r_{r+s}\,{}^{m-r}_{|m-r|+\ell}}{(|m-r|+\ell)(|m-r|+\ell+1)} + \sigma^m_j\,\omega^m_{m+nj}$$

$$+ h_j\left(\theta^{*m}_{m+nj} - \theta^m_{m+nj}\right) - d^m_{nj}\,\theta^m_{m+nj} \quad (4.35)$$

for $m = 0$, $n = 1,2,3,4,5,6$;

$$m = 2,4,6, \quad n = 0,1,2 \ ;$$

$$j = 2,4,\cdots 16.$$

$$\theta^m_{mnj} = C^m_{nj}\left(\zeta^m_{m+n-1\,j-1} - \zeta^m_{m+n-1\,j+1}\right) + C^m_{n+1\,j}\left(\zeta^m_{m+n+1\,j-1} - \zeta^m_{m+n+1\,j+1}\right) \qquad (4.36)$$

$$m = 0, \quad n = 1, 2, 3, 4, 5, 6;$$
$$m = 2, 4, 6, \quad n = 0, 1, 2;$$

where

$$j = 2, 4, \cdots 16$$

$$a^m_n = \frac{1}{m+n}\left[\frac{(2m+n)\,n}{(2(m+n)-1)(2(m+n)+1)}\right]^{\frac{1}{2}}$$

$$a^m_{nj} = \frac{a^m_n\, 2\Omega}{P_{j-1} - P_{j+1}}$$

$$d^m_{nj} = \frac{(m+n)(m+n+1)}{a^2}\, E_j$$

$$g^m_{nj} = \frac{(m+n+2)(m+n-1)}{a^2}\, E_j$$

$$b^m_n = \frac{2\Omega\, m}{(m+n+1)(m+n)}$$

$$C^m_{nj} = \frac{a^m_{nj}\, a^2\, P^K_{e*}}{(m+n)\, R\, P^{K-1}_j}$$

$$L^{m_1\ m_2\ m_3}_{n_1\ n_2\ n_3} = \frac{1}{2}\int_{-1}^{+1} P^{m_1}_{n_1}(\mu)\left\{m_2\, P^{m_2}_{n_2}(\mu)\frac{dP^{m_3}_{n_3}}{d\mu} - m_3\, P^{m_3}_{n_3}(\mu)\frac{dP^{m_2}_{n_2}}{d\mu}\right\}\, d\mu$$

$$\left.\right\} \quad (4.37)$$

In equation (4.35) the ζ^m_{nj} must be interpolated.

The equations with negative m are duplicates of these once real and imaginary parts are taken. The vorticity equation has an extra term to be added for $j = 1$ representing boundary forcing given by (4.24). The non-linear terms involving Jacobians, and the effects of the earth's vorticity on the flow give rise to the interaction coefficients $L^{m_1\ m_2\ m_3}_{n_1\ n_2\ n_3}$, the a^m_{nj} and the C^m_{nj} as shown in the appendix. The method used for calculating the former is also described.

The system of equations has become a spectral system of simultaneous complex ordinary differential equations, and may be solved by matrix inversion as outlined in Section 6.1.

4.5 Numerical Values of Parameters

The parameters involved in the equations of the model are assigned values on the basis of previous experience of other authors with models, and from observations of the real atmosphere. Models of the lower stratosphere and troposphere are abundant, as are observations, but data at higher levels are rare and somewhat uncertain. Models of the region are virtually nonexistent.

(a) Values of θ_j representing January conditions in the N.H. were chosen from Murgatroyd (1970), see Fig. 1, and U.S. Standard Atmosphere Supplements (1966). Thus a mean temperature was used to evaluate the static stability and the k, k' . The static stability values were later modified slightly as described in Section 6.3. See Table 1.

(b) Following Charney (1959) and Peng (1965) the coefficient of ground friction was taken as $k_1 = 2 \times 10^{-6} \sec^{-1}$. The vertical eddy coefficient μ was assumed to be inversely proportional to the static stability, with $\mu_0 = 225$ gm cm^{-1} sec^{-1} (Charney, 1959). Thus k, k' may be calculated, see Table 1.

(c) The lateral eddy viscosity coefficient and eddy diffusion coefficient, E_v and E_T , are difficult to estimate. Peng (1965) chose $E_v = 10^5$ m^2 sec^{-1} and $E_T = 0$. Phillips (1956) put

p (mb)	σ $^\circ mb^{-1}$	T_0 $^\circ K$	μ gm cm^{-1} sec^{-1}	k 10^{-7} sec^{-1}	k' 10^{-7} sec^{-1}	E m^{2}sec^{-1}	h 10^{-6} sec^{-1}	h^{-1} days	T_1^{*0}	T_2^{*0}	T_3^{*0}	θ_1^{*0}	θ_2^{*0}	θ_3^{*0}
									unnormalized					
1000	.048		225											
800				20	10.7	10^5								
600	.047	267	200			10^4	.926	12½	11.4	-34.4		77.57	-17.8	
450				14.3	6.13	10^5								
300	.14	236	108			10^4	.680	17	10.3	-23.0		8.42	-14.54	
200				10.2	1.11	5×10^4								
120	.8	209	13.5			10^4	.222	52	15.5	-5.0	4.5	16.42	-4.10	3.12
70				2.51	.373	10^4								
40	4.5	214	2.4			10^3	.297	39	20.4	-10.4	8.8	29.6	-11.65	8.34
20				.995	.1036	10^3								
10	34.	231	.318			10^2	.587	20	24.0	-12.0	12.0	52.0	-20.1	17.02
5				.388	.0309	10^2								
2	280.	263	.039			10	2.20	5	21.6	-12.0	14.4	69.2	-31.7	32.2
1				.165	.0672	10								
0.5	880.	256	.0123			1	2.77	4	19.5	-4.0	13.0	98.2	-15.6	42.9
0.2				.252	.032	1								
0.1	6400.	221	.0017			0	2.31	5	4.8	0	3.2	38.5	0	16.8
0.05				.128	0	0								

Table 1. Values of parameters at pressure levels p. T_n^{*0} values are the unnormalized temperature values corresponding to θ_n^{*0}. Other parameters are defined in text.

$E_v = E_\tau = 10^5 \, m^2 \, sec^{-1}$. It seems E_τ should be somewhat less than E_v, and probably both should decrease with height, since short waves are largely absent at higher levels, see Table 1.

(d) Diabatic heating satisfies the equation

$$\frac{d\theta_j}{dt} = h_j(\theta_j^* - \theta_j)$$

Mean values of θ_j have been chosen. Below 10 mb values of $\frac{d\theta_j}{dt}$ were taken from Newell et al. (1970) and include estimates of latent heat, boundary layer heating, and radiative heating or cooling. θ^* values were estimated, principally making use of Manabe and Strickler (1964) calculations, with some adjustment at low levels as indicated by Manabe and Möller (1961). Only a smoothed θ^* profile was chosen as best fit, using the first 3 modes. Thus $\theta_4^{*o} = \theta_5^{*o} = \theta_6^{*o} = 0$ at all levels. The values chosen represent solstice conditions and the annual heating cycle was incorporated as discussed in Section 4.6. Above 10 mb, the procedure given in Section 4.2 was used. The Newtonian cooling coefficient k_r was estimated from work by Kuhn and London (1969) and Murgatroyd and Goody (1958). $\left(\frac{\partial q_s}{\partial T}\right)_e$ is found from (4.16) and thus the enhanced Newtonian coefficients h_j were found. θ^* is difficult to estimate owing to the nonlinear nature of heating with temperature, but with the aid of Murgatroyd (1970), Murgatroyd and Goody (1958), and Kuhn and London (1969), the values in Table 1 were chosen. At 10 mb, both procedures were used and a compromise value chosen. The enhanced Newtonian coefficients agree very well with Dickinson (1968c).

The complete T^* field is presented in Fig. 3 and may be compared to the equilibrium field given by Murgatroyd (1970). The resemblance is very strong at lower levels but differs considerably where photochemical damping plays an important role.

(e) As indicated earlier, the major heating is caused by the land-sea contrast, and is predominantly in wave 2. We shall consider only wave 2 nonzonal heating, i.e. $\theta^{*4}_{nj} = \theta^{*6}_{nj} = 0$.

The net asymmetric heating is not well known, and difficulties in obtaining estimates are highlighted by Clapp (1961) who used two methods, the results of which were quite different. Katayama (1964) also presented estimates of tropospheric heating which were used to evaluate the $\theta^{*\lambda}_{nj}$ for this study. The heating was arbitrarily distributed at the two tropospheric levels in the model in the ratio of 10:1 at 600 and 300 mb. Thus

$$\frac{\partial T_2}{\partial t} = 1.07 \ \sin 2(\lambda + 45°)$$

$$\frac{\partial T_4}{\partial t} = .107 \ \sin 2(\lambda + 45°)$$

By making use of the observed amplitudes of the mean fields we find

$$\sum_n \theta^{*\lambda}_{n2} = 22.38 \ \sin 2(\lambda + 35°)$$

$$\sum_n \theta^{*\lambda}_{n4} = 5.0 \ \sin 2(\lambda + 35°)$$

where the h_j found for the zonal heating were used. The latitudinal profile was selected to produce a maximum effect at 45°N. A compromise
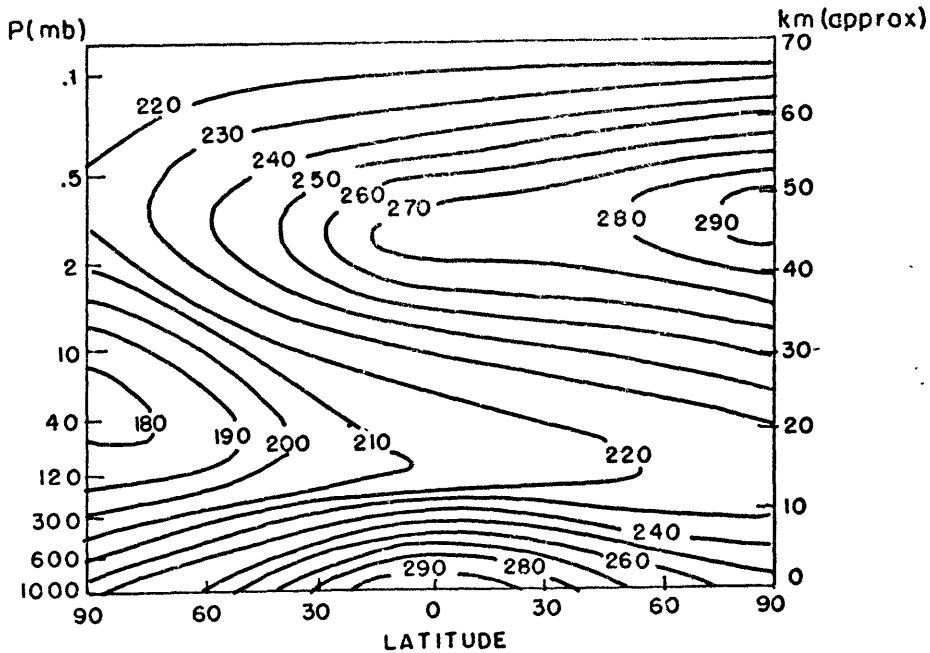
Fig. 3. T^* equilibrium temperature field for the solstices

value was chosen, which would produce only a small peak in the S.H. and small gradients at the equator, given by

$$\tfrac{1}{5}T_2^2 + \tfrac{2}{15}T_3^2 + \tfrac{2}{15}T_4^2 = \cos^2\phi \left(7\sin^2\phi + 2\sin\phi - 2/5\right);$$

where T_n^m are the unnormalized P_n^m, see the appendix. This function produces a maximum of 2.3 near 44N, and 0.9 near 50S, and a minimum of 0.4 near 8S. The θ^{*2} values are given in Table 2 with a generalized phase angle γ, where $\gamma = 145°$ (or $-35°$).

	600 real	600 imag	300 real	300 imag.
θ_2^{*2}	$2.17 \sin 2\gamma$	$-2.17 \cos 2\gamma$	$.49 \sin 2\gamma$	$-.49 \cos 2\gamma$
θ_3^{*2}	$2.73 \sin 2\gamma$	$-2.73 \cos 2\gamma$	$.61 \sin 2\gamma$	$-.61 \cos 2\gamma$
θ_4^{*2}	$4.17 \sin 2\gamma$	$-4.17 \cos 2\gamma$	$.93 \sin 2\gamma$	$-.93 \cos 2\gamma$

Table 2.

The values in Table 2 were chosen to be representative values
of the heating in wave 2. No attempt was made to represent the varia-
tion of phase with latitude or with height. Note that the amplitude
and phase of the heating agrees very well with that used by Derome
and Wiin-Nielsen (1971) for their wave 2 component.

The phase of the mountains in wave 2 was chosen as 35E. There-
fore peak warming will occur to the east of the mountains, and cooling
to the west, which should produce an approximate in-phase reinforcement
of the two effects. The exact relation will depend on the vertical
structure of the wave.

(f) Lower Boundary Mechanical Forcing.

From (4.24)

$$\nabla \cdot f \nabla \chi_0 \sim - f_0 \rho_0 g \, J(\psi, h)$$

Again using only wave 2, we select the latitudinal variation of
h to have a peak in mid-latitudes of the N.H., but smaller values in
the S.H. and equatorial regions. The profile chosen was a peak of
1050 m (amplitude 525 m) near 45°N. A peak of 334 m (amplitude 167 m)
then appears 90° out of phase near 30°S. The profile is given by

$$\tfrac{2}{3} T_3^2 + \tfrac{4}{15} T_4^2 + \tfrac{2}{21} T_5^2 = \cos^2 \phi \; (15 \sin^3 \phi + 14 \sin^2 \phi + 5 \sin \phi - 2)$$

Thus

$$h = (210 \, P_3^2 + 128 \, P_4^2 + 63 \, P_5^2) \cos 2(\lambda - 35^\circ)$$

For computation purposes, the reference phase was taken as
$\lambda_0 = 35^\circ$E. The truncated spectral expansion of $\nabla \cdot f \nabla \chi_0$ is then

given by

$$\frac{f_0 \rho_0 g}{100} \sum_{n=0,2\cdots6} \sum_{\ell=1,2,3} \left[\left(210\, L^{2\ 2\ 0}_{\ell+2\ 3\ n} + 128\, L^{2\ 2\ 0}_{\ell+2\ 4\ n} + 63\, L^{2\ 2\ 0}_{\ell+2\ 5\ n}\right)\right.$$

$$\left.\cdot\frac{1}{\lambda}\left[\frac{(S^{\lambda}_{2\ell,1} + S^{-\lambda}_{2+2,1})}{(\ell+2)(\ell+3)} Y^0_n - \frac{S^0_{n1}}{n(n+1)}\left(Y^{\lambda}_{2+\ell} + Y^{-\lambda}_{2+\ell}\right)\right]\right] \qquad (4.38)$$

where
$f_0 = 10^{-4}\ \mathrm{sec}^{-1}$

$\rho_0 = 1.21\ \mathrm{kg\ m}^{-3}$

$g = 9.8\ \mathrm{m\ sec}^{-2}$

and the factor of 100 is a unit conversion factor.

The approximation involved in (4.24), as discussed in 4.3, will have the effect of producing the response to orography in the S.H. a half wavelength out of phase of the actual orography used, so that in effect (4.38) is the response to orography with a peak of 1050 m near 45°N and a peak of 334 m near 30S at the same longitude.

4.6 Annual Heating Cycle

The heating function was considered with an annual cycle defined as follows. Heating components asymmetric about the equator $(\Theta^{*0}_1, \Theta^{*0}_3)$ were made to vary sinusoidally with time. Θ^{*0}_2 was kept constant.

Above the tropopause, the phase of the variation was set equal to the sun; i.e. the scale factor (SS) multiplying $\Theta^{*0}_1, \Theta^{*0}_3$ was unity at the solstices, and zero at the equinoxes. At lower levels,

(600 mb and 300 mb) a phase lag of three weeks was included since the primary heat source of the troposphere is the surface of the earth. The observed phase lag varies considerably between the centers of continents, coastal regions and the oceans. The value chosen, combined with the time constant of the heating, should provide a phase lag in the temperature field about one month behind the sun. This scale factor (ST) was also used for all components of the nonzonal heating. Thus

$$SS = \sin \frac{2\pi}{365}(t_o - t)$$

$$ST = \sin \frac{2\pi}{365}(t_o - t + 21)$$

where t_o is chosen so that SS = 1 at t = Dec. 22, (t in days).

CHAPTER V

MODEL ENERGETICS

This chapter presents the forms of energy and conversions between them in spectral form. The hemispheric formulation is presented in detail.

The reader who is not interested in the mathematical details may skip this chapter without loss of continuity, but is referred to Fig. 4 which explains the form of presentation of the energetics in later chapters.

5.1 Energy Transformations for the Model

As shown in Section 4 we chose a system of equations which were energetically consistent. We now derive the form of the energy equations and conversion terms in the spectral representation. The equations will conserve energy in the absence of diabatic heating and frictional effects.

Much of our later analysis will be based on the changes in these terms with time at different levels, in the manner of the observational studies discussed in Section 2. We note however, that many of these studies are based on the energetics of only part of the globe, often not even a whole hemisphere, and thus differences in definitions will exist.

We shall determine the global energetics, thereby averaging the summer and winter regimes, and will also consider each hemisphere

separately. Whereas the global kinetic energy is the mean of the hemispheric values (per unit area), a similar relation may not hold for available potential energy. The latter depends on the deviation of the temperature field from the mean for the layer, and thus depends on the area over which the mean is determined. We shall use a global mean, as does Newell et al. (1970), so that the global A is the mean of the hemispheric values. However this is not the case in most observational studies, which utilize a hemispheric mean temperature.

Certain problems arise in expressing the energy equations in spherical harmonics on a hemispheric basis. The truncation of the spectral series prevents non-linearities from overly dispersing the spectra, but may cause mathematical equilities to no longer hold when expressed in truncated spectral form. For this reason the energetics are presented in considerable detail. It also indicates some of the effects of the truncation on the internal model mechanisms.

We define

$$(\overline{\ }) = \frac{1}{2\pi} \int_0^{2\pi} (\ ) \, d\lambda$$

$$(\ )' = (\ ) - (\overline{\ })$$

$$\{(\ )\} = \epsilon \int_{\phi_0}^{\phi_1} (\ ) \cos\phi \, d\phi$$

$$= \epsilon \int_{\mu_0}^{\mu_1} (\ ) \, d\mu$$

where $\mu = \sin\phi$, and λ, ϕ are the longitude and latitude,

$$\left.\begin{array}{l} \mu_1 = 1 \;,\; (\phi_1 = \pi/2) \\[2mm] \mu_0 = -1 \;,\; (\phi_0 = -\pi/2) \\[2mm] \varepsilon = 1/2 \end{array}\right\} \text{ global, or } \left.\begin{array}{l} \mu_1 = 1 \;,\; (\phi_1 = \pi/2) \\[2mm] \mu_0 = 0 \;,\; (\phi_0 = 0) \\[2mm] \varepsilon = 1 \end{array}\right\} \text{ N.H.}$$

A_j and K_j are the Available potential energy, and Kinetic energy in the layer $P_{j-1} - P_{j+1}$. We have

$$A = AZ + AE = \sum_j (AZ_j + AE_j) \;,\quad j = 2,4,\text{---}\; 16 \qquad (5.1)$$

$$K = KZ + KE = \sum_j (KZ_j + KE_j) \;,\quad j = 1,3,\text{---}\; 17 \qquad (5.2)$$

where these are the zonal and eddy parts of the energy defined below. From (4.28)

$$A_j = \frac{R P_{oo}^{-\varkappa}}{2g} \frac{(P_{j-1} - P_{j+1})}{\sigma_j} P_j^{\varkappa-1} \left\{ \overline{(\theta_j - \{\overline{\theta_j}\})^2} \right\}$$

then

$$AZ_j = \frac{R P_{oo}^{-\varkappa}}{2g} \frac{(P_{j-1} - P_{j+1})}{\sigma_j} P_j^{\varkappa-1} \left\{ \overline{\theta}_j^2 - \{\overline{\theta}\}^2 \right\} \qquad (5.3)$$

$$AE_j = \frac{R P_{oo}^{-\varkappa}}{2g} \frac{(P_{j-1} - P_{j+1})}{\sigma_j} P_j^{\varkappa-1} \left\{ \overline{\theta_j'^2} \right\} \qquad (5.4)$$

From (4.29)

$$K_j = \frac{1}{2g} (P_{j-1} - P_{j+1}) \left\{ \overline{\nabla \psi_j \cdot \nabla \psi_j} \right\}$$

$$= \frac{1}{2g} (P_{j-1} - P_{j+1}) \left[\left\{ \overline{\nabla \cdot (\psi_j \nabla \psi_j)} \right\} - \left\{ \overline{\psi_j \nabla^2 \psi_j} \right\} \right]$$

then

$$K z_j = \frac{1}{2q}(P_{j-1} - P_{j+1})\left\{\nabla \cdot (\overline{\psi_j \nabla \psi_j}) - \overline{\psi_j \nabla^2 \psi_j}\right\} \tag{5.5}$$

$$K \varepsilon_j = \frac{1}{2q}(P_{j-1} - P_{j+1})\left\{\nabla \cdot (\overline{\psi_j' \nabla \psi_j'}) - \overline{\psi_j' \nabla^2 \psi_j'}\right\} \tag{5.6}$$

Globally, the divergence terms in (5.5) and (5.6) vanish, but a term is introduced on a hemispheric basis.

We introduce the following notation

$$\int_0^1 P_{m+n}^m P_{m+\ell}^m \, d\mu = I_{n\ell}^m \quad\Bigg\} \tag{5.7}$$

and

$$P_{m+n}^m \frac{\partial P_{m+\ell}^m}{\partial \mu}\bigg|_{\mu=0} = J_{n\ell}^m \quad\Bigg\}$$

$I_{n\ell}^m$ is symmetric in n, ℓ and has non-zero values for $n = \ell$ and if n, ℓ are not both even or odd. $J_{n\ell}^m$ is not symmetric, and takes non-zero values only if n is even and ℓ is odd. As we consider only even m, $I_{n\ell}^m = I_{n\ell}^{-m}$; $J_{n\ell}^m = J_{n\ell}^{-m}$. As a further form of shorthand we write

$$IJ_{n\ell}^m = I_{n\ell}^m - \frac{J_{n\ell}^m}{(m+\ell)(m+\ell+1)}$$

The divergence term in (5.5) and (5.6) is of the form

$$\left\{\overline{\nabla \cdot (B_1 \nabla B_2)}\right\} = \frac{1}{2\pi}\iint\left[\frac{\partial}{\partial\lambda}\left(\frac{B_1}{a^2 \cos\phi}\frac{\partial B_2}{\partial\lambda}\right) + \frac{\partial}{\partial\mu}\left(\frac{1}{a^2}B_1 \cos\phi\frac{\partial B_2}{\partial\phi}\right)\right] d\mu \, d\lambda$$

$$= \frac{1}{2\pi}\int_0^1\left[\frac{B_1}{a^2(1-\mu^2)}\frac{\partial B_2}{\partial\lambda}\right]\bigg|_0^{2\pi} d\mu + \frac{1}{2\pi}\int_0^{2\pi}\left[\frac{B_1(1-\mu^2)}{a^2}\frac{\partial B_2}{\partial\mu}\right]\bigg|_0^1 d\lambda$$

The first integral will always vanish owing to the cyclic nature of B_1 and B_2. We are left with

$$\left\{ \overline{\nabla \cdot (B_1 \nabla B_2)} \right\} = - \frac{\overline{B_1}}{a^2} \frac{\partial B_2}{\partial \mu} \Big|_{\mu=0} \tag{5.8}$$

which is the origin of the $J_{n\ell}^m$ term which appears in the hemispheric kinetic energy equations.

The following are the spectral form of energy expressions.

Global

$$AZ_j = \frac{R P_{oo}^{-\kappa}}{2g} \frac{(P_{j-1} - P_{j+1})}{\sigma_j} P_j^{\kappa-1} \sum_n \Theta_{nj}^{o}{}^2 \qquad n = 1,2,\cdots 6 \tag{5.9}$$

$$AE_j = \frac{R P_{oo}^{-\kappa}}{g} \frac{(P_{j-1} - P_{j+1})}{\sigma_j} P_j^{\kappa-1} \sum_m \sum_n \Theta_{m+nj}^{m} \Theta_{m+nj}^{-m} \qquad \begin{array}{l} m = 2,4,6 \\ n = 0,1,2 \end{array} \tag{5.10}$$

$$KZ_j = \frac{a^2}{2g} (P_{j-1} - P_{j+1}) \sum_n \frac{S_{nj}^{o}}{n(n+1)} \qquad n = 1,2\cdots 6 \tag{5.11}$$

$$KE_j = \frac{a^2}{g} (P_{j-1} - P_{j+1}) \sum_m \sum_n \frac{S_{m+nj}^{m} S_{m+nj}^{-m}}{(m+n)(m+n+1)} \qquad \begin{array}{l} m = 2,4,6 \\ n = 1,2,3 \end{array} \tag{5.12}$$

N.H.

$$AZ_j = \frac{R P_{oo}^{-\kappa}}{2g} \frac{(P_{j-1} - P_{j+1})}{\sigma_j} P_j^{\kappa-1} \sum_n \sum_\ell \Theta_{nj}^{o} \Theta_{\ell j}^{o} I_{n\ell}^{o} \qquad n,\ell = 1,2,\cdots 6 \tag{5.13}$$

$$AE_j = \frac{R P_{oo}^{-\kappa}}{2g} \frac{(P_{j-1} - P_{j+1})}{\sigma_j} P_j^{\kappa-1} \sum_m \sum_n \sum_\ell \left(\Theta_{m+nj}^{m} \bar{\Theta}_{m+\ell j}^{-m} + \bar{\Theta}_{m+nj}^{-m} \Theta_{m+\ell j}^{m} \right) I_{n\ell}^{m} \tag{5.14}$$
$$m = 2,4,6 ; \quad n,\ell = 0,1,2.$$

$$KZ_j = \frac{a^2}{2g} \frac{(P_{j-1} - P_{j+1})}{n(n+1)} \sum_n \sum_\ell S_{nj}^{o} S_{\ell j}^{o} IJ_{n\ell}^{o} \qquad n,\ell = 1,2\cdots 6 \tag{5.15}$$

$$KE_j = \frac{a^2}{2g} (P_{j-1} - P_{j+1}) \sum_m \sum_n \sum_\ell \frac{\left(\bar{S}_{m+nj}^{-m} S_{m+\ell j}^{m} + S_{m+nj}^{m} \bar{S}_{m+\ell j}^{-m} \right) IJ_{n\ell}^{m}}{(m+n)(m+n+1)} \tag{5.16}$$
$$m = 2,4,6 ; \quad n,\ell = 1,2,3.$$

Now consider the rate of change of these quantities.

$$\frac{dA}{dt} = \sum_j \left(\frac{dAZ_j}{dt} + \frac{dAE_j}{dt} \right) \qquad j = 2, 4 \cdots 16$$

$$\frac{dK}{dt} = \sum_j \left(\frac{dKZ_j}{dt} + \frac{dKE_j}{dt} \right) \qquad j = 1, 3 \cdots 17$$

and

$$\frac{dA_j}{dt} = \frac{R\, P_{oo}^{-\kappa}}{g} \frac{(P_{j-1} - P_{j+1})}{\sigma_j} P_j^{\kappa - 1} \left\{ \overline{\theta_j \frac{\partial \theta_j}{\partial t}} \right\}$$

where

$$\theta_j \frac{\partial \theta_j}{\partial t} = -\theta_j J(\psi_j, \theta_j) + \sigma_j \theta_j \nabla^2 \chi_j$$

$$+ h_j \theta_j (\theta_j^* - \theta_j) - \varepsilon_{v_j} \theta_j \nabla^2 \theta_j$$

$$= -J(\psi_j, \tfrac{1}{2}\theta_j^2) \qquad \text{(a)}$$

$$+ \sigma_j \nabla \cdot (\theta_j \nabla \chi_j - \chi_j \nabla \theta_j) \qquad \text{(b)}$$

$$+ \sigma_j \chi_j \nabla^2 \theta_j \qquad \text{(c)}$$

$$+ \theta_j \left(h_j (\theta_j^* - \theta_j) - \varepsilon_{v_j} \nabla^2 \theta_j \right) \qquad \text{(d)}$$

(5.17)

$$\frac{dK_j}{dt} = \frac{1}{g}(\rho_{j-1} - \rho_{j+1})\left\{\overline{\nabla\psi_j \cdot \frac{\partial}{\partial t}\nabla\psi_j}\right\}$$

where

$$\nabla\psi_j \cdot \frac{\partial}{\partial t}\nabla\psi_j = \nabla\cdot(\psi_j \frac{\partial}{\partial t}\nabla\psi_j) - \psi_j \frac{\partial}{\partial t}\nabla^2\psi_j$$

$$= \nabla\cdot(\psi_j \frac{\partial}{\partial t}\nabla\psi_j) - \psi_j J(\psi_j, \nabla^2\psi + f)$$

$$- \frac{\psi_j \nabla\cdot f\nabla(x_{j-1} - x_{j+1})}{(\rho_{j-1} - \rho_{j+1})} + E_{Tj}(\nabla^2 + 2/a^2)\nabla^2\psi_j$$

$$+ \psi_j\left[k_j\nabla^2(\psi_j - \psi_{j-2}) + k_j'\nabla^2(\psi_j - \psi_{j+2})\right]$$

$$= \nabla\cdot(\psi_j \frac{\partial}{\partial t}\nabla\psi_j) \qquad (a)$$

$$- J(\tfrac{1}{2}\psi_j^2, \nabla^2\psi_j) \qquad (b)$$

$$- J(\tfrac{1}{2}\psi_j^2, f) \qquad (c)$$

$$- \frac{1}{(\rho_{j-1} - \rho_{j+1})}\nabla\cdot(\psi_j f\nabla(x_{j-1} - x_{j+1}) - (x_{j-1} - x_{j+1})f\nabla\psi_j) \qquad (d)$$

$$- \frac{1}{(\rho_{j-1} - \rho_{j+1})}(x_{j-1} - x_{j+1})\nabla\cdot f\nabla\psi_j \qquad (e)$$

$$+ \psi_j\left[E_{Tj}(\nabla^2 + 2/a^2)\nabla^2\psi_j + k_j\nabla^2(\psi_j - \psi_{j-2}) + k_j'\nabla^2(\psi_j - \psi_{j+2})\right] \qquad (f)$$

$$\left.\right\} \quad (5.18)$$

Term 5.18 (e) may be rewritten

$$+ \frac{1}{g}\left[x_{j+1}\nabla\cdot f\nabla\psi_{j+1}\right. \qquad (g)$$

$$- x_{j-1}\nabla\cdot f\nabla\psi_{j-1} \qquad (h)$$

$$+ x_{j+1}\nabla\cdot f\nabla(\psi_j - \psi_{j+2})\cdot(1 - r_{j+1}) \qquad (i)$$

$$\left. - x_{j-1}\nabla\cdot f\nabla(\psi_j - \psi_{j-2})\cdot r_{j-1}\right] \qquad (j)$$

where use has been made of

$$\psi_{j+1} = (1-\Gamma_{j+1})\psi_{j+2} + \Gamma_{j+1}\psi_j \qquad \text{and} \qquad \Gamma_{j+1} \;(\angle 1) \qquad \text{is}$$

the ratio representing linear interpolation between levels P_j and P_{j+2}.

Identification of these terms follows. Since a Jacobian may be expressed as a horizontal divergence, terms (5.17a) and (5.18) (b) and (c) vanish globally. Internal changes in the composition of A and K are produced by nonlinear interactions between waves, and thus exchanges between the zonal and eddy forms of energy occur, (CA and CK). Term (5.17d) is the rate of generation and dissipation of A by diabatic heating and cooling, and by diffusion (GZ and GE). Term (5.18f) is the dissipation of K by friction and diffusion (DZ and DE). Terms (5.18) (g) and (h) clearly represent the vertical propagation of energy out of and into the jth layer $(\nabla\bar{\phi}z \;\; and \;\; \nabla\bar{\phi}\epsilon)$. Terms (5.18) (i) and (j) combine with the level above or below to produce a term equal and opposite to (5.17c) when use is made of the thermal wind equation. They represent the conversion of A to K (CZ and CE). The remaining terms (5.17b), (5.18) (a) and (d) become boundary terms and vanish globally.

5.2 Global Conversion Terms

The energy budget may thus be written

$$\frac{\partial A z}{\partial t} = GZ - CZ - CA \qquad\qquad (5.19)$$

$$\frac{\partial AE}{\partial t} = GE - CE + CA \tag{5.20}$$

$$\frac{\partial KZ}{\partial t} = CZ + CK - DZ \tag{5.21}$$

$$\frac{\partial KE}{\partial t} = CE - CK - DE \tag{5.22}$$

where

$$GZ = \frac{Rp_{oo}^{-\kappa}}{g} \sum_j p_j^{\kappa-1} \frac{(p_{j-1}-p_{j+1})}{\sigma_j} \sum_n \left[h_j(\theta_{nj}^{*0} - \theta_{nj}^0) - \frac{E_j}{a^2} n(n+1)\theta_{nj}^0 \right] \theta_{nj}^0$$
$$n = 1,2,\cdots 6 ; \; j = 2,4 \cdots 16 \tag{5.23}$$

$$GE = \frac{Rp_{oo}^{-\kappa}}{g} \sum_j p_j^{\kappa-1} \frac{(p_{j-1}-p_{j+1})}{\sigma_j} \sum_m \sum_n \left[h_j(\theta_{mnj}^{*m} - \theta_{mnj}^m) - \frac{E_j}{a^2}(m+n)(m+n+1)\theta_{mnj}^m \right] \theta_{mnj}^{-m}$$
$$m = 2,4,6 ; \; n = 0,1,2 ; \; j = 2,4,\cdots 16 \tag{5.24}$$

$$CZ = -\frac{R}{g} p_{oo}^{-\kappa} \sum_j p_j^{\kappa-1} (p_{j-1}-p_{j+1}) \sum_n \omega_{nj}^0 \, \theta_{nj}^0$$
$$n = 1,2\cdots 6 ; \; j = 2,4,\cdots 16 \tag{5.25}$$

$$CE = -\frac{R}{g} p_{oo}^{-\kappa} \sum_j p_j^{\kappa-1} (p_{j-1}-p_{j+1}) \sum_m \sum_n \omega_{mnj}^{-m} \, \theta_{mnj}^m$$
$$m = \pm 2,4,6 ; \; n = 0,1,2 ; \; j = 2,4\cdots 16 \tag{5.26}$$

$$CK = \frac{a^2}{g} \sum_j (p_{j-1}-p_{j+1}) \sum_m \sum_n \sum_\ell \sum_s \frac{L_n^0 \, m_{\ell s}^m \, m_{s\ell}^{-m} \, \zeta_{nj}^0}{(m+\ell)(m+\ell+1) \, n(n+1)} \mathcal{I} (\zeta_{m s j}^m \zeta_{m \ell j}^{-m} - \zeta_{m\ell j}^m \zeta_{m s j}^{-m})$$
$$m = 2,4,6 ; \; n = 1,2\cdots 6 ; \; \ell,s = 1,2,3 ; \; j = 1,3,\cdots 17 \tag{5.27}$$

$$CA = \frac{Rp_{oo}^{-\kappa}}{g} \sum_j p_j^{\kappa-1} \frac{(p_{j-1}-p_{j+1})}{\sigma_j} \sum_m \sum_n \sum_\ell \sum_s \frac{L_n^0 \, m_{\ell s}^m \, m_{s\ell}^{-m} \, \theta_{nj}^0}{(m+\ell)(m+\ell+1)} \mathcal{I} (\zeta_{m\ell j}^m \theta_{m s j}^{-m} - \theta_{m s j}^m \zeta_{m\ell j}^{-m})$$
$$m = 2,4,6 ; \; n = 1,2\cdots 6 ; \; \ell = 1,2,3 , s = 0,1,2 ; \; j = 2,4,\cdots 16 \tag{5.28}$$

$$DZ = \frac{a^2}{g}(p_{j-1}-p_{j+1}) \sum_n \left[k_j(\zeta_{nj}^0 - \zeta_{nj-2}^0) + k_j'(\zeta_{nj}^0 - \zeta_{nj+2}^0) - \frac{E_T}{a^2}\zeta_{nj}^0 (n(n+1)-2) \right] \frac{\zeta_{nj}^0}{n(n+1)}$$
$$n = 1,2\cdots 6 ; \; j = 1,3\cdots 17 \tag{5.29}$$

$$DE = \frac{a^2}{g}(p_{j-1}-p_{j+1}) \sum_m \sum_n \left[k_j(\zeta_{mnj}^m - \zeta_{mnj-2}^m) + k_j'(\zeta_{mnj}^m - \zeta_{mnj+2}^m) \right.$$
$$\left. - \frac{E_T}{a^2}\zeta_{mnj}^m ((m+n)(m+n+1)-2) \right] \frac{\zeta_{mnj}^{-m}}{(m+n)(m+n+1)} \tag{5.30}$$
$$m = \pm 2,4,6 ; \; n = 1,2,3 ; \; j = 1,3,\cdots 17$$

where $\mathcal{J}(\quad)$ is the imaginary part of $(\quad)$.

These expressions may be further resolved into the contribution of the jth layer, and into the eddy terms corresponding to wave m contribution only. The following expressions then become necessary.

$$V\oint z_j = \frac{a^2}{g}(P_{j-1} - P_{j+1}) \sum_n \left(\frac{a^o_{nj}}{n} \omega^o_{n-1 j} + \frac{a^o_{n+1 j}}{n+1} \omega^o_{n+1 j} \right) \varsigma^o_{nj} \qquad (5.31)$$

$$n = 1,2 \cdots 6; \quad j = 2,4,\cdots 16$$

$$V\oint E_j = \frac{a^2}{g}(P_{j-1} - P_{j+1}) \sum_n \left(\frac{a^m_{nj}}{m+n} \omega^m_{m+n-1 j} + \frac{a^m_{n+1 j}}{m+n+1} \omega^m_{m+n+1 j} \right) \varsigma^{-m}_{m+nj} \qquad (5.32)$$

$$m = \pm 2,4,6; \quad n = 1,2,3; \quad j = 2,4,\cdots 16.$$

The interactions in our model are limited. If we consider the interaction of wave $r + (m-r) \longrightarrow m$, the change in K^m_j is KF^m_j where

$$KF^m_j = \frac{a^2}{g}(P_{j-1} - P_{j+1}) \left\{ \overline{\psi^m_j J(\psi^{m-r}_j, \nabla^2 \psi^r_j)} \right\}$$

We combine this with the contribution of $(m-r) + r \longrightarrow m$, and consider the negative of these as well to get

$$KF^m_j = \frac{a^2}{g}(P_{j-1} - P_{j+1}) \mathcal{J} \sum_n \sum_\ell \sum_s \left[\frac{L^m_{n+s} \quad n s \quad \overline{|m-r|+\ell}}{(|m-r|+\ell)(|m-r|+\ell+1)(m+n)(m+n+1)} \right.$$

$$\left(\varsigma^r_{r+sj} \varsigma^{m-r}_{|m-r|+\ell j} \varsigma^{-m}_{m+nj} - \varsigma^{-r}_{r+sj} \varsigma^{-m+r}_{|m-r|+\ell j} \varsigma^m_{m+nj} \right) +$$

$$\frac{L^m_{m+n} \quad |m-r|+s \quad n\ell}{(r+\ell)(r+\ell+1)(m+n)(m+n+1)} \left(\varsigma^{m-r}_{|m-r|+sj} \varsigma^r_{r+\ell j} \varsigma^{-m}_{m+nj} - \varsigma^{-|m-r|}_{|m-r|+sj} \varsigma^{-r}_{r+\ell j} \varsigma^m_{m+nj} \right)$$

$$n,s,\ell = 1,2,3; \quad j = 1,3 \cdots 17. \qquad (5.33)$$

Similarly

$$AF_j^m = \frac{R}{q} P_\infty^{-K} P_j^{X-1} \frac{(P_{j-1} - P_{j+1})}{\sigma_j} \sum_n \sum_\ell \sum_3 \} [$$

$$\frac{L_{m+n}^m \, _{r+s}^r \, _{|m-r|+\ell}^{m-r} \, \ell}{(|m-r|+\ell)(|m-r|+\ell+1)} \left(\theta_{r+sj}^r \, \varsigma_{|m-r|+\ell j}^{m-r} \, \theta_{m+nj}^m - \theta_{r+sj}^{-r} \, \varsigma_{|m-r|+\ell j}^{-m-r} \, \theta_{m+nj}^m \right) +$$

$$\frac{L_{m+n}^m \, _{|m-r|+s}^{m-r} \, _{r}^r \, \ell}{(r+\ell)(r+\ell+1)} \left(\theta_{|m-r|+sj}^{m-r} \, \varsigma_{r+\ell j}^r \, \theta_{m+nj}^m - \theta_{|m-r|+sj}^{-m-r} \, \varsigma_{r+\ell j}^{-r} \, \theta_{m+nj}^m \right)]$$

$$n, s = 0, 1, 2; \quad \ell = 1, 2, 3; \quad j = 2, 4, \cdots 16. \qquad (5.34)$$

Contributions to wave m come from each interaction $r + (m-r) \longrightarrow m$ summed over r . We have the following two sets only

m	$m-r$	r	$m-r$	r
2	4	-2	-4	6
4	2	2	6	-2
6			2	4

When orographical effects are introduced at the lower boundary, it produces an interchange between KZ and KE at the lowest level.

$$BKZ = \frac{\rho_o \rho_o}{12} a^2 \sum_m \sum_\ell \frac{(\varsigma_{\ell+\ell}^2 + \varsigma_{\ell+\ell}^{-2}) \varsigma_{n_1}^0}{(2+\ell)(3+\ell)(n+1)n} [$$

$$210 \, L_{\ell+\ell}^2 \, _3^2 \, _n^0 + 128 \, L_{\ell+\ell}^2 \, _4^2 \, _n^0 + 63 \, L_{\ell+\ell}^2 \, _5^2 \, _n^0] \qquad (5.35)$$

and

$$BKE = -BKZ$$

5.3 N.H. Conversion Terms

In much of the following discussion, the constants in the

$$K_j \quad , \quad \left(\frac{a^2}{q} (p_{j-1} - p_{j+1}) \quad = \quad K_o \quad \text{say} \right), \text{ and the } A_j$$

$$\left(\frac{R}{q} \, p_{oo}^{-x} \, p_j^{x-1} \, \frac{(p_{j-1} - p_{j+1})}{\sigma_j} \quad = \quad A_o \quad \text{say} \right), \text{ expressions, and}$$

the subscript j referring to the level will be understood.

$$\frac{\partial AZ}{\partial t} = GZ - CZA - CAZ + BAZ \tag{5.36}$$

$$\frac{\partial AE}{\partial t} = GE - CEA + CAE + BAE \tag{5.37}$$

$$\frac{\partial KZ}{\partial t} = CZK + CKZ - DZ + BKZ \tag{5.38}$$

$$\frac{\partial KE}{\partial t} = CEK - CKE - DE + BKEH + BKE \tag{5.39}$$

where the conversion terms are explained and derived below.

The conversion terms in (5.17) will take a similar form to AZ

and AE in (5.13) and (5.14) for the N.H., as compared to (5.9) and (5.10).

GZ and GE follow this form exactly. Similarly, the conversion terms in

(5.18) will take a similar form to KZ and KE in (5.15) and (5.16) for

the N.H. as compared to (5.11) and (5.12). DZ and DE follow this form.

The remaining terms are considerably complicated by the presence

of boundary terms.

Term (5.17b) forms boundary terms

$$BAZ = A_0 \sum_n \sum_s \frac{\theta_n^0 \omega_s^0}{s(s+1)} \left(J_{ns}^0 - J_{sn}^0 \right) \qquad n,s = 1,2,\cdots 6 \qquad (5.40)$$

$$BAE = A_0 \sum_m \sum_n \sum_s \left(\theta_{m+n}^m \bar{\omega}_{m+s}^m - \theta_{m+n}^m \bar{\omega}_{m-s}^m \right) \left(J_{ns}^n - J_{sn}^m \right) \qquad (5.41)$$

$$m = 2,4,6; \quad n,s = 0,1,2.$$

where we have used (5.8). In deriving these expressions, we make use of

$$\int \nabla \cdot (\theta \nabla \chi - \chi \nabla \theta) \, dH = \int (\theta \nabla^2 \chi - \chi \nabla^2 \theta) \, dH \qquad \text{, which produces}$$

an identity in spectral form

$$J_{sn}^m - J_{ns}^m = \left[(m+n)(m+n+1) - (m+s)(m+s+1) \right] I_{ns}^m. \qquad (5.42)$$

BAZ and BAE arise through the rearrangement of the temperature field by the divergent part of the flow at the equator.

When considering (5.17a) and (5.18a) and (5.18b) in zonal and eddy forms, or as individual waves, the term can no longer be expressed as a Jacobian. In the AZ equation, (5.17a) becomes

$$-\bar{\theta} \, J(\overline{\psi', \theta'}) \qquad \text{(a)}$$

and in the AE equation it becomes

$$-\theta' \, J(\bar{\psi}, \theta') \qquad \text{(b)}$$

$$-\theta' \, J(\psi', \bar{\theta}) \qquad \text{(c)} \qquad \qquad (5.43)$$

$$-\theta' \, J(\psi', \theta') \qquad \text{(d)}$$

$$+\theta' \, J(\overline{\psi', \theta'}) \qquad \text{(e)}$$

Term (5.43e) vanishes immediately upon integration over longitude. Term (5.43b) may be rewritten $-J(\bar{\psi}, \frac{1}{2}\theta'^2)$ and thus as a boundary

term. Hence it vanishes in the global equations and should vanish on a hemisphere. In spectral form (5.43b) =

$$- \oint \sum_m \sum_k \sum_s \sum_n \left(\theta_{n+k}^{-m} \theta_{m+s}^{m} - \theta_{n+k}^{m} \vartheta_{m+s}^{-m} \right) \frac{s_{\ell}^{o}}{\ell(\ell+1)} L_{m+n}^{m} \underset{\ell}{i} \underset{m+s}{m} I_{nk}^{m} \qquad (5.44)$$

It would vanish if

$$\sum_n L_{m+n}^{m} \underset{\ell}{i} \underset{m+s}{m} I_{nk}^{m} = \sum_n L_{m+n}^{m} \underset{\ell}{i} \underset{m+k}{m} I_{ns}^{m} \qquad (5.45)$$

While this identity holds for a sum over n from o to ∞ , truncation of the series makes it invalid, and thus (5.44) is non-zero. We shall consider it combined with (5.41). The interpretation is of a redistribution of AE by the zonal flow, resulting in an exchange of AE between the hemispheres.

Terms (5.43) (a) and (c) are equal and opposite in the global case, forming the conversion CA. On a hemispheric basis, boundary effects are included and equality no longer holds. We find

$(5.43 a) \longrightarrow$

$$CAZ = A_o \oint \sum_m \sum_k \sum_n \sum_s \sum_\ell \theta_n^o \left(\theta_{m+s}^{-m} \zeta_{m+\ell}^{m} - \theta_{m+s}^{m} \zeta_{m+\ell}^{-m} \right) \frac{}{(m+\ell)(m+\ell+1)} L_{m+s}^{m} \underset{k}{i} \underset{m+\ell}{m} I_{nk}^{o}$$

$$m = 2,4,6; \; n,k = 1,3\cdots6; \; s = 0,1,2; \; \ell = 1,2,3 \qquad (5.46)$$

$(5.43c) \longrightarrow$

$$CAE = A_o \oint \sum_m \sum_k \sum_n \sum_s \sum_\ell \theta_n^o \left(\theta_{m+s}^{-m} \zeta_{m+\ell}^{m} - \theta_{m+s}^{m} \zeta_{m+\ell}^{-m} \right) \frac{}{(m+\ell)(m+\ell+1)} L_{m+k}^{m} \underset{n}{i} \underset{m+\ell}{m} I_{ks}^{m}$$

$$m = 2,4,6; \; k,s = 0,1,2; \; n = 1,2\cdots6; \; \ell = 1,2,3 \qquad (5.47)$$

CAZ is the conversion of $(AZ)_{N.H.}$ to $(AE)_{GLOBAL}$, and CAE is the gain in $(AE)_{N.H.}$ by conversion from $(AZ)_{GLOBAL}$.

The remaining term (5.17d) may be compared to the global form

(5.34). Now we find

$$
\begin{aligned}
AF^m = A_0 \Bigg\{ \sum_r \sum_s \sum_k \Bigg[& \frac{(\theta^{-m}_{m+k}\, \theta^r_{m+s}\, \zeta^{m-r}_{|m-r|+\ell} - \theta^m_{m+k}\, \theta^{-r}_{r+s}\, \zeta^{-m-r}_{|m-r|+\ell})}{(|m-r|+\ell)(|m-r|+\ell+1)} L^m_{m+n}\, \overset{r}{,}\, \overset{m-r}{|m-r|+\ell} \\
+ & \frac{(\theta^{-m}_{m+k}\, \theta^{m-r}_{|m-r|+s}\, \zeta^r_{r+\ell} - \theta^m_{m+k}\, \theta^{-m-r}_{|m-r|+s}\, \zeta^{-r}_{r+\ell})}{(r+\ell)(r+\ell+1)} L^m_{m+n}\, \overset{m-r}{|m-r|+s}\, \overset{r}{r+\ell} \Bigg] I^m_{k n}
\end{aligned}
$$

$$
m, r = 2,4,6 \;;\; n,k,s = 0,1,2 \;;\; \ell = 1,2,3 \qquad (5.48)
$$

The mth component of this expression, is the gain in $(A^m)_{N.H.}$ from

$(A^{m-r})_{GLOBAL}$ and $(A^r)_{GLOBAL}$, by nonlinear interactions between

waves.

A similar analysis to that applied to (5.17a) may be applied to

(5.18b), plus the portion of (5.18a) with the same form. Term (5.18b) is

then written;

for $K\ell$ $\qquad -\overline{\psi}\, J(\overline{\psi'},\, \nabla^2\psi')$ $\qquad$ (a)

for $K\epsilon$ $\qquad -\psi'\, J(\overline{\psi},\, \nabla^2\psi')$ $\qquad$ (b)

$\qquad\qquad\qquad -\psi'\, J(\psi',\, \nabla^2\overline{\psi})$ $\qquad$ (c) $\qquad$ (5.49)

$\qquad\qquad\qquad -\psi'\, J(\psi',\, \nabla^2\psi')$ $\qquad$ (d)

$\qquad\qquad\qquad +\psi'\, J(\overline{\psi'},\, \nabla^2\psi')$ $\qquad$ (e)

Term (5.49e) vanishes upon integration over the domain. Term

(5.49c) vanishes globally, and for the N.H. should take the form of a

boundary term.

$$
BKEH = K_0 \Bigg\{ \sum_m \sum_n \sum_k \overset{\ell}{} \zeta^0_n \frac{(\zeta^m_{m+s}\, \zeta^{-m}_{m+\ell} - \zeta^{-m}_{m+s}\, \zeta^m_{m+\ell})}{(m+\ell)(m+\ell+1)(m+s)(m+s+1)} L^n_{m+k}\, \overset{0}{n}\, \overset{m}{m+s}\, IJ^m_{\ell k}
$$

$$
m = 2,4,6 \;;\; n,s,\ell,k = 1,2,3. \qquad\qquad (5.50)
$$

Making use of (5.45), this expression would be expressible as a
boundary term, giving rise to an exchange of K^m across a latitude
circle. However the truncation of the spectral equations cause it to
produce an internal redistribution of K^m as the waves interact with
the zonal flow. Thus the label BKEH is somewhat misleading for the
model.

Terms (5.49) (a) and (b) are equal and opposite in the global
case, forming the conversion CK. But with boundary effects included,
the conversion of $(KE)_{GLOBAL}$ to $(KZ)_{N.H}$ (= CKZ) in (5.49a), no longer
equals the conversion of $(KE)_{N.H}$ to $(KZ)_{GLOBAL}$ (= CKE) in (5.49b).

$$CKZ = K_0 \oint \sum_m \sum_{\substack{k \\ n}} \sum_{\substack{s \\ \ell}} S_n^0 \frac{(S_{m+s}^m S_{m+\ell}^{-m} - S_{m+s}^{-m} S_{m+\ell}^m)}{n(n+1)(m+\ell)(m+\ell+1)} L_{m+s}^m {}_k^0 {}_{m+\ell}^m IJ_{nk}^0$$

$$m = 2,4,6; \quad k,n = 1,2,\cdots 6; \quad s,\ell = 1,2,3 \tag{5.51}$$

$$CKE = K_0 \oint \sum_m \sum_{\substack{k \\ n}} \sum_{\substack{s \\ \ell}} S_n^0 (S_{m+s}^m S_{m+\ell}^{-m} - S_{m+s}^{-m} S_{m+\ell}^m) L_{m+s}^m {}_n^0 {}_{m+k}^m IJ_{\ell k}^m$$

$$m = 2,4,6; \quad n = 1,2\cdots 6; \quad s,\ell,k = 1,2,3 \tag{5.52}$$

Term (5.49d) is the gain in $(K^m)_{N.H.}$ from $(K^{m-r})_{GLOBAL}$ and
$(K^r)_{GLOBAL}$ by non-linear interactions.

$$KF^m = K_0 \oint \sum_r \sum_{\substack{n \\ s}} \sum_{\substack{\ell \\ k}} \left[L_{m+n}^m {}_{s}^r {}_{m-r+\ell}^{m-r} \frac{(S_{m+k}^{-m} S_{r+s}^r S_{m-r+\ell}^{m-r} - S_{m+k}^m S_{r+s}^{-r} S_{m-r+\ell}^{-m+r})}{(m-r+\ell)(m-r+\ell+1)(m+k)(m+k+1)} \right.$$

$$\left. + L_{m+n}^m {}_{m-r+s}^{m-r} {}_{r+\ell}^r \frac{(S_{m+k}^{-m} S_{m-r+s}^{m-r} S_{r+\ell}^r - S_{m+k}^m S_{m-r+s}^{-m+r} S_{r+\ell}^{-r})}{(r+\ell)(r+\ell+1)(m+k)(m+k+1)} \right] IJ_{kn}^m$$

$$m,r = 2,4,6; \quad n,s,\ell,k = 1,2,3. \tag{5.53}$$

While term (5.18c) vanishes, the similar contribution from
(5.18a) does not, and becomes

$$\int 2\text{-}\Omega m \; \frac{(\zeta^m_{m+n} \zeta^{-m}_{m+2} - \zeta^{-m}_{m+n} \zeta^m_{n+\ell}) J^m_{\ell n}}{(m+n)(m+n+1)(m+2)(m-\ell+1)(m+n)(m+n+1)}$$

$$m = 2,4,6 \;; \quad \ell = 2 \;; \quad n = 1,3.$$

(5.54)

This term will be considered along with BKEH, as it is a boundary term arising from an exchange of K^m between the hemispheres due to advection of the earth's angular momentum across the equator.

The terms yet to be considered are (5.18d), (5.18e) and (5.17c). Use was made of the expression

$$\psi \nabla . f \nabla \chi - \nabla . (\psi f \nabla \chi) = f \nabla \psi . \nabla \chi - \chi \nabla . f \nabla \psi - \nabla . (\chi f \nabla \psi)$$

(5.55)

On a global integration, the divergence terms vanish and the remaining terms are equal, even when expressed in spectral form. Upon integration over a hemispheric domain the presence of f ensures that the divergence terms should again vanish. But in truncated spectral form it is not so. Expression (5.55) produces the identity in spectral form

$$\frac{(m+\ell+2) a^m_{\ell+1} I^m_{n\ell+1} + (m+\ell-1) a^m_{\ell} I^m_{n\ell-1}}{(m+n)(m+n+1)} = \frac{(m+n+2) a^m_{n+1} I^m_{\ell n+1} + (m+n-1) a^m_n I^m_{\ell n-1}}{(m+\ell)(m+\ell+1)}$$

for $n, \ell \geqslant 1.$

(5.56)

Once again, owing to truncation of the spectral series (5.56) cannot always be applied. In effect the center term in (5.55) takes different values depending on whether the expression (A8) (see appendix   ) is applied to disperse ψ or χ .

Thus (5.18d) and (5.18c) when combined with the contribution from (5.18a) produces expressions for the conversion of $(A)_{GLOBAL}$ into $(K)_{N.H.}$ (CZK and CEK), and for the vertical propagation of geopotential energy ($V\Phi Z$ and $V\Phi E$). Conversely term (5.17c) represents the conversion of $(A)_{N.H.}$ into $(K)_{GLOBAL}$, (CZA and CEA).

$$CZK = K_o \left[(n+1) a^o_{nj} \omega^o_{n-1j} + n\, a^o_{n+1j} \omega^o_{n+1j} \right] \left(\frac{\zeta^o_{\ell j+1} - \zeta^o_{\ell j-1}}{\ell(\ell+1)} \right) I J^o_{\ell n}$$

$$\ell, n = 1, 2, \cdots 6 \qquad (5.58)$$

$$CEK = K_o \left[(m+n+1) a^m_{nj} \omega^m_{m+n-1j} + (m+n) a^m_{n+1j} \omega^m_{m+n+1j} \right] \left(\zeta^{-m}_{m+\ell j+1} - \zeta^{-m}_{m+\ell j-1} \right) I J^m_{\ell n}$$

$$\frac{}{(m+\ell)(m+\ell+1)}$$

$$m = \pm 2, 4, 6 \; ; \; \ell, n = 1, 2, 3. \qquad (5.59)$$

$$V\Phi Z = K_o \left[(n+1) a^o_{nj} \omega^o_{n-1j} + n\, a^o_{n+1j} \omega^o_{n+1j} \right] \frac{\zeta^o_{\ell j}}{\ell(\ell+1)} I J^o_{\ell n}$$

$$\ell, n = 1, 2, \cdots 6 \qquad (5.60)$$

$$V\Phi E = K_o \left[(m+n+1) a^m_{nj} \omega^m_{m+n-1j} + (m+n) a^m_{n+1j} \omega^m_{m+n+1j} \right] \frac{\zeta^{-m}_{m+\ell j}}{(m+\ell)(m+\ell+1)} I J^m_{\ell n}$$

$$m = \pm 2, 4, 6 \; ; \; \ell, n = 1, 2, 3 \qquad (5.61)$$

$$CZA = A_o \frac{n(n+1)}{s(s+1)} \omega^o_s \theta^o_n I^o_{ns}$$

$$n, s = 1, 2, \cdots 6 \qquad (5.62)$$

$$CEA = A_o \frac{(m+n)(m+n+1)}{(m+s)(m+s+1)} \left(\omega^{-m}_{m+s} \theta^m_{m+n} + \omega^m_{m+s} \theta^{-m}_{m+n} \right) I^m_{ns} \qquad (5.63)$$

$$m = 2, 4, 6 \; ; \; n, s = 0, 1, 2.$$

The topographical term follows the pattern set by CKZ and CKE in (5.51) and (5.52). Thus the loss of KZ in one hemisphere may appear as a gain in KE in either hemisphere, and BKE and BKZ must be evaluated separately.

5.4 Energetics Presentation

Fig. 4 shows the 4-box diagram usually used for presenting energetics analyses, but with each box isolated. Whereas the boxes may be connected in a global treatment of the energetics, the hemispheres are not closed energetically owing to the boundary at the equator and to the limited degrees of freedom caused by truncation of the spectral equations.

Arrows will be used to indicate the direction of the conversions. In parentheses below the value of the form of energy, the change necessary for the contributions into each box to balance will be given.

The model atmosphere will be subdivided into three regions for comparing the model energetics with the atmosphere. The layer 1000-200 mb will be considered as the troposphere, 200-20 mb as the lower stratosphere, and the region above 20 mb as the upper stratosphere. The latter region also includes the mesosphere. The divisions are necessarily somewhat artificial, but will suffice for our purposes.

5.5 Angular Momentum and Temperature Budgets and Velocity Fields

The expressions for the velocity components, the p-velocity and temperature are presented below

$$\bar{u}_j = a \sum_n \frac{\zeta_{nj}^o}{n(n+1)} \frac{\partial P_n^o}{\partial \phi} \qquad n = 1,2,\cdots 6 \; ; \; j = 1,3,\cdots 17 \qquad (5.64)$$

$$\bar{v}_j = a \sum_n \frac{(\omega_{nj-1}^o - \omega_{nj+1}^o)}{(P_{j-1} - P_{j+1}) n(n+1)} \frac{\partial P_n^o}{\partial \phi} \qquad n = 1,2,\cdots 6 \\ j = 1,3,\cdots 17. \qquad (5.65)$$
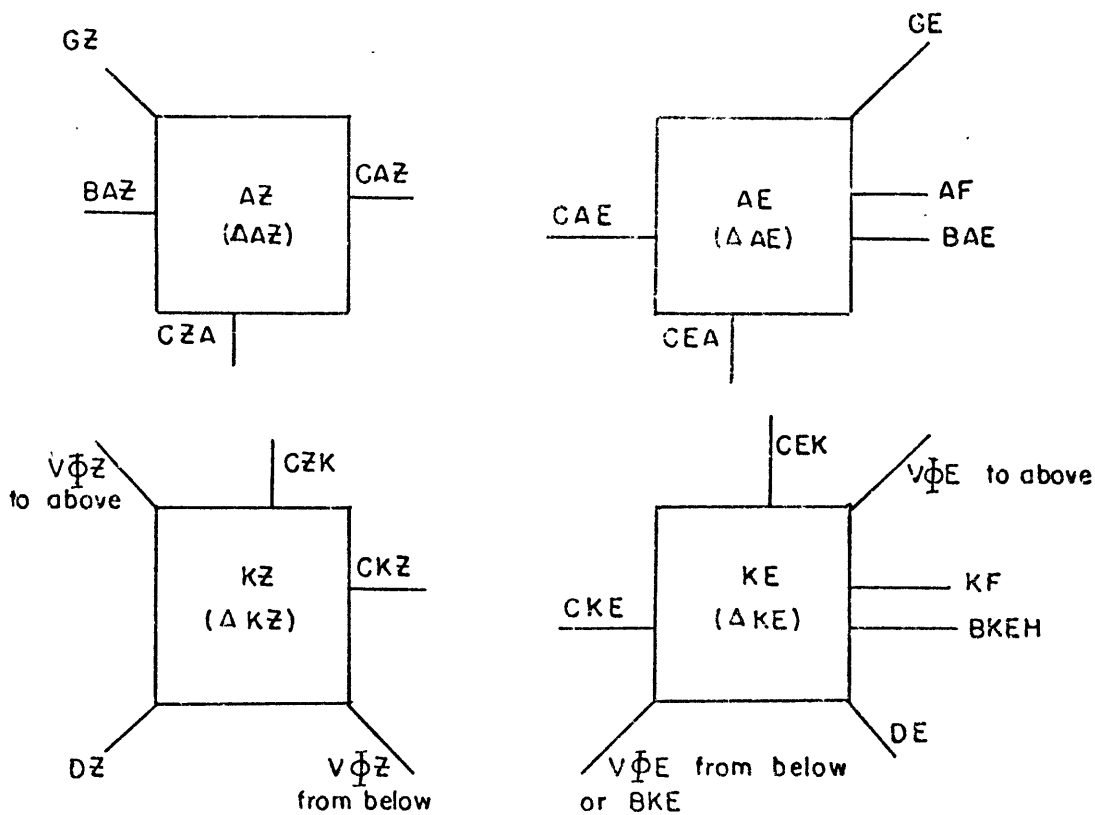
Fig. 4. Representation of Energetics in model.

$$\bar{\omega}_j = \sum_n \omega^o_{nj} P^o_n \qquad n=1,2,\cdots 6; \quad j=2,4,\cdots 16 \qquad (5.66)$$

$$\bar{T}_j = T_{oj} + (P_j/P_{oo})^{\kappa} \sum_n \theta^o_{nj} P^o_n \qquad \begin{matrix} n=1,2,\cdots 6 \\ j=2,4,\cdots 16 \end{matrix} \qquad (5.67)$$

The angular momentum (M) per unit area is given by

$$M = \int \rho \left(u a \cos\phi + \Omega a^2 \cos\phi \right) dz$$

and thus

$$\frac{\partial M}{\partial t} = \frac{a^2}{g} \sum_j (P_{j-1} - P_{j+1}) \sum_n \frac{\frac{\partial S^o_{nj}}{\partial t}}{n(n+1)} \frac{\partial P^o_n}{\partial \phi} \cos\phi \qquad (5.68)$$

$$n=1,2\cdots 6; \quad j=1,3,\cdots 17$$

We may substitute for $\frac{\partial \zeta_j^o}{\partial t}$ from (4.34) and (4.38). The interaction term is the redistribution of M by the eddies. The ω terms vanish when summed over j , indicating that the quasigeostrophic nature of the model produces no meridional cell contribution other than a vertical exchange of relative angular momentum between layers, due to a conversion between the earth's angular momentum and relative angular momentum by the meridional circulation. The lack of a net transport is caused by the requirement that there be no net mass transport across a latitude circle. The inclusion of (4.38) produces a mountain torque term. The frictional term produces a vertical exchange of relative angular momentum which is conserved except at the ground, thus simulating surface friction. The horizontal diffusion term redistributes relative angular momentum within each layer.

The temperature budget may be directly determined from (4.35). Thus we may evaluate the contributions due to (i) the advection by the eddies, (ii) adiabatic effects from vertical motion, (iii) diabatic heating and cooling, and (iv) horizontal diffusion.

CHAPTER VI

PRELIMINARY SOLUTIONS

6.1 Method of Numerical Solution

The system of spectral equations has been reduced to a system of complex simultaneous ordinary differential equations (4.32), (4.35) and (4.36). The θ_{nj}^{m} are determined by the thermal wind equation and a solution is found for the unknowns $\frac{d\zeta_{nj}^{m}}{dt}$ and ω_{nj}^{m} . It is determined from a set of matrix equations.

$$A^{m} Z^{m} = B^{m} \qquad \text{for} \quad m = 0,2,4,6 \qquad (6.1)$$

where A^{m} is a constant real matrix, (102x102 for $m = 0$, and 51x51 for $m = 2,4,6$); Z^{m} is a column matrix, whose complex elements consist of the unknowns $\frac{d\zeta_{nj}^{m}}{dt}$ and ω_{nj}^{m} ; B^{m} is a column matrix whose complex elements are generally non-linear functions of θ_{nj}^{m} and ζ_{nj}^{m} .

By inverting the coefficient matrices A^{m} , we solve for the elements Z^{m}

$$Z^{m} = A^{m^{-1}} B^{m} \qquad \text{for} \quad m = 0,2,4,6 \qquad (6.2)$$

For $m \neq 0$, the equations are complex, and when separated into real and imaginary parts combine to produce 408 real ordinary differential equations. The ω_{nj}^{m} are immediately determined from (6.2). A set of equations of the form $\dot{x} = Fx$ remain; where $\dot{x}$, x are column matrices of the 216 real and imaginary parts of $\frac{d\zeta_{nj}^{m}}{dt}$, ζ_{nj}^{m} respectively; and F is a 216x216 matrix.

The finite difference scheme used for the time integration is that proposed by Lorenz (1971). The order of the scheme equals the number of steps required, and the algorithm is as follows for N^{th} order:

If Z_i is a set of numbers with arbitrary initialization,

let $a = 0$, $b = N/\Delta T$,

1. Replace Z_i by $\left[a Z_i + F_i(x_i)\right] / b$

2. Replace x_i by $x_i + Z_i$

3. Replace a by $a - 1/\Delta T$; b by $b - 1/\Delta T$

4. If $b > 0$ return to step 1; if $b = 0$ the procedure

is complete.

The scheme is equivalent to choosing coefficients so that

$$x(t_0 + \Delta T) = \sum_{k=0}^{N} F^k x(t_0) \frac{\Delta t^k}{k!}$$

Lorenz shows $\Delta T/N$ may be considered as the fundamental time step, and provided it is short enough (less than about 1/17th of the period of the waves), the N-cycle scheme becomes increasingly accurate as N is increased.

6.1.1 Computations

The computations were performed on an IBM 360/65 machine at the M.I.T. computation center. All computations of the matrix inversion and interaction coefficients were performed in double precision, (single precision denotes a word of 4 bytes or 32 bits). In the main integration, the order of the scheme used was $N = 4$. The largest time step sufficient for a stable scheme with adequate accuracy was $\Delta T = 6$ hours ($\Delta T/N = 1.5$ hours). The real time taken to integrate the model for one day and perform

the energetics and supplementary calculations was about 22 sec.

In the preliminary calculation without eddies (Section 6.2), a considerably longer time step of ΔT = 24 hours, ($\Delta T/N$ = 6 hours) was used.

6.2 Preliminary Integrations

The steady state solution under solstice conditions was found as a test of the parameters chosen. The solutions are not presented here, but the temperature field is very similar to that in Fig. 3.

Following the conventional procedure for setting up a numerical experiment with an atmospheric general circulation model, a symmetric zonal flow was allowed to develop at equinoctial heating. After 60 days, the annual heating cycle was introduced into the model and a run made for 1 year without eddies.

The results are presented, as they provide a background for considering the effects of the eddies in the full scale response of the model. As both hemispheres are identical, only 6 months are considered. Temperature and velocity fields are presented at 30 day intervals, corresponding to the dates shown, in Fig. 5. A schematic diagram of the meridional circulation accompanying these fields is also given. These contours were drawn to represent streamlines, but are not spaced to account for the strength of the flow.

The maximum winds appeared a few weeks after the solstice with westerlies of 180 m sec^{-1} and easterlies of 40 m sec^{-1}. The easterlies
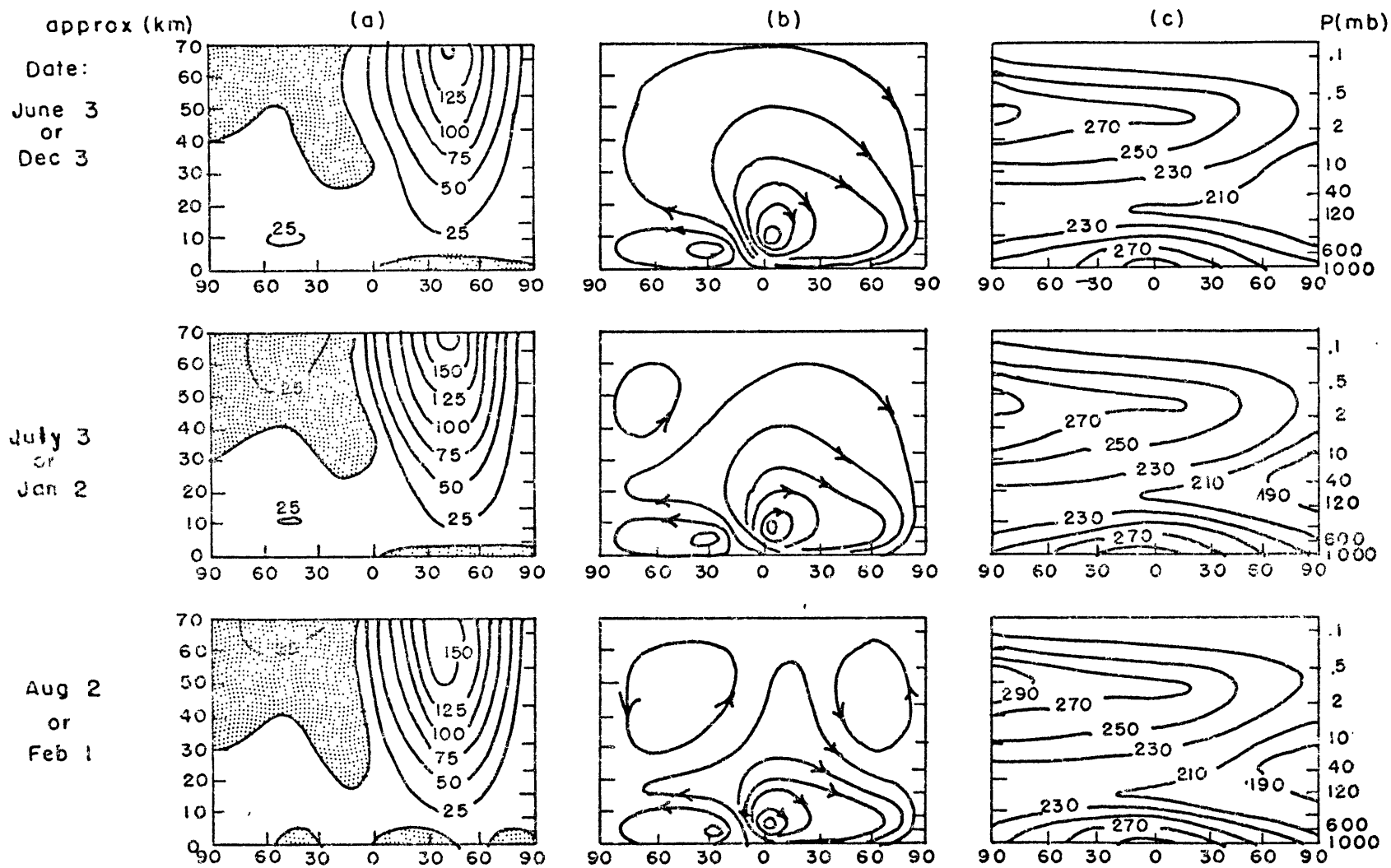
Fig. 5. Zonal wind (m sec^{-1}) Schematic meridional cell Temperature ($^{\circ}$K).
Easterlies are shaded. streamlines.
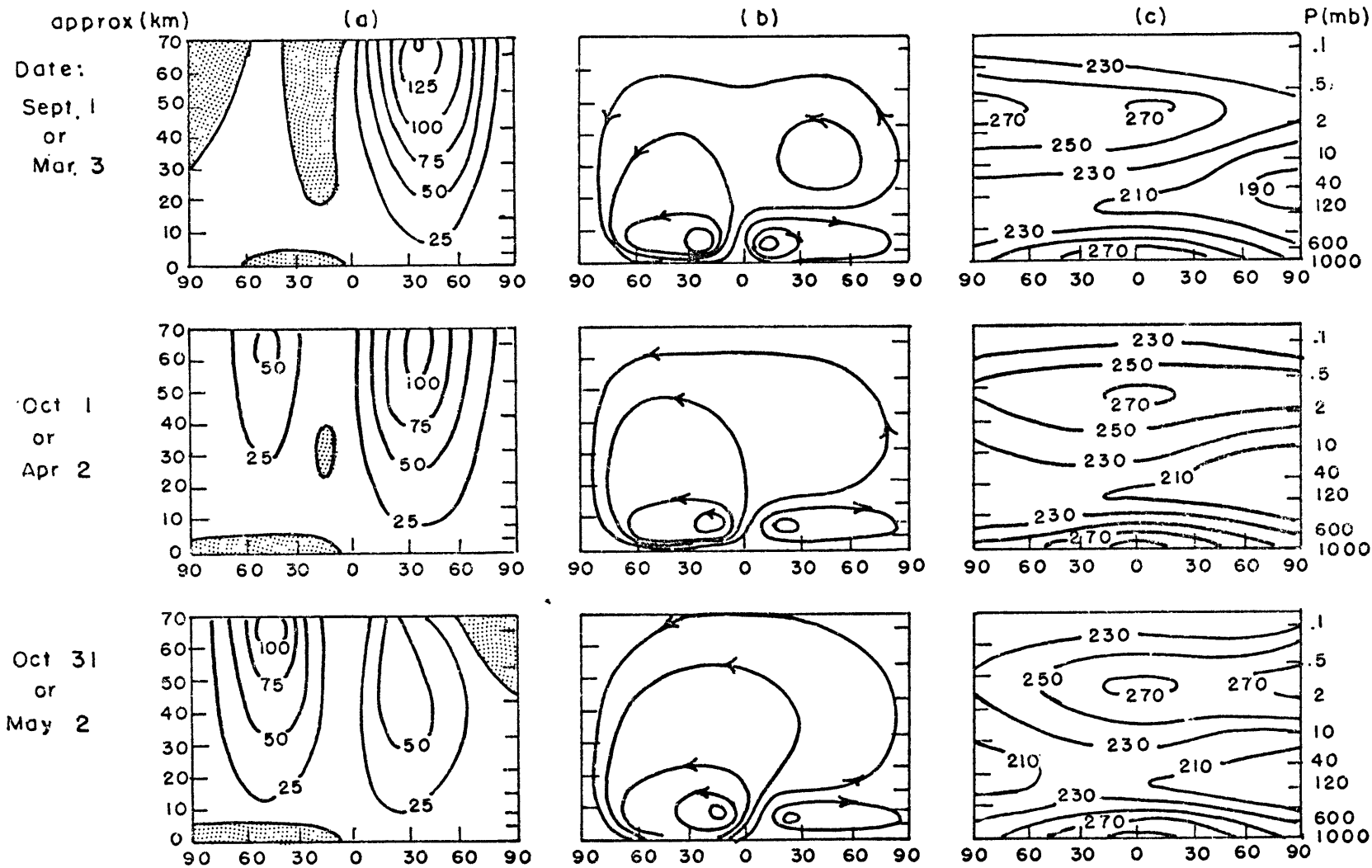
approx (km) (a)   (b)   (c)   P(mb)

Date:
Sept. 1
or
Mar. 3

Oct 1
or
Apr 2

Oct 31
or
May 2

Fig. 5. Zonal wind (m sec^{-1})   Schematic meridional   Temperature ($^{\circ}$K).
Easterlies are shaded.   cell streamlines.

are not as strong as observed, nor do they extend to sufficiently low levels. This was expected to be helped considerably by the inclusion of eddies, which should also reduce the westerly maximum

The greatest amplitude of the meridional velocity at the upper levels in our model occurred in April and October of .25 m sec^{-1} near 60 km. The differential heating near the stratopause, which is the forcing field for the motions, is weak prior to the solstice and reverses shortly thereafter owing to the progress of seasons. Hence the meridional circulations are somewhat weaker at the time of the solstice, as may be seen from Fig. 5. The strongest meridional flow in the troposphere occurred during January and July.

It is of interest to compare Fig. 5 with the stratospheric Hadley circulations presented by Leovy (1964). He considered the circulation at the solstice as driven by heating in that region, with a lower boundary at 22.5 km. Thus tropospheric influence on the upper atmospheric circulation was neglected. Eddy fluxes of heat and momentum were allowed for, but only zonally symmetric circulations were considered.

The circulation at the time of the solstice in Fig. 5 is quite different from that given by Leovy (1964). The introduction at the eddy fluxes may make his solution more comparable to the period prior to the solstice, but even if the maximum meridional circulation in our model is considered, the strength is still much less than half that found by Leovy. Some differences are caused by the upper boundary in this model, but are primarily due to the inclusion of the troposphere.

This allows the presence of a substantial return flow at the low levels, whereas Leovy's model required this to be above 22.5 km.

Leovy (1964) found the forced meridional cell could cause the very low temperatures observed at the summer pole in the mesosphere. Our model does not extend this high, but the adiabatic cooling at .1 mb from this effect was not sufficient to reverse the weak temperature field set up by the externally imposed heating field. Thus the presence of the upper boundary does not allow us to test this mechanism, although it is likely that the effects would be less than found by Leovy.

6.3 Baroclinic Growth Rates

In order to obtain a model which behaved like the real atmosphere, parameters were chosen from real data. However, owing to the truncation of the spectral representation and the limited vertical resolution, it was recognised that the model would not correspond exactly, and might even have a solution considerably different in some respects. Therefore it might prove desirable to choose somewhat different parameters in order to gain the best resemblance between those features of the flow deemed important. With this in mind, the model was investigated to learn more about its properties and how we might change the parameters in order to better the simulation.

After the initialization of the model without eddies, perturbations in waves 4 and 6 were introduced. Wave 4 grew faster than wave 6, and the growth rate was still greater even with friction and heating excluded. Since the real atmosphere and baroclinic instability studies

have waves with greatest growth rates at a wavelength near 2500 km

(e.g. Sanders, 1971), a similar but further simplified model was used

to perform a baroclinic instability analysis. We shall refer to this

model and analysis as 'M3', and the full scale model as 'M9'.

We consider a model with about the same vertical tropospheric

resolution, namely an atmosphere divided into 3 equal layers so that

$\Delta p = P_{j-1} - P_{j+1} = 333$ mb = const. The equations (4.25), (4.26),

and (4.27) were used with heat and friction, excluded, and a perturba-

tion analysis made. We put

$$\psi = \overline{\psi} + \psi' \quad , \quad \theta = \overline{\theta} + \theta' \quad , \quad X = \overline{X} + x'$$

and assume a solution

of the form

$$\nabla^2 \psi' = S_n^m Y_n^m e^{-imct}$$

$$\theta' = \theta_n^m Y_n^m e^{-imct}$$

$$\nabla^2 x' = \omega_n^m Y_n^m e^{-imct}$$

Consistency in the resulting equations imposes conditions upon c,

and requires that c be the solution to a cubic equation. The eigen-

values will be one real and two complex, or three real solutions. In

the former case, the imaginary part of the root determines the growth

rate of the wave.

The basic current was represented by two modes P_1^0 and P_3^0 for

the vorticity profile and P_2^0 for the temperature profile. A linear

dependence on pressure was assumed in the vertical

$$\nabla^2 \overline{\psi} = (b_1 P_1^0 + b_3 P_3^0)(P_{00} - P).$$

The cases chosen for study were such that the vertical wind shear at

45° latitude was $\left[\dfrac{du}{dp}\right]_{45^o} = .5$ m sec^{-1} cb^{-1}. Two cases were

considered, $b_3 = 0$ (solid rotation, but with a vertical shear) and such that the N-S velocity profile of the basic current was proportional to $(10 \sin^2\phi + 1)\cos\phi$, which is more like that observed; see Fig. 6 (a) and (b).

In each case, only single modes were chosen to represent the vorticity field of each wave, combined with one or two temperature modes. We considered the combinations

(A) $\quad \zeta^m_{m+1}$, θ^m_m

(B) $\quad \zeta^m_{m+1}$, θ^m_m , θ^m_{m+2}

(C) $\quad \zeta^m_{m+3}$, θ^m_{m+2}

This extreme truncation cannot provide realistic looking solutions, and clearly the solutions are not independent. For example, ζ^m_{m+1} and ζ^m_{m+3} both depend on θ^m_{m+2} through the thermal wind equation. However the inclusion of single vorticity modes precludes barotropic interactions, so that wave growth can only be baroclinic. Brown (1969) found barotropic instability processes could be of significance, particularly for long waves, when horizontal shear was included.

The parameters varied in the analysis apart from the basic current were the static stabilities $(\sigma = \frac{d\theta}{dp})$ defined at $666^2/3$ mb $(= \sigma_2)$ and $333^1/3$ mb $(= \sigma_4)$. The following values were considered, in $(^{\circ}\text{mb}^{-1})$

	(i)	(ii)	(iii)	(iv)
σ_2	.054	.047	.05	.05
σ_4	.085	.11	.06	.12

Case (i) represents values originally chosen for model 'M9'. (The

slightly different resolution requires σ to be defined at different levels in model 'M3'). Case (ii) is the values finally selected, and cases (iii) and (iv) were used to show the effect of changing the upper static stability. Only waves 2 to 10 were considered.

The cubic equation for c had very complicated coefficients and hence is not presented here. The solutions to the equation were found numerically using the IBM subroutine POLRT, which utilizes the Newton-Raphson iterative technique.

Fig. 7 (a), (b) presents growth rates for the basic state given in Fig. 6a, and Fig. 8 shows the growth rates for the basic state given in Fig. 6b. Curves are labelled A, B or C corresponding to the combination of modes labelled above. Whereas the disturbances have only integral wave numbers, results have been presented as continuous curves for more graphic representation.

Of interest is the second region of instability for the planetary scale waves (best depicted by case B), which corresponds to the extra region of instability first noted by Green (1960). Green found this long wave region of instability to contain very small growth rates, but he considered only waves of infinite N-S extent and used a β-plane. Thus his result may be better compared to Fig. 8 where the correspondence is greater. Since this model is formulated on a sphere, rather than on a β-plane, and β is very small close to the pole, the stabilizing effect of β is small at high latitudes. This may be the source of the greater growth rates found in the long wave region.
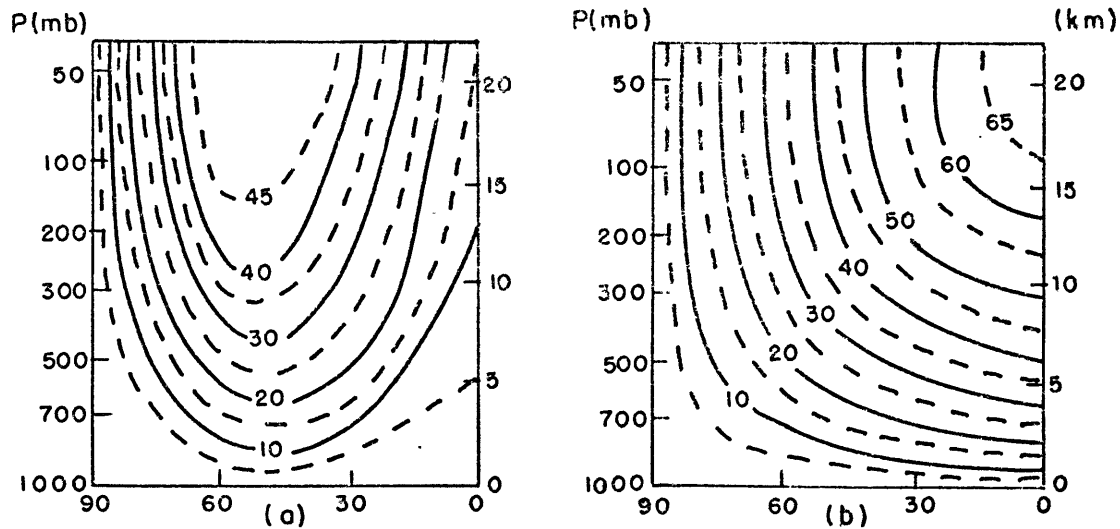
Fig. 6. Basic state velocity profiles used in baroclinic
growth studies (m sec^{1}).

We further note that wavelength is a function of latitude so that for

example wave 2 at 69° latitude has the same wavelength as wave 4 near

45° latitude. No second long wave region of instability was found for

case C.

A comparison of Fig. 8 with 7 (a) and (b) reveals the effect of

choosing a basic state with N-S shear. The presence of the added N-S

shear has destabilized the very short waves in all cases. In case (A)

and (B), the neutral wave has moved from wave 2-3 to wave 4-5 resulting

in a stabilizing of the moderately long waves 4,5,6. However the very

long wave 2 is also destabilized by N-S shear. In case C waves 2,3,4

are all stabilized by N-S shear. This effect is not to be confused with

the separate effects of barotropic growth or damping, which are not

present here.

The neutral wave separating the two regions of instability encom-

passes a number of wavelengths. This appears to be caused by the reduced

FIG. 7a

FIG. 7b
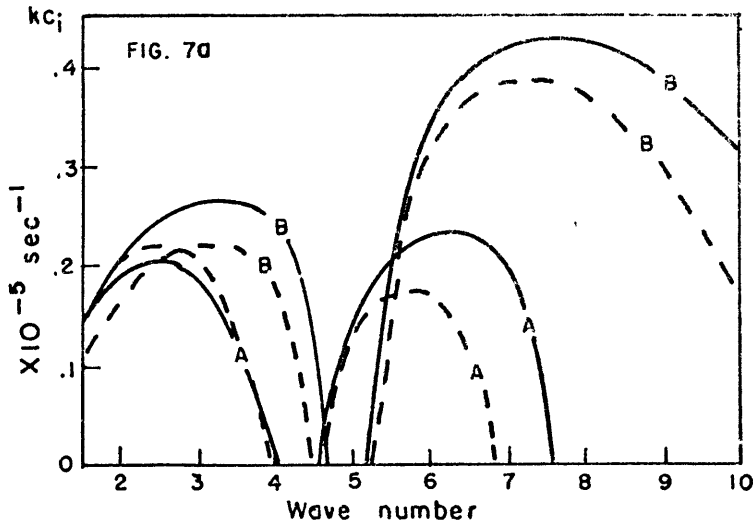
FIG. 8

Fig. 7 and 8

Baroclinic growth rates for modes.

A ζ^m_{m+1} , θ^m_m

B ζ^m_{m+1} , θ^m_m , θ^m_{m+2}

C ζ^m_{m+3} , θ^m_{m+2}

Fig. 7
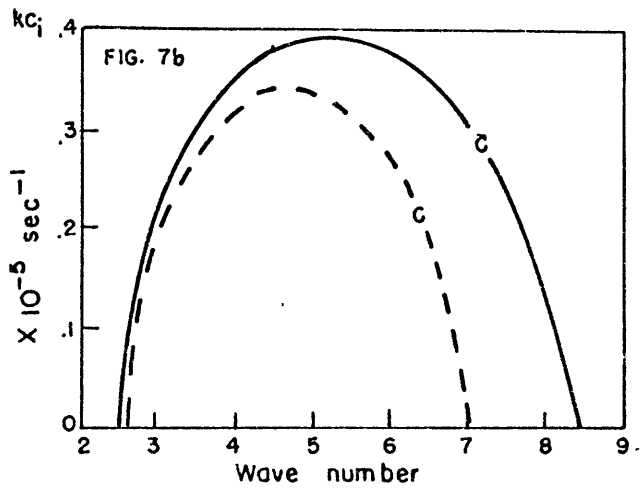
Growth rate vs wave number corresponding to the basic state in fig. 6a; and for static stabilities.

solid curve $\begin{cases} \bar{\sigma_2} = .047 \\ \bar{\sigma_4} = .11 \end{cases}$ %/mb

dashed curve $\begin{cases} \bar{\sigma_2} = .054 \\ \bar{\sigma_4} = .085 \end{cases}$ %/mb

Fig. 8

Growth rate vs wave number corresponding to the basic state in fig. 6b;

solid curve $\begin{cases} \bar{\sigma_2} = .05 \\ \bar{\sigma_4} = .12 \end{cases}$ %/mb

dashed curve $\begin{cases} \bar{\sigma_2} = .05 \\ \bar{\sigma_4} = .06 \end{cases}$ %/mb

number of degrees of freedom in the vertical, which is also the cause

of the short wave cut off, and strongly affects the short waves in

all cases.

In Fig. 9 (a), (b) and (c) are presented the phase speeds of the

neutral (N) and unstable (U) waves, for the cases A,B, and C, corres-
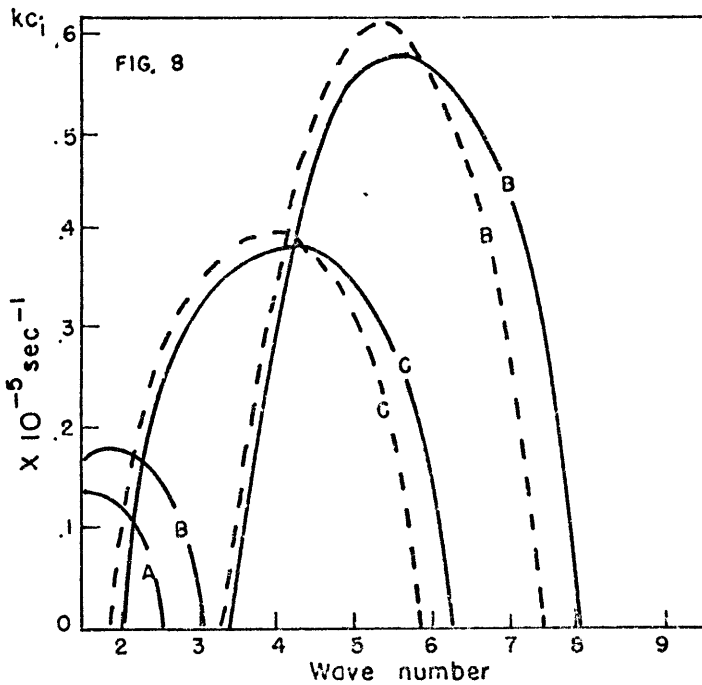
ponding to Figs. 7 and 8.

In the case where the solution to the cubic equation produces

only neutral waves, there are three phase speeds, one for each solution.

When a growing wave solution exists there is a coupled solution which

is damped at an equal but negative growth rate, and has the same phase

speed. Thus when an unstable solution exists only two values of phase

speed appear in Fig. 9, one for the neutral wave and one representing

the growing and damping waves.

In Fig. 9 (a) and (b) the neutral waves at short wavelengths

(large m) are progressive and the phase speeds vary little with m ,

whereas the long wavelength neutral waves are retrogressive and the

phase speeds increase greatly as m decreases. The phase speeds of

the unstable waves do not vary much with m . They are mostly pro-

gressive, travelling somewhat slower than the basic current. The short

unstable waves vary from about $-2 < c_r < 8$ ^{o} day^{-1}, while the long

unstable waves vary from $0 < c_r < 15$ ^{o} day^{-1}.

We note that in the neutral wave region separating the two

unstable sets of waves, one of the neutral waves is stationary.

Fig. 9a

Corresponding to solid curves
in fig. 7.

$\sigma_2 = .047 \quad \sigma_4 = .110$

Fig. 9b

Corresponding to dashed curves
in fig. 7

$\sigma_2 = .054, \sigma_4 = .085$

Fig. 9c

Corresponding to solid curve
in fig. 8.
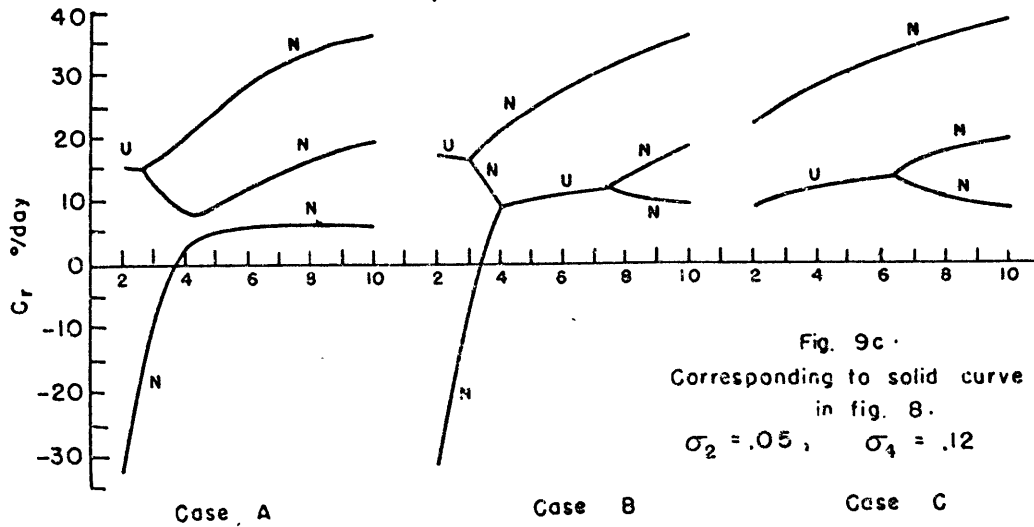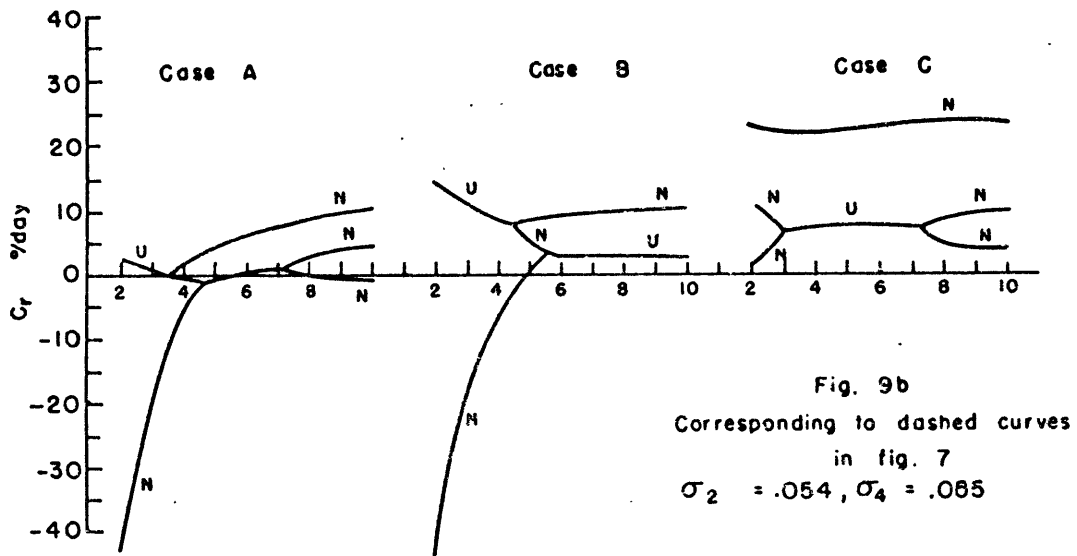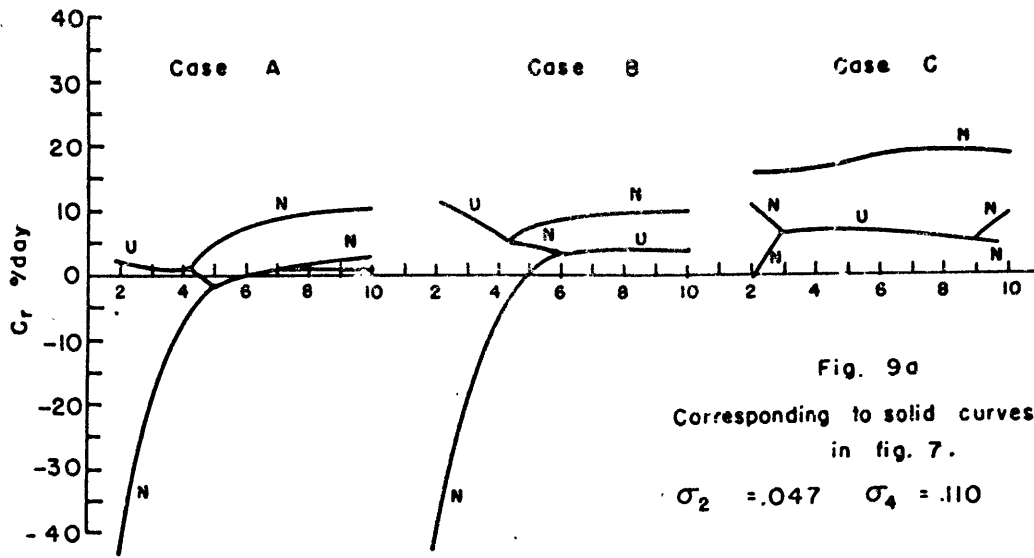
$\sigma_2 = .05, \quad \sigma_4 = .12$

Fig. 9. Phase speed of growing waves versus wavenumber.

Fig. 9 (c) reveals that the effect of increasing the westerlies in equatorial regions is to markedly increase the eastward component of the waves.

Examination of the individual modes in model 'M9' revealed nearly all the growth to be in ζ_7^4 and ζ_9^6, and the growth rate corresponded extremely well to that given in Fig. 7(b) for the original static stability values, (case (i)). This shows that wave 4 should indeed grow faster than wave 6. Mode ζ_7^6 grew slowly ($\sim .13 \times 10^{-5}$ sec^{-1}), while ζ_5^4 grew mainly by non-linear processes, showing fair agreement with Fig. 7(a).

As shown by the main region of instability in Fig. 8, an increase in σ_4 at 333 1/3 mb tends to destabilize the shorter waves and stabilize the long waves. This finding also applied to the other basic state considered (not presented here). Eady (1949) and Green (1960) found similar results when comparing the effect of a rigid top to a stratospheric layer over the baroclinic region.

A lower static stability at low levels destabilizes all waves. Thus the static stability values in case (ii) were chosen to produce a more realistic response, since the greatest effect is to destabilize the short waves considerably. Mode ζ_9^6 should now grow faster than ζ_7^4 in model 'M9', which proved to be the case.

Wave 6 is clearly a wave commonly regarded as 'baroclinic', whereas wave 2 is likely to have the different characteristics of very long waves. Wave 4 should be close to the transition point.

6.4 Model Response to the Introduction of Eddies: Day 0-40, no Nonzonal

  Forcing.

Perturbations in waves 4 and 6 were introduced at all tropospheric

levels into the zonally symmetric solution corresponding to October 1.

There was neither orography nor non-zonal heating included at this stage

which would distinguish each hemisphere, but for convenience we shall

refer to the spring hemisphere as south, and autumn hemisphere as north.

Both waves grew by baroclinic processes while interacting to pro-

duce a perturbation in wave 2. After day 7 wave 2 began to grow baro-

clinically and at day 11 waves 4 and 6 began to decay (see Figs. 12 and

13). Wave 2 also ceased to increase in amplitude in the troposphere but

continued to be strongly baroclinic in the sense that the process

$AZ \longrightarrow AE \longrightarrow KE$ continued at a much greater rate than KE was dissip-

ated. As a result, the increase in K2 (i.e. the kinetic energy in wave

2) occurred in the stratosphere and large quantities of energy were

propagated upwards.

By day 20 the wave energy had reached the uppermost level (0.05 mb)

and was trapped by the upper boundary. The vertically propagating energy

was accompanied by a polewards transport of heat and $AZ \longrightarrow AE$, which

induced meridional cells $KZ \longrightarrow AZ$, and a downward flux of geopotential

energy by the zonal flow. As a result the zonal westerlies weakened

considerably.

In the S.H. the trapping of the energy at the uppermost level

eventually resulted in the formation of easterlies at high latitudes

along with a reversal of the mean zonal temperature gradient, whereupon the process changed. This part of the atmosphere then responded in the manner of the lower stratospheric region of the atmosphere and was driven by the vertically propagating energy

$$V \phi E_{up} \longrightarrow KE \longrightarrow AE \longrightarrow AZ \longrightarrow KZ \longrightarrow V \phi Z_{Down}$$ which continued to

modify the zonal flow and brought about a sudden stratospheric warming type of phenomenon. The processes involved are discussed at greater length in Chapter 8.

The events considered above were predominant in the spring hemisphere, however similar processes were taking place in the autumn hemisphere to a lesser degree. A sudden warming did take place, but the appearance of easterlies in the zonal wind field occurred 5 days after their first appearance in the spring hemisphere and, of more significance, were centered at the 20 mb level. The warming intensified at this level subsequently having some effects at the 5 mb level but not above there, and hence this warming was neither induced nor affected by the upper boundary.

The spring warming was concentrated polewards of $40^{o}S$, and by day 29 had progressed down to the 20 mb level. The autumn warming was limited to high latitudes and was largely concentrated below about 20 mb throughout the lower stratosphere.

The situation on day 25 (Oct. 26) is presented in Fig. 10 (a) and (b). Fig. 10a may be compared to the corresponding figures when no eddies were present in Fig. 5. The most obvious change is the breakdown

KM
(APPROX)

(a)

← S   N →

← S   N →

← S   N →

P
(MB)

Streamlines
for selected
levels on
day 25.
(Oct. 26)

(b)

N
S

N
S

800MB — INTERVAL 0.5×10^{-7} m^2 sec^{-1}

200MB — INTERVAL 2.5×10^{-7} m^2 sec^{-i}

20MB — INTERVAL 4×10^{-7} m^2 sec^{-1}
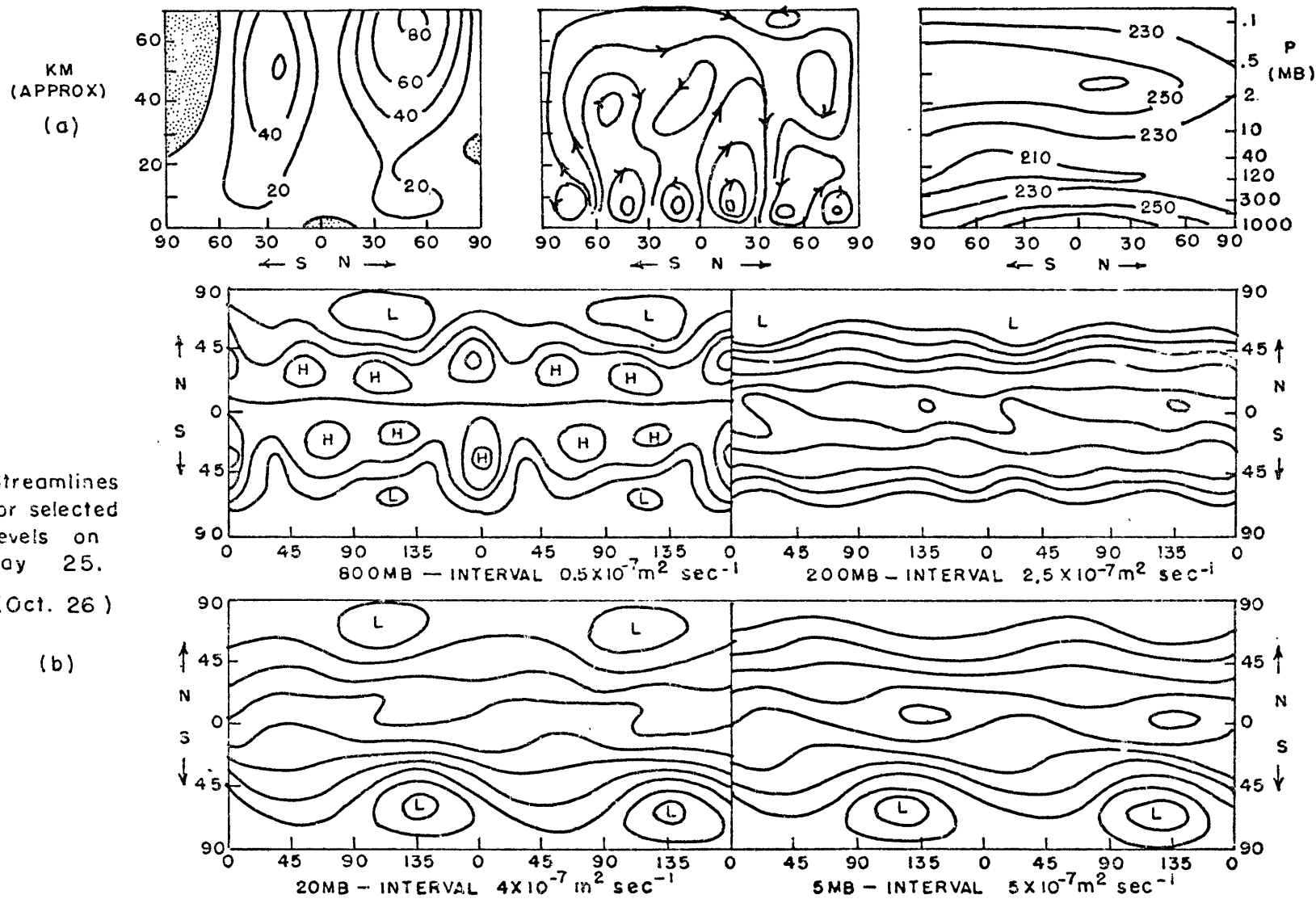
5MB — INTERVAL 5×10^{-7} m^2 sec^{-i}

Fig. 10a. As for Fig. 5; and Fig. 10b. Streamlines at selected levels as a function of latitude and longitude.

of the single Hadley cell in the troposphere of both hemispheres into
3-cell systems, and the appearance of a 2-cell system in each hemisphere
in the stratosphere along with the global pole to pole Hadley circula-
tion. The westerlies have been weakened in the N.H. and the easterlies
are more extensive in the S.H. Further discussion on the effects of
the eddies and on the sudden warmings will be pursued upon presentation
of the rest of the experiments.

Fig. 10b shows the streamlines at representative levels. As only
even wave numbers were included the pattern repeats itself after 180° of
longitude. The 800 mb and 200 mb levels reveal tropospheric flow
patterns. The 20 mb chart is similar to the 70 mb chart except for a
phase shift in the waves, and the levels 5 mb and above are similar.
The closed low pressure systems extend from 70 mb to the top of the model
(0.05 mb) in the S.H. with a westward slope with height. But a closed
low is present only at the 70 and 20 mb levels in the N.H.

A diagram which reveals further features of the vertical struc-
ture and movement of the waves is shown in Fig. 11. The movement of a
constant phase of each wave at 45° latitude in each hemisphere was
plotted at each level of the model at 3-day intervals from day 25 to 40.
The phase angle is arbitrary to the extent that it is plus or minus one
or more wavelengths. The exact relation of the phase at each level
relative to those above and below can best be determined by a complete
time series. The structure shown is representative of about polewards
of 35° latitude. At low latitudes it differed chiefly in the lower
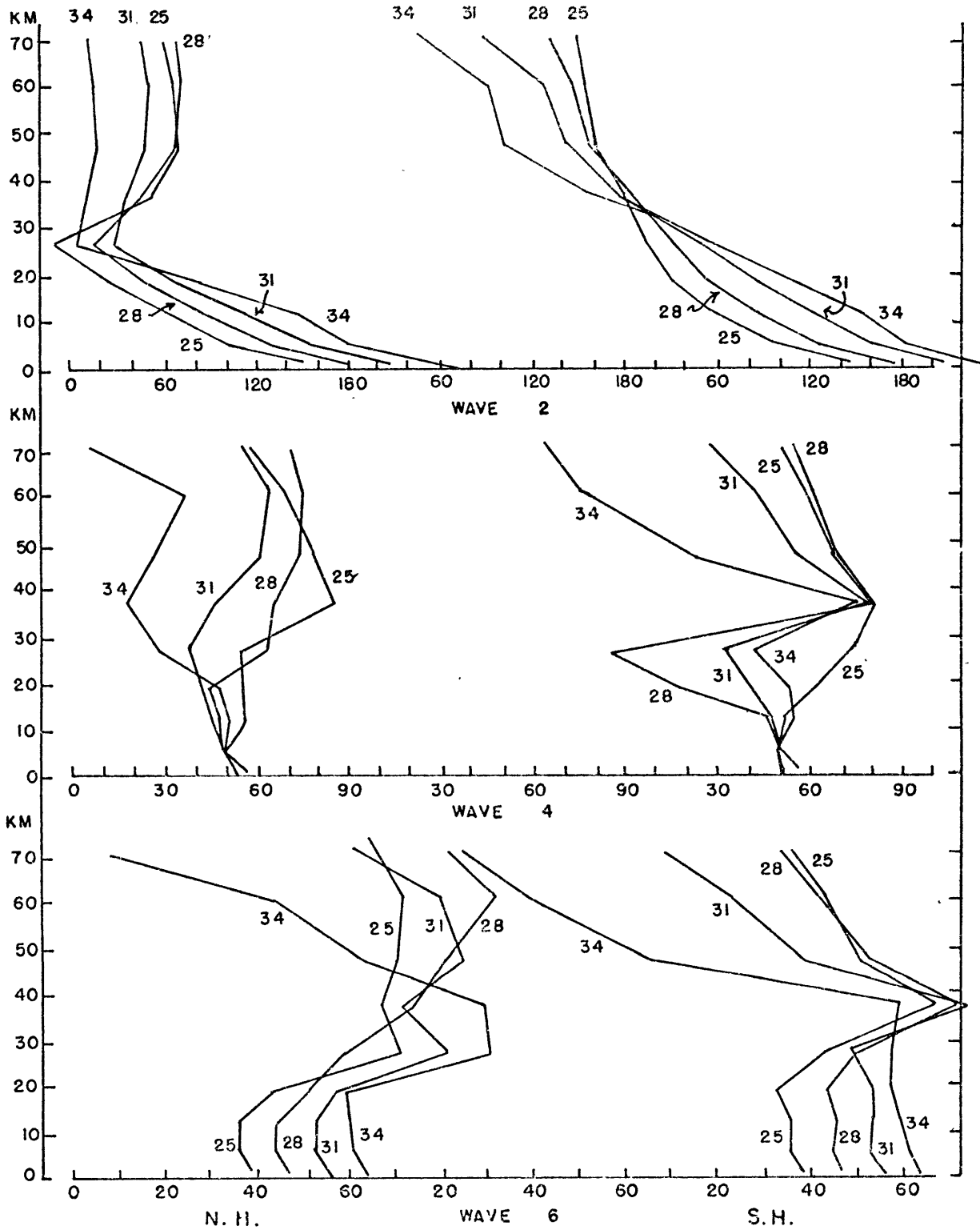stratosphere.

Fig. 11. The structure of waves 2, 4 and 6 at 45N (left) and
45S (right) at 3-day intervals.

Wave 2: In the troposphere this wave progressed at a mean speed of 9° day^{-1} in both hemispheres and sloped strongly westward with height.

Above 200 mb wave 2 reached peak amplitude on day 29 when the vertical flux of eddy geopotential energy diminished, and subsequently it began to move westward. By day 34 the top four levels were no longer connected to those below.

In the N.H. the wave did not reach peak amplitude till day 34 and was almost vertical throughout the upper stratosphere. The 20 mb level, where the high latitude easterlies became established, also separated the continually progressive motion below from the initially progressive, but by day 28 increasingly retrogressive motion above.

Wave 4: The behavior of wave 4 as a slightly baroclinic wave with almost no movement in the troposphere during this period, appears to be a characteristic of the model for this basic state. The linear baroclinic analysis gave such indications. The wave was unable to propagate far into the stratosphere and was formed at high levels chiefly through non-. linear interactions between different modes of wave 2. It remained small in amplitude and its movement, like that of wave 2, was first progressive then rapidly retrogressive.

Wave 6: This wave progressed regularly at about 3° day^{-1} in the troposphere. It was strongly baroclinic but the energy was trapped below about 70 mb. At high levels, it was formed chiefly through non-linear interactions of wave 4 with wave 2 and had very small amplitude.

Wave 2 moved about 3 times as fast as wave 6 in the troposphere, thus maintaining an almost constant phase relation throughout this period of integration, and the result was an added source of energy for wave 2 from non-linear interactions of wave 6 with the almost stationary wave 4.

All waves had roughly the same phase in each hemisphere in the troposphere, which is not unexpected at this time since the basic current and initial perturbation were fairly symmetric. This was not the case in the stratosphere, see Fig. 10.

The above discussion has been about the events triggered by the introduction of eddies into the troposphere of a model with a lower stratosphere unlike that observed. A rapid adjustment and change in structure of the atmosphere resulted. However apart from unrealistic way in which the events were triggered, the stratospheric adjustment was not unlike that observed during sudden warmings. To that extent it reinforces our assertion that an abrupt large scale change in the forcing of the stratosphere from below would produce such changes.

CHAPTER VII

RESULTS

Whenever such a simple model as ours is used to investigate a complicated dynamical system, the capability of duplicating a given phenomenon does not necessarily imply the correctness of the model in describing the responsible mechanism of the real phenomenon. In order to ascertain the validity of any results, we therefore consider the performance of the model in explaining related phenomena. Thus we shall first compare the features of the model circulation with those observed.

In this chapter points of agreement and deficiencies in the model will be brought out. The likely causes of the deficiencies will be deduced and the suitability of the model for our experiments ascertained. We shall be primarily concerned with average features of the circulation, and the details of daily variations and how the experiments apply to our central theme will be delayed to chapter 8.

7.1 Southern Hemisphere Winter Simulation: No Non-Zonal Forcing, Ex. A.

In the first run all non-zonal forcing was excluded so that the winter hemisphere should more closely resemble a S.H. winter. However, in the discussion we shall continue to refer to the winter hemisphere as North.
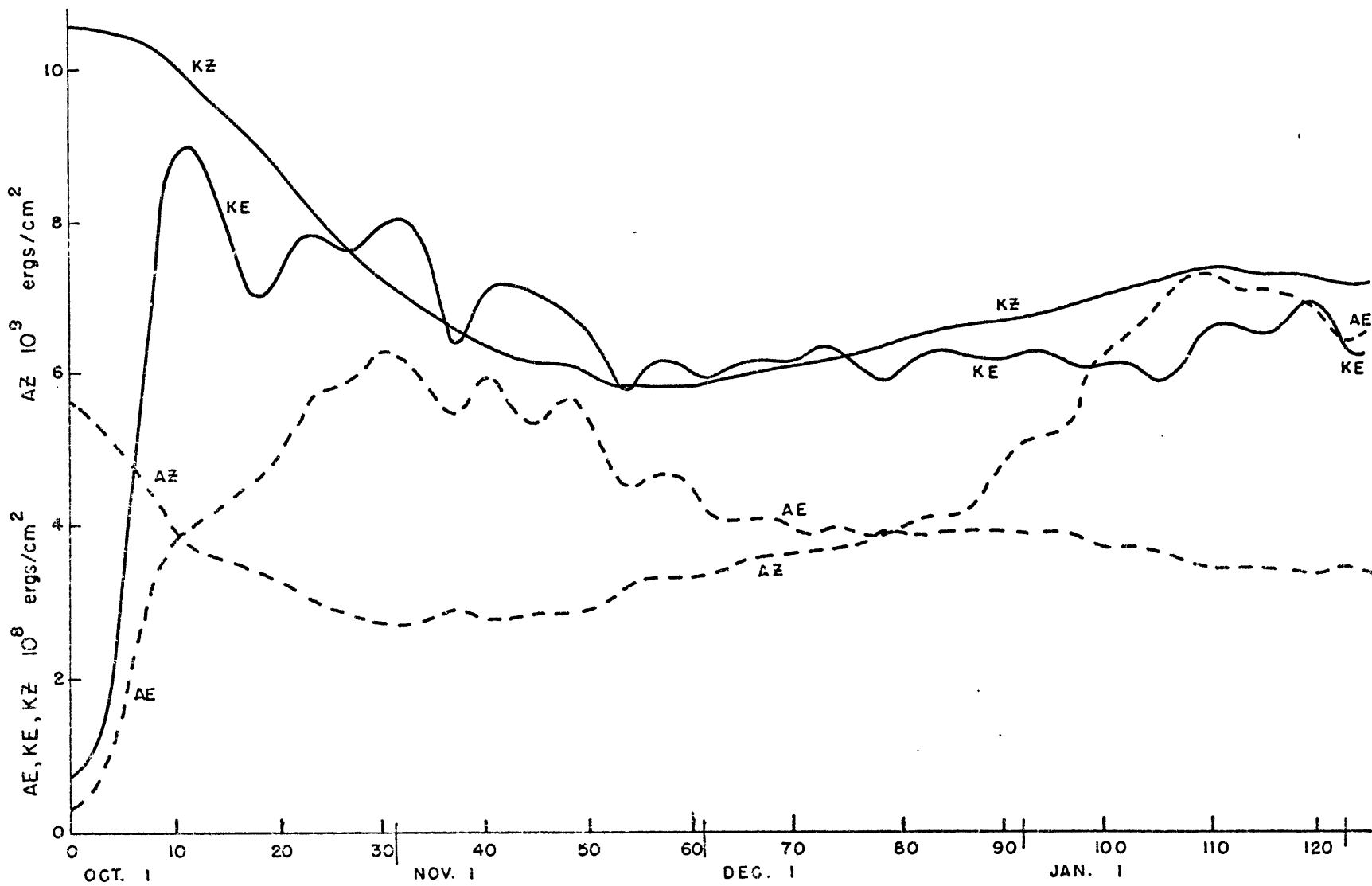
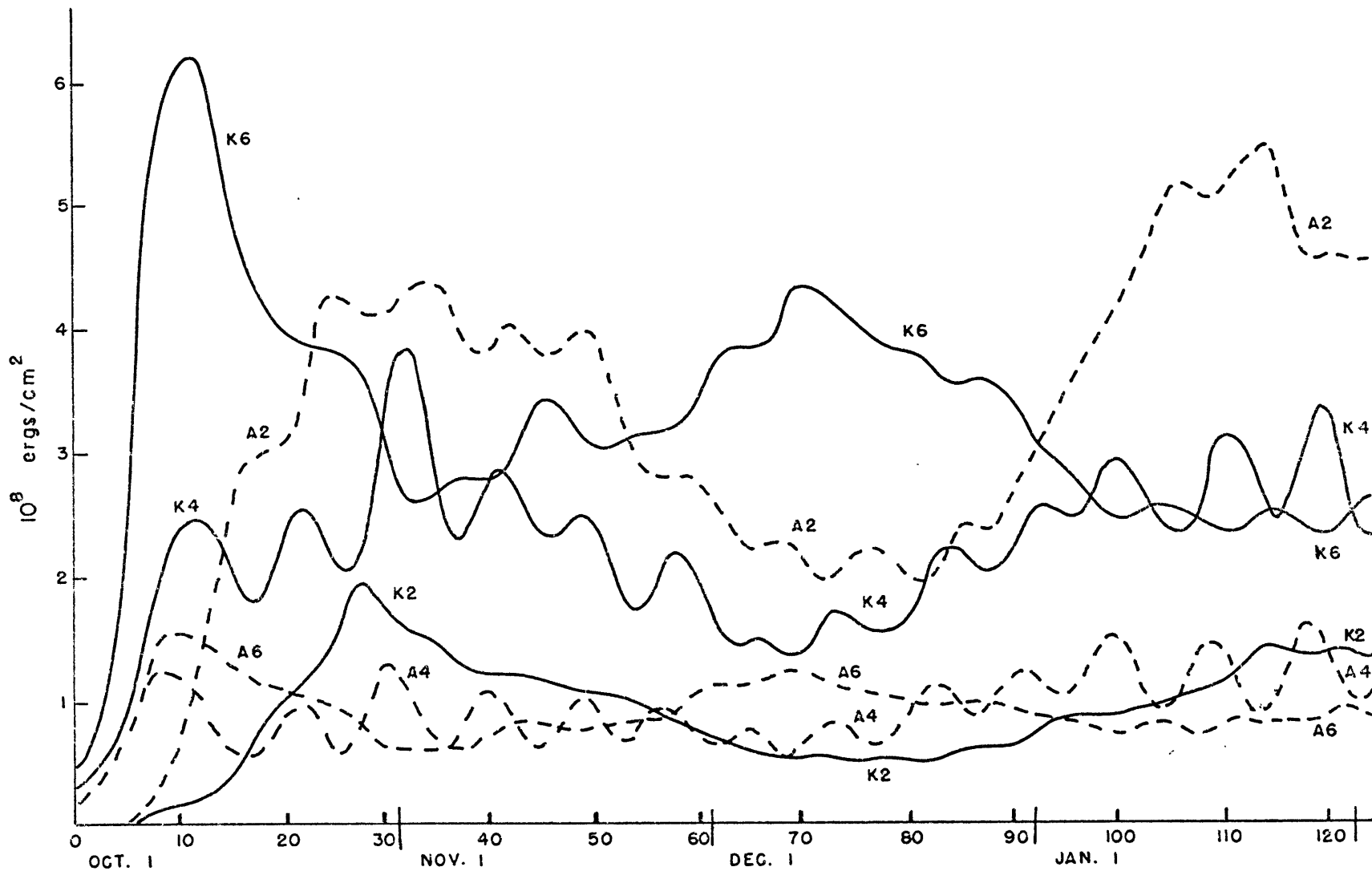Fig. 12. Daily variation of vertical integral of global forms of energy in Ex. A.

Fig. 13. As for Fig. 12 but for the eddy components in waves 2,4 and 6.

In Fig. 12, time series of the vertically integrated global forms of the zonal and eddy energy are presented. Figure 13 shows the breakdown of the eddy terms into wave numbers. These diagrams indicate that it is not until at least day 50 that the model can be said to have become adjusted to the eddies and approaching a statistically steady state with a seasonal trend superposed.

7.1.1 Zonally Averaged Fields

Fig. 14 shows the zonal temperature and wind fields and meridional cell streamlines at monthly intervals for the dates shown at left. These dates are the same as those for the similar presentation without eddies in Fig. 5. The zonal wind and temperature fields do not change very rapidly and daily values are representative of the monthly means. The meridional circulation is more subject to shorter period changes and thus 5 day mean values are presented. The principal features are evident from these diagrams.

Zonal Wind Field.

The strength of the model tropospheric jet in both hemispheres is in excellent agreement with observations given by Newell et al. (1970). These values differ somewhat from the idealized values given in Fig. 1. The latitude of the model tropospheric jets and their seasonal variation is also remarkably good for such a simple modeling.

Easterlies are present in the model troposphere tropics at 800 mb but are absent above there. This extension of the winter westerlies into equatorial regions at most levels above 800 mb is a feature of
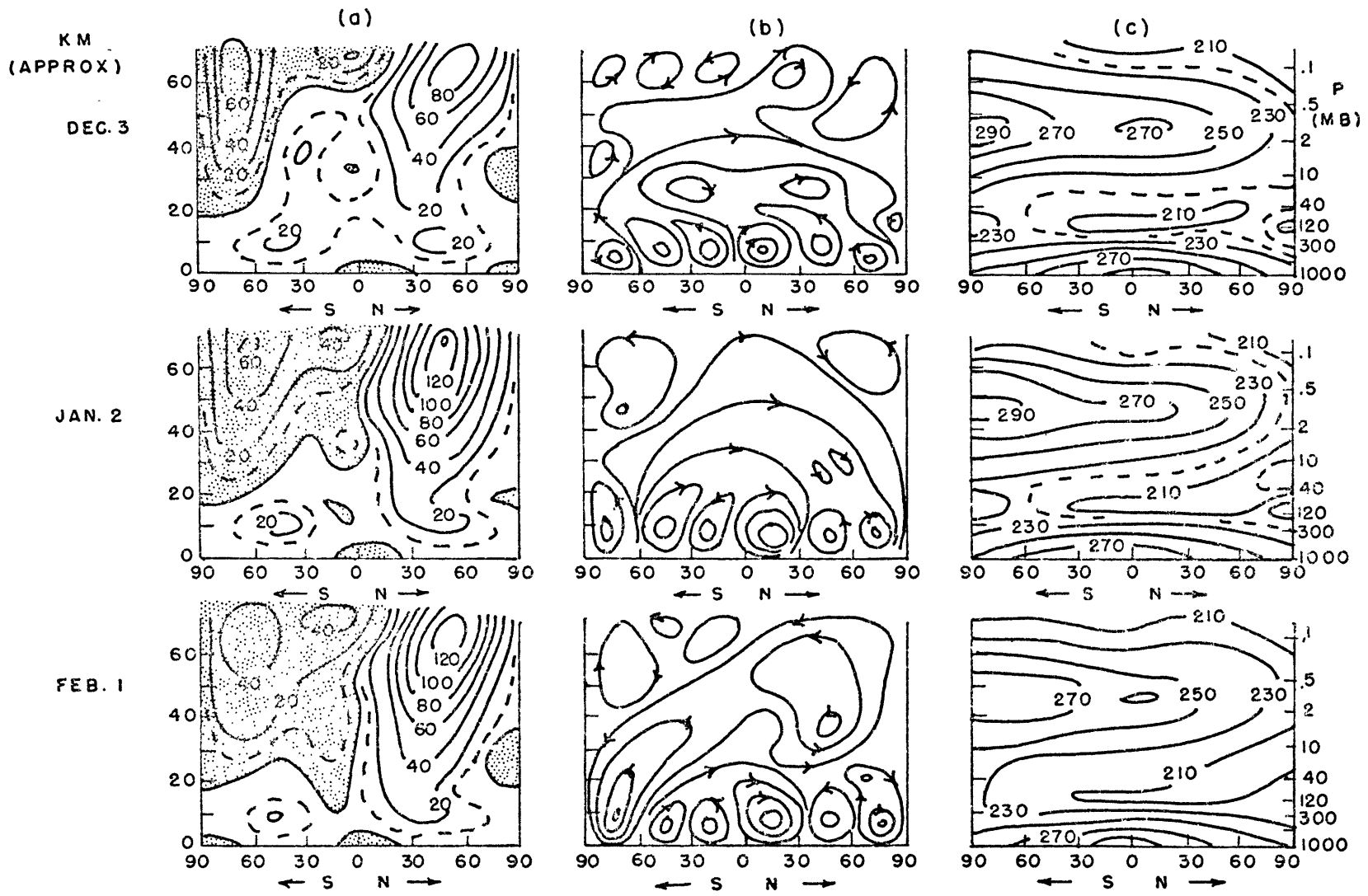
Fig. 14.   (a) Zonal wind (m sec^{-1})   (b) Schematic meridional   (c) Zonal temperature
Ex. A   Easterlies are shaded   wind streamlines   (^{0}K)

the model that is not observed. A single maximum of easterly winds is present at the lowest level where the Hadley cells in each hemisphere converge. In reality the doldrum region exists there with the trade winds forming a double maximum on either side.

The general pattern of the model upper atmospheric winds is in general agreement with the observed. The secondary easterly maximum at 70 km in low latitudes is not observed, but excellent agreement exists with the location and strength of the primary easterly maximum. However, at lower levels the maximum observed easterlies extend into low to mid-latitudes, whereas the model maintained strong easterlies at high latitudes.

The location of the westerly jet maximum was at either .2 or .05 mb (60 to 70 km) in good agreement with that observed. The maximum winds of 140 m sec^{-1}, although more realistic than the 180 m sec^{-1} in the no-eddy run (Fig. 5), are still too strong. In fact the strength of the westerlies throughout the N.H. stratosphere is slightly greater than that of the observed mean winds. The westerly wind maximum extends down into the lower stratosphere at lower latitudes than observed and has a tendency to be connected to the tropospheric jet.

Hence the wind field and its seasonal variation has been rather well simulated overall, and main discrepancies present are: i) in the lower stratosphere, where the summer easterlies and winter westerlies are not at the observed latitudes; ii) the presence of westerlies over the equator; and iii) stratospheric westerlies which are too strong.

Zonal Temperature Field

Since the temperature field is related to the wind field through the thermal wind equation, the degree to which each resembles the observed field should be similar. Thus we also find a pleasing agreement in most respects between the simulated temperature field and the observed, see Fig. 1 and Newell et al., (1970).

At 600 mb, the model temperature gradient between equator to pole was 50°K in winter and 30°K in summer. As values representative of the lower troposphere they compare favorably with the observed. When compared to the symmetric circulation run in Fig. 5, we find the temperature gradients to have been reduced by about 5°K. The means by which this was accomplished was in poleward heat transports by the large scale eddies, plus a contribution due to the direct meridional cells. The intensity of the latter were enhanced by the baroclinic eddies.

The most notable discrepancies in the model temperature field are apparent in the lower stratosphere. The tropical tropopause is not as cold and intense as observed. The increasing temperatures toward the pole are correctly simulated in the summer lower stratosphere, but the same pattern is also seen in the winter hemisphere. In the atmosphere a mid-latitude temperature maximum is found in winter.

The Meridional Circulation

The seasonal mean meridional circulation has been evaluated for the lower atmosphere by Newell et al., (1970), and will be compared with the model.

The 3-cell tropospheric circulation was present throughout the experiment and showed the dominance of a direct cell extending across the equator from the winter hemisphere. The latitude where the rising motion reached a maximum was near 10°S with subsidence in the subtropics. These features resemble the observed pattern remarkably well.

The strength of the rising motion in the convergence region averaged about 19×10^{-5} mb sec^{-1} at 600 mb, which is more than twice the value found for the symmetric run (Fig. 5).

The Ferrel cell in mid-latitudes of both hemispheres seems weaker, and the high latitude direct cell stronger, than observed, (the intensities were not computed). These features are particularly noticeable in the lower stratosphere where a two-cell circulation in each hemisphere should be formed from the extension of the low latitude Hadley cell and the mid-latitude Ferrel cell to higher levels, (e.g. Manabe and Hunt, 1968; Holloway and Manabe, 1971). This did occur at times in the model when the eddies were particularly strong, e.g. see Fig. 10a.

In the upper atmosphere the meridional circulation tends to be a global Hadley cell, although variations did exist. The beginning of the reversal of this cell can be seen in Fig. 14 on January 2. Although the heating field begins to reverse at this time, the change was primarily due to the eddies, as may be seen by comparing the meridional circulation for February 2 with the corresponding date in Fig. 5.

Newell (1968) has speculated on the meridional motions in the upper atmosphere. By neglecting the effects of eddies in a steady state

solution, Newell deduced rising motions to be present in the summer

hemisphere at 50 km, accompanied by equatorward drifts of 3-5 cm sec^{-1}.

In the model, the presence of eddies produced daily changes in the

Hadley cell, so that the 5-day mean values were somewhat weaker than the

daily values. In Table 3, the meridional velocity is given at each level

in the upper stratosphere, for summer, at 0, 30, 60 S, for the 5 day

period centered on January 2. Positive values are northward.

Approx. Height (km)	P (mb)	Latitude			
		60	30	0	S
71	.05	-7	-0	15	
61	.2	+1	1	5	
48	1	-2	4	9	
36	5	+6	5	11	
26	20	+0	9	12	

Table 3. Zonal average of the northward merid-
ional velocity (cm sec^{-1}) for summer
hemisphere.

The zonally averaged vertical motion accompanying these values

at 2 mb (43 km), was greatest in mid-latitudes of about -10^{-7} mb sec^{-1}

(roughly .4 mm sec^{-1}). At .5 mb (53 km) the maximum was in low latitudes

of about -1 to 2×10^{-8} mb sec^{-1} (about .3 mm sec^{-1}).

These values are of the same order as those deduced by Newell.

They are also similar to those in our solution without eddies for this

date, but are much lower than the values found by Leovy (1964); see the

discussion in Section 6.2.

7.1.2 Energy Budget

Fig. 15 (a) and (b) shows the 4-box diagrams for the (i) troposphere (1000-200 mb), (ii) lower stratosphere (200-20 mb), and (iii) upper stratosphere (above 20 mb), where the meaning of the diagram is explained in Fig. 4 and Section 5.4. The global, as well as N.H. (winter), and S.H. (summer) energetics are shown for the months of December (Fig. 15a) and January (Fig. 15b). Energy values are 10^5 ergs cm^{-2} and conversions ergs cm^{-2} sec^{-1}.

All calculations were checked by comparing the net contribution of the conversion terms to each box with the measured change in each energy component. In experiments B, C and D, the energetics calculations were made once each day and the agreement in the above check procedure was excellent. In this experiment, the hemispheric energetics were computed with a two-day sampling interval. The agreement between the calculated and measured change was still good, but included some small sampling errors.

We shall compare the values in Fig. 15 with estimates for the atmosphere and other numerical models. The best estimates currently available are those by Newell et al. (1970), who have computed global, N.H. and S.H. values for the 1000-100 mb layer.

The Troposphere: Ex. A.

Allowance must be made for the 200-100 mb layer and other differences in the regions considered. When this is done, agreement between the values of AZ, KZ, and KE, in both the hemispheres with the observed

GLOBAL

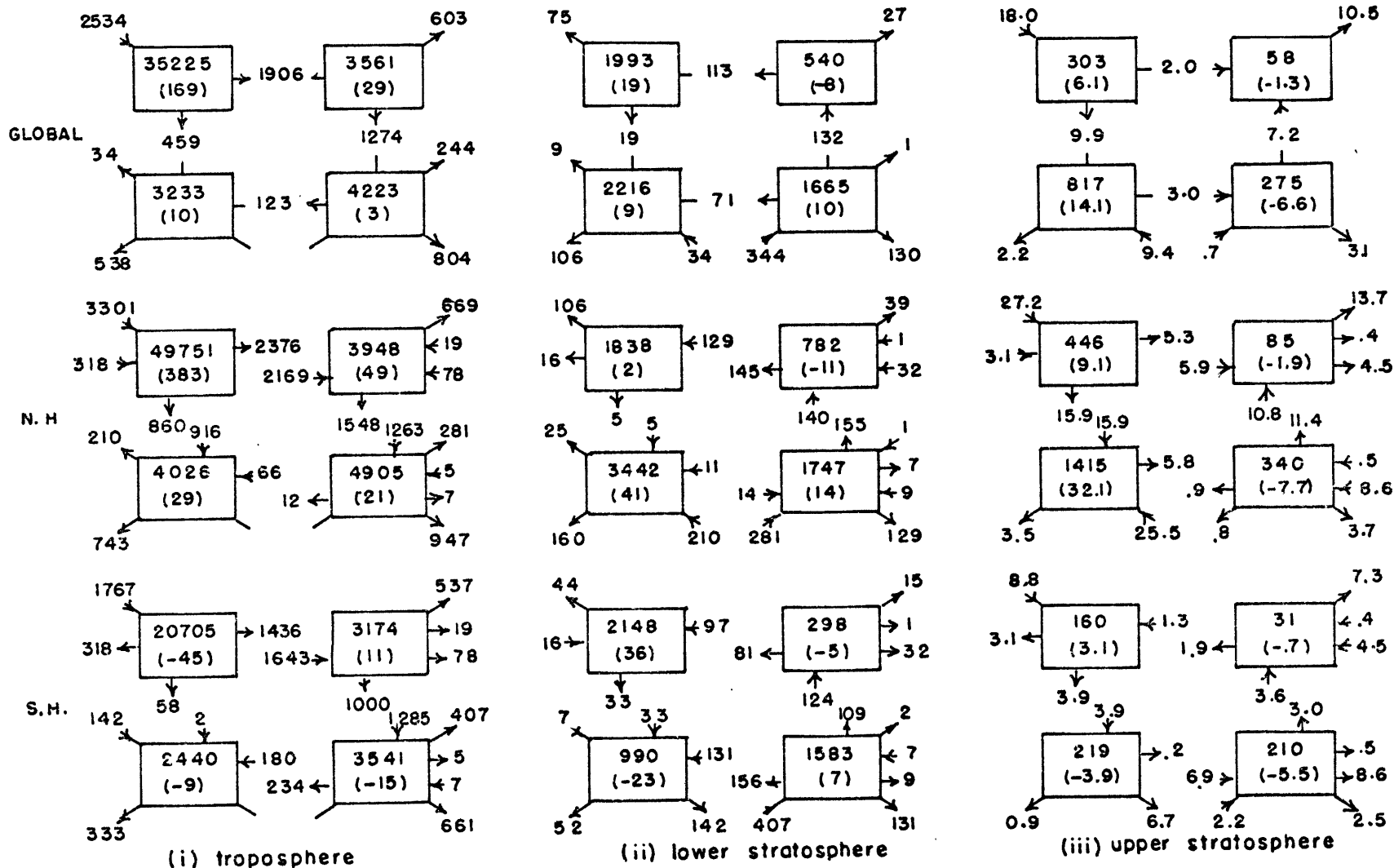(i) troposphere (ii) lower stratosphere (iii) upper stratosphere

N. H

S.H.

Fig. 15a. Energetics for December in Ex. A. Energy values are 10^5 ergs cm^{-2}, and conversions ergs cm^{-2} sec^{-1}.
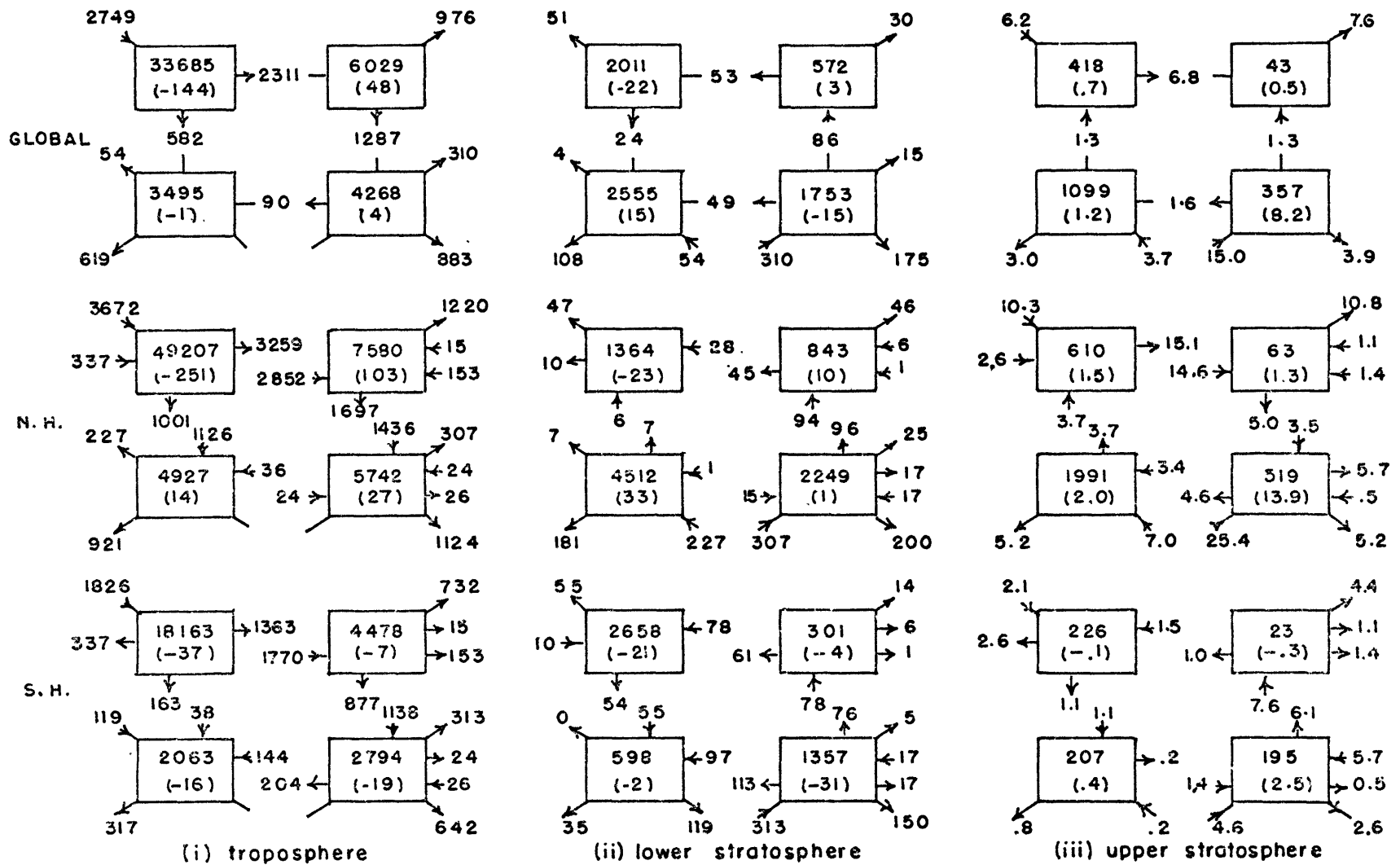
Fig. 15b. Energetics for January in Ex. A.

is extremely good. The ratio of KE to KZ is close to unity, as may also be seen in Fig. 12. This observed feature of the atmosphere has been sadly lacking in the more sophisticated primitive equation models (e.g. Manabe et al., 1970).

The value of AE has not been determined by Newell's group. Oort (1964b) finds AE to be about twice the value of KE and KZ. Our model values are similar to those found in the G.F.D.L. models which exclude nonzonal effects, (Manabe et al., 1970). This value is probably too low. It is most likely due to the lack of waves 1 and 3 in the model, which along with wave 2 contain most of the AE in the atmosphere. Fig. 13 clearly indicates how the ratio of AE to KE changes with wave number. It also shows a marked increase in A2 going into January which is reflected in the monthly values in Fig. 15. The lack of nonzonal forcing in this experiment with the model is most likely a factor, but this will be remedied in later experiments.

The uncertainty in the conversion terms for the atmosphere is apparent from the wide range of values present in the literature. Further confusing the issue is the natural variability of the atmosphere itself. We find the model to compare very favorably in all but three conversions. The conversion CZ (AZ ——→ KZ) is too large in the model in winter indicating the dominance of the direct cells in the meridional circulation. This is partly due to truncation as noted in Section 7.1.4. As a result of this source of KZ, the conversion CK is somewhat lower than observed in the winter hemisphere.

GE has the opposite sign in the model from that observed. Since there was no nonzonal heating in this experiment, GE could act only as a sink to AE. This feature is also present in the G.F.D.L. dry models, where the hydrologic cycle is omitted, (e.g. Manabe et al., 1970). The inclusion of nonzonal heating should decrease this dissipation of AE. However, without water vapor in the model, we cannot obtain the gain in AE in transient cyclone scale waves due to condensation east of the trough, as described by Manabe et al., (1970).

The intensity of the energetics is indicated by the total production of A, total dissipation of K, or the conversion between them (CZ + CE). In a long term average these should all be equal. In January, in the N.H., there was a marked increase in the intensity of the tropospheric circulation. As may be seen from Fig. 13 this was largely brought about by wave 2. The very large increase in AE which resulted was accompanied by a decrease in AZ so that there was a maximum AZ in December. This kind of response has also been noted in the atmosphere by Krueger et al. (1965) who found a double maximum of AZ in December and March to be normal.

The increased intensity resulted in an increased eddy flux of energy into the lower stratosphere and particularly into the upper stratosphere.

We conclude that the simulation of the tropospheric circulation in both summer and winter hemispheres has been very successful.

The Lower Stratosphere

The model lower stratosphere energetics of both summer and winter hemispheres are similar in overall characteristics and resemble those of Manabe and Hunt (1968). The circulation is driven from below by the vertical eddy flux of geopotential.

Dopplick (1971) has recently calculated monthly values of the atmospheric energetics for 1964 for the 100-10 mb layer, 90°N to 20°N. This and other energetics studies (see Section 2.2) reveal the baroclinic nature of the winter lower stratosphere, which is not apparent in the model. This point was mentioned in the previous section as a deficiency of the model simulation of the temperature field. However we note that Manabe and Hunt (1968) correctly simulated the winter temperature field of the lower stratosphere, but the directions of the energy conversions in their model are the same as those in Fig. 15. This indicates the importance of the $0-20^\circ$N region which was omitted in Dopplick's study.

The zonal flux of geopotential ,$(v\Phi z)$, was in the observed direction in the winter hemisphere but is in the opposite direction to Dopplick's values in summer. A detailed comparison is hampered by the lack of the region $0-20^\circ$N in Dopplick's calculations.

The model conversion CK is small in winter (as it is in the troposphere), but large in the summer hemisphere, whereas the reverse seems true in the atmosphere. Newell et al. (1970) related the modulations in CK to those of the vertical eddy flux of geopotential. We note that this appears to be true here.

The model lower stratosphere energetics resembles the pattern now regarded as typical of the region, but is in error at high latitudes in winter.

The Upper Stratosphere

The upper stratosphere is considered distinct from the lower stratosphere because of the different nature of the energetics. It is a region where the summer and winter circulations are no longer alike in any respect. In winter there is an in situ source of energy from GZ, and baroclinic conversion terms CA and CE may become positive in the westerlies. GZ is also positive in summer, but the easterlies are quite steady and the conversion CZ should maintain the kinetic energy, see for example Newell (1968).

In our model, the differences between the months of December and January are quite large, especially in the winter hemisphere. The difference is also apparent in Fig. 14.

The Upper Stratosphere in Winter

In December, the Hadley cell driven by the heating field was the dominant part of the energetics, so that the symmetric part of the flow prevailed. KZ increased throughout the month to reach a seasonal peak. In January, GZ was negative above 5 mb and the reversal in the meridional circulation produced a source of AZ through the conversion CZ. The changes were stimulated by the increased eddy flux of energy into the region from below. As a result CA, CE and CK all became positive. However the changes in AE and KE were not particularly great although

the change in the energy cycle was pronounced. This seems to be a feature of the effects of transient wave vertical propagation of energy and will be considered further in chapter 8. The change in the energetics of the region was associated with the sharp increase in wave 2 energy in the troposphere that we noted earlier, see Fig. 13, and it was largely a coincidence that the change occurred at about the time of the solstice.

The energetics of the upper stratosphere in the model of Manabe and Hunt (1968) is qualitatively similar to that of our January simulation of the winter hemisphere.

The Mesosphere in Winter

Included within the upper stratosphere as we have defined it, is the region above 60 km which is actually part of the mesosphere. Newell (1968) discussed the energetics of this region distinct from the layer below. Using a diagnostic approach he deduced the region to be one of forced motions somewhat analogous to the lower stratosphere. The forcing could either originate from the baroclinic waves generated in situ in the 25-60 km region, or from leakage of the vertically propagating energy from the troposphere.

In our model, the top layer did indeed behave in this manner, although was most likely affected to some degree by the upper boundary. Unlike all layers below, GZ was negative for both months. The details of the energetics of this layer, (from .2 mb (61 km) to the top of the model), are shown in Fig. 16. The values of AZ, AE and KE changed little

GZ = .25   GE = .55

BAZ = .05 ← [AZ .8]   [AE 1.2] ← .15
                                        CA

CZ = .15   CE = .7

[KZ 81] .8 ← [KE 4.7]
         CK

DZ = .01   VφZ = .2   VφE = 1.7   DE = .01
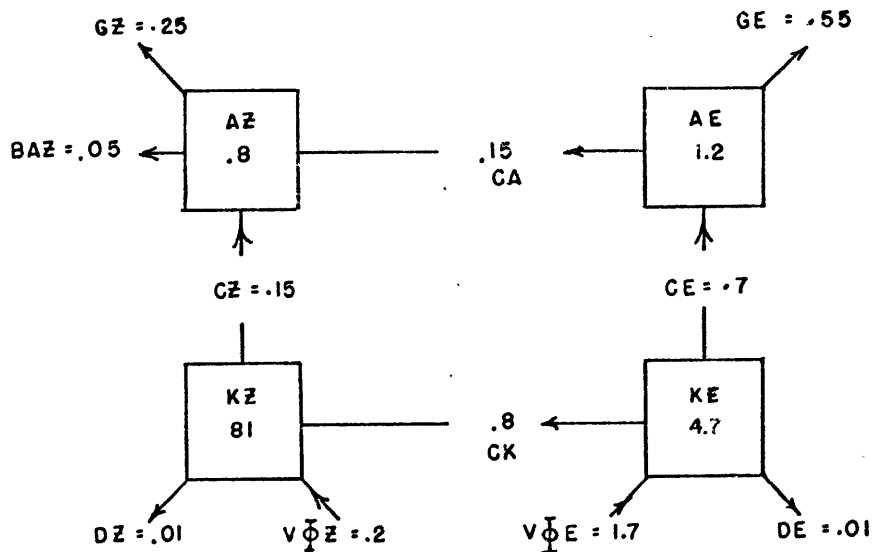
Fig. 16. Energetics for layer above .2 mb (61 km),
mean for December and January for the N.H.
Energy values 10^5 ergs cm^{-2}, conversions
ergs cm^{-2} sec^{-1}.

throughout the period, but KZ increased to a peak in mid January and

showed a net gain for the period of nearly 1 ergs cm^{-2} sec^{-1}.

The horizontal boundary terms at the equator were small and are

not shown except for BAZ. The conversion terms are average values,

(e.g. CK = $\frac{1}{2}$(CKE + CKZ)), and are accurate to $\pm$ .1 ergs cm^{-2} sec^{-1}.

As may be seen from this figure, the energetics are similar to

that of the lower stratospheric region and are driven from below by the

vertical flux of eddy geopotential energy. Throughout the period the

highest temperatures in the N.H. at .1 mb ($\sim$ 66 km) were in mid-latitudes

near 45°N. Thus the structure of this region, with cold temperatures at

the equator and polar regions, and a mid-latitude maximum, is like that

observed for the winter lower stratosphere (but not present in the model

lower stratosphere), see Fig. 14.

The Upper Stratosphere in Summer

In the summer upper stratosphere, energetics conversions are small in comparison and seem reasonable. However, since the model easterlies were less extensive than observed, the energetics are not completely representative of an easterly regime. Thus the horizontal boundary fluxes into the region are taking place mostly in westerlies at the equator, and the vertical fluxes are occurring in the low-mid latitude westerlies at 20 mb.

Newell (1965) speculated that a source of energy for the summer upper stratosphere may be required since GZ is small and the vertical flux of energy would be absorbed in the lower stratosphere. He concluded that this energy might be derived from the winter hemisphere.

As is apparent from Fig. 15, the month of December was dominated by the symmetric terms driven by the differential heating in the region. In January this forcing was no longer effective and GZ became negative at the higher levels. All conversions were small but the increase in the importance of the eddies is evident.

However it is not very clear what the mechanism and source of this energy is. A more detailed analysis, (not presented here), shows the mean $\overline{v\Phi}$ to be positive in the S.H. at .5 mb and .1 mb. Time series of the daily fluctuations in this vertical flux are more revealing. There is a very good correlation between the direction of this quantity

in each hemisphere, although the N.H. values are considerably larger.
Thus it is possible that the limited degrees of freedom in the model
may well be providing a spurious source of energy in the S.H. in the
manner discussed in Chapter 5.

The horizontal boundary fluxes of energy do not seem to be of
importance in the model, but the issue is clouded since eddy motions
may have been induced in the S.H. by the more vigorous motions in the
N.H. winter circulation through unrealistic restraints imposed upon the
motions by truncation.

Interhemispheric Exchanges

If we now consider the boundary fluxes at the equator and differ-
ences in conversions such as CAE and CAZ (see Section 5.4), we find the
interhemispheric exchange of energy. Table 4 shows this change in
AZ + AE + KZ + KE, for the winter hemisphere, for December and January,
in ergs cm^{-2} sec^{-1}.

	Troposphere	Lower Stratosphere	Upper Stratosphere
Dec.	-79	+13	+.6
Jan.	+20	-7	-3.3

Table 4. Gain in energy by N.H. in ergs cm^{-2} sec^{-1} through
interhemispheric exchange.

These values are small compared to the other conversions and the
changing sign of the exchange in each month seems to indicate that the
transport is not significant. A possible exception is the effect on
the summer upper stratosphere as already discussed.

Certain terms are large and consistently in one direction, but are balanced by other terms. For example, in the troposphere for both months, considering AZ contributions, we find that BAZ is large and positive into the N.H. and is supported by the difference between CZA and CZK, but the contribution is cancelled to a large degree by the difference between CAZ and CAE.

Most energetics studies of the troposphere have ignored boundary fluxes of energy. Dopplick (1971) showed them to be small in the lower stratosphere. Our model also shows most of these terms to be small, or to be cancelled by another term of similar nature. As the energetics of the troposphere and lower stratosphere in each hemisphere are of the same order, it is expected that there is no large systematic interhemispheric exchange caused by a lack of degrees of freedom, as may be present in the upper stratosphere.

7.1.3 Angular Momentum Budget

As shown in Section 5.5, the reasons for the changes in the angular momentum of the atmosphere may be evaluated. Fig. 17 shows the net change for a vertical column averaged around a latitude circle as a function of the sine of the latitude. This represents the net balance due to contributions by the surface friction mechanism, and by the redistribution of angular momentum by the eddies. The contribution due to the horizontal diffusion has been included with the surface friction, and is very small. Values are in 10^7 gm sec^{-2}.

DECEMBER

changes due to
--- eddies
...... friction, etc
—— net

JANUARY

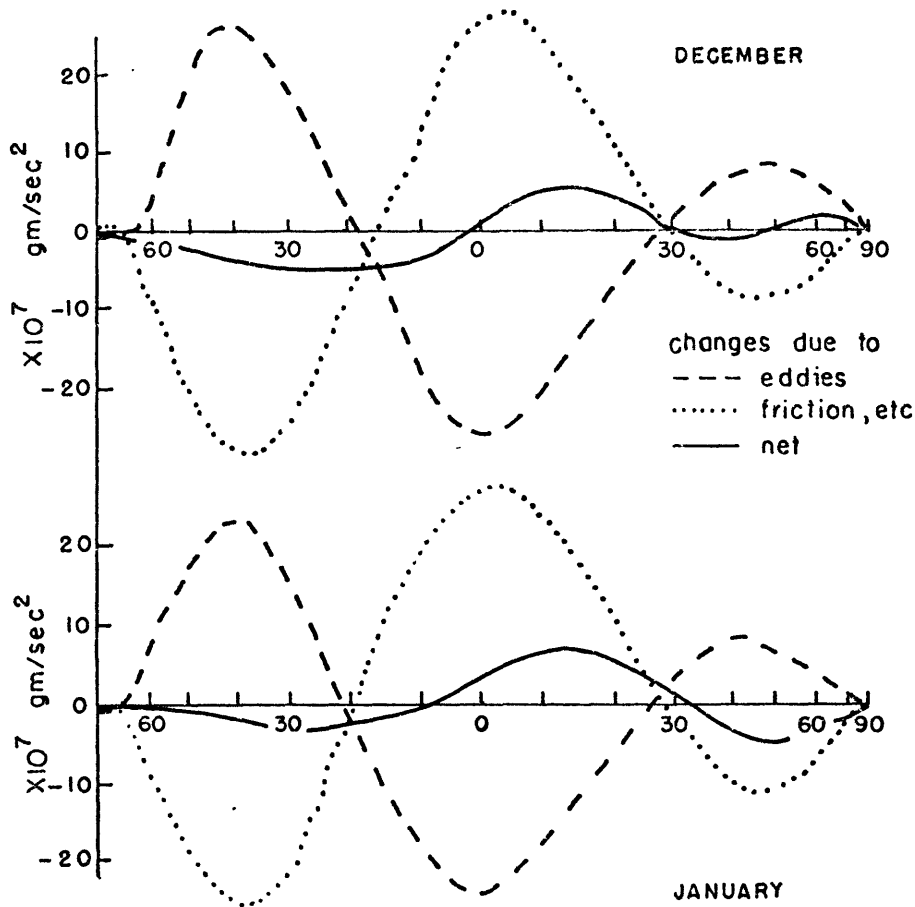Fig. 17.

Angular
Momentum
Budget
$(10^7 \frac{gm}{sec^2})$

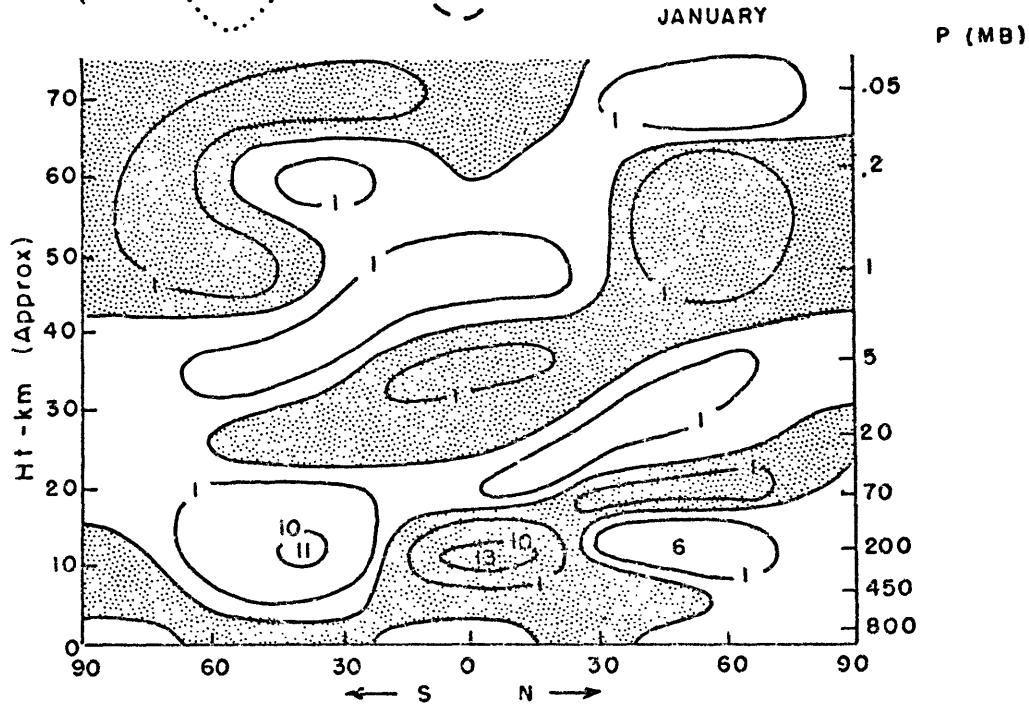

Fig. 18. Angular momentum change due to eddies for Ex.A
for 5-day period centered on January 2.
Contours are 1 or 10×10^5 gm sec^{-2} mb^{-1}.

While the angular momentum is conserved on a global basis, (i.e. the positive and negative areas under the friction curve balance), there is nowhere near a balance on a hemispheric basis. Thus there is quite a large eddy transport of angular momentum across the equator out of the winter hemisphere. This feature has also been found in the real atmosphere, e.g. Kidson and Newell, (1969). The flux into the summer hemisphere in the model is entirely due to the eddies and is about 10×10^{25} g cm^2 sec^{-2} in December, and 6×10^{25} g cm^2 sec^{-2} in January, which shows surprisingly excellent agreement with the values of Kidson and Newell.

The seasonal variation in the wind fields is revealed in the angular momentum budget by the net gain in westerly momentum in the winter hemisphere, while offset by the increase in easterly, (or decrease in westerly), momentum in the summer hemisphere. In the N.H. the net change curve illustrates the shift in latitude and increase in the westerly maxima as both the tropospheric and stratospheric jets intensify and move equatorwards. These features are also evident from Fig. 14.

The above aspects of the wind fields and angular momentum budget clearly cannot be reproduced in models which do not incorporate a seasonal cycle, or which are symmetric about the equator while using the truncated spectral representation.

The details of the curves in Fig. 17 do not resemble those for the atmosphere in the tropics, (see for example the frictional torque on the atmosphere given by Newton, 1971, and the contributions of the eddies,

mean cell and friction torque in the G.F.D.L. model, Manabe et al.,
1970). The lack of a doldrum region in the model tropics was commented
on earlier, and the single maximum of easterly winds near the equator
produces the profile of frictional angular momentum change in Fig. 17.
The angular momentum transport by the mean meridional cells in low lat-
itudes is significant in the atmosphere, but is omitted by the quasi-
geostrophic formulation. However, the pattern polewards of 35° is in
qualitative agreement with observations, although the values of the
frictional torque are only about half those given by Newton (1971) and
Manabe et al. (1970).

Figure 8 shows the mean latitudinal-height distribution of the
momentum change for the 5 day period centered on Jan. 2. The pattern
in the troposphere did not change much throughout the two month period
and is well represented by Fig. 18, but daily variations occurred above
20 km, and the pattern there is not representative of a long term mean.

As observed in the atmosphere, (e.g. Newell et al., 1970; and
see also Manabe et al., 1970), the largest changes are taking place near
the tropopause at 200 mb. The angular momentum transports by the large
scale eddies are clearly important in maintaining the structure of the
tropospheric jet.

No such transports by the eddies appeared to be of any long term
significance in the stratosphere of the model. Manabe and Hunt (1968)
noted the tendency for the changes in this region due to eddies and the
meridional circulation to balance. The polar night jet in their model

was maintained by convergence of angular momentum by the eddies while being destroyed by the meridional circulation. However the indirect cell which dominated the high latitude stratospheric region of their model was mostly absent here. The lack of this indirect cell and of a compensating eddy flux in the angular momentum budget must be regarded as a flaw in the model.

7.1.4 Source of Discrepancies

Many of the differences between the model and the real atmosphere were expected. Some are probably due to the lack of nonzonal forcing and may be remedied in the following experiments. Defects caused by the lack of water vapor and clouds in the model are not very large in the mean zonal fields, but were noticeable in the energetics. The quasigeostrophic formulation is deficient in the tropics and may be responsible for some of the discrepancies present there. The lack of any transports of angular momentum by the meridional cells is a feature of a quasigeostrophic model that was particularly evident in the angular momentum budget.

Manabe and Hunt (1968) found the general features of the lower stratosphere to be much better simulated with a high resolution model. Of particular note is the improvement in the mid-latitude temperature maximum in the winter hemisphere and the low latitude tropical tropopause. The vertical resolution of our model will probably also preclude the possibility of linear baroclinic instability in the stratosphere, (Murray, 1960; Mc Intyre, 1970).

Undoubtedly a major source of discrepancy is the external heat-
ing used here. However the parameterization could very likely be im-
proved without increasing the complexity by changing the formulation.
The strength of the westerlies in the upper stratosphere, and the loca-
tion of the maximum easterlies and westerlies in each hemisphere of the
lower stratosphere can probably be improved in this way. The formulation
of the heating itself, although undoubtedly in error for some problems,
seems sufficient for the purposes of this experiment.

The truncation of the spectral representation of the variables is
undoubtedly another major source of error. Since we kept six modes to
represent the zonal flow, but only three to represent each wave, the
added degrees of freedom act to enhance the symmetric effects and increase
the efficiency of the mean cells relative to the eddies. Thus the ratio
of the number of retained modes in the zonal flow to the number in each
wave is at least partly responsible for the dominance of the direct cells
throughout the model atmosphere.

Apart from this balance, some atmospheric events may have been
excluded by the truncation of the modes. For example Kikuchi (1968) found
a 4-cell meridional structure to be present in the troposphere when block-
ing occurs.

Some of the above defects in the model were expected and regarded
as acceptable. The general performance of the model in view of the many
simplifications is extremely good. The simple manner in which the sea-
sonal variation was introduced was surprisingly successful. However some

defects may affect the results of the experiments planned. The effects of the eddies on the stratosphere were fairly small, and the above discussion reveals the causes of the dominance of the meridional cells as being due to truncation and vertical resolution. Since we are especially interested in the effects of the vertical propagation of energy by the eddies, we may then expect to obtain an underestimate. Also, the winter lower stratosphere of our model does not have a baroclinic region at high latitudes, and this structure is less favorable for vertical energy propagation.

Conversely, with the location of the westerly jet at low latitudes in the lower stratosphere, there is a tendency for easterlies to form quite readily at high latitudes in the winter hemisphere.

7.2 The Introduction of Non-Zonal Forcing

For the purposes of discussing results, the phase angle (δ) of a wave will refer to a point of constant phase measured from the datum longitude, modulo one wavelength. The datum is chosen so that the phase of the topographical forcing is 0° (see Section 4.5), and γ is the phase of the forced diabatic heating. We let ϵ denote the phase of the temperature perturbation which accompanies the wave of phase angle δ.

The initial state for all the further experiments was Day 40 (Nov. 10) of Experiment A.

7.2.1 Experiment B: The Inclusion of Non-Zonal Heating

A priori the response expected in this experiment was as follows:
a reinforcement of the temperature perturbation, and thus a decrease in
dissipation of AE when

$$\gamma - \frac{\pi}{4} < \epsilon < \gamma + \frac{\pi}{4}$$ for wave 2.   A progressive

wave would be retarded by this effect for $\gamma < \epsilon < \gamma + \frac{\pi}{2}$; and

accelerated for $\gamma - \frac{\pi}{2} < \epsilon < \gamma$.

This would produce a residual wave in the mean flow where it
moves slowest and is greatest in magnitude, i.e. near $\epsilon = \gamma + \frac{\pi}{4}$.
If the wave is to become quasistationary and maintained baroclinically,
as occurs in winter (see Section 2.3.1), it would then be in a position

$$\gamma + \frac{\pi}{4} < \epsilon < \gamma + \frac{\pi}{2}$$.

The above features were deduced from a knowledge of the structure
of the quasistationary waves as revealed by Saltzman (1965) and Holo-
painen (1970).

Brief runs were made for differing γ's , the longest of which
was a 20-day integration with $\gamma = 110°$, as found for the atmosphere
in Section 4.5.[#] The a priori expectations appeared to hold reasonably
well but non-linear effects were also present.   In particular, the AE
variations were much greater than the simple analysis above would
expect, and was caused by the changes in the baroclinicity of the wave
as its slope changed with height.   Hence, when the temperature perturba-
tion was reinforced by diabatic heating, increased polewards heat

transports resulted with a large increase in CA and subsequently CE. This was particularly the case for $\gamma < \epsilon < \gamma + \pi/4$. The net result was a transient wave 2 which underwent large fluctuations in the baroclinicity with a period of three to four weeks.

This large response may have been partially caused by the concentration of the heating at essentially a single tropospheric level.

The results of this run are not presented, but further discussion relating to it will be given when we consider both nonzonal heating and orography in the model (Section 7.3).

7.2.2 Experiment C: The Inclusion of Orography

The presence of mountains on a flow produces a mechanical disturbance with a tendency for a trough to form to the lee side. In the model this implies the existence of a perturbation 1/4 wavelength out of phase with the orography, i.e. for $\delta = 3\pi/4$. This results in a pressure difference across the mountain which imposes a torque on the atmosphere and slows it down. Thus the earth speeds up slightly as the mountain torque acts as a sink to the atmospheric angular momentum.

However, pre-existing waves will interact with the orography to produce an exchange of kinetic energy between the zonal flow and the eddies. The mountain torque may then act as a source or sink of angular momentum, depending upon the location of the wave.

Newton (1971) has recently evaluated mountain torques for the atmosphere, and indicates that the net result is a mixture of the effect

due to the mechanical disturbance of the flow by mountains, and that due to unequal temperatures on either sides of the mountain. The latter appears to dominate, and the presence of a westward torque on the atmosphere in the N.H. winter is mostly due to the presence of a very strong pressure gradient between the Siberian High and Aleutian Low, across the generally low North Asiatic mountains, while the effects of the Himalayas are small.

In the model the baroclinicity of wave 2 was dominant, and the wave continued to progress eastwards while moving in and out of phase with the orography. The result was a transient wave alternately reinforced and cancelled by orographical forcing.

However, the movement of the wave was strongly influenced by two different effects. Distortion of the flow produces a stationary component, which would appear as acceleration of the wave for $\frac{\pi}{4} < \delta < \frac{3\pi}{4}$ or retardation for $-\frac{\pi}{4} < \delta < \frac{\pi}{4}$. The second effect is that due to the change in advection as the zonal wind fluctuates from the interaction. In this case, the zonal flow should become stronger westerly (or weaker easterly) for $0 < \delta < \pi/2$.

In the model the most pronounced change in the eastward motion of the wave was for acceleration for $\frac{\pi}{4} < \delta < \frac{\pi}{2}$ and retardation for $\frac{3\pi}{4} < \delta < \pi$, in excellent agreement with the above analysis. This was evident throughout the troposphere.

Experiment C consisted of a 50 day integration with orographic effects, so that the month of December was again simulated.

The mountain torque served to enhance the surface friction by a factor of roughly 2/3 northwards of 40N. This drain on the westerlies was offset somewhat by an increased flux of angular momentum into the region by the large scale eddies.

There was little change in the energetics from that shown in Fig. 15a although the intensity of the N.H. circulation in the troposphere decreased somewhat. The mean exchange for the entire month between KE and KZ due to orography was 9 ergs cm^{-2} sec^{-1} going from KE to KZ in the N.H., and 1 erg cm^{-2} sec^{-1} in the same direction in the S.H. Hence the exchange was insignificant.

7.2.3 Experiment D: Inclusion of Non-Zonal Heating and Orographical Forcing.

As indicated in experiments B and C, the presence of the nonzonal forcing in the model failed to produce a quasistationary wave. Therefore a cyclic response resulted from alternate reinforcement and cancellation by the interaction with the external forcing, with a period of about 3 to 4 weeks.

With both kinds of forcing included, the net response of the wave will include the separate effects of the nonzonal forcing and the baroclinicity of the wave, and will clearly be nonlinear. The relative phase of the two kinds of forcing will be of importance.

We set $\gamma = 110^{o}$. The slope of wave 2 from 800 mb to 600 mb in Ex. A was about 25° of longitude, (e.g. see Fig. 11). The phase of the temperature perturbation lags about 1/4 wavelength behind, so that $\epsilon_{600} \sim \delta_{300} - 70^{o}$. Hence reinforcement of the wave by heating, and

the ensuing change in baroclinicity, should occur 45° out of phase with the orographic reinforcement. At the observed mean speed of wave 2 in Ex. A of 9° day^{-1}, this is a lag of about 5 days behind the orography.

Experiment D was a complete run, from day 40 to day 124, so that both months of December and January were again simulated. The results of this integration are compared to Ex. A in the following section.

7.3 Northern Hemisphere Winter Simulation: Both Orographic and Non-Zonal Heating Effects included: Ex. D.

In this section, results for this integration will be presented, and a comparison made with Ex. A and the atmosphere. Again we shall confine our attention to averages and details of the daily variations, particularly with regard to the sudden warmings, will be delayed until Chapter 8.

7.3.1 Zonally Averaged Fields

The comparable figure to Fig. 14 for this experiment is shown in Fig. 19. Once again the dates are the same as shown in Figs. 5 and 14. However the zonal wind and temperature fields are less representative of the longer period mean values. This was due to fairly large changes, especially at 10 mb in the N.H., which were caused by sudden warming type events. These effects were considerably more noticeable in the 5-day mean meridional circulation. However the principal features are present and details are discussed below.
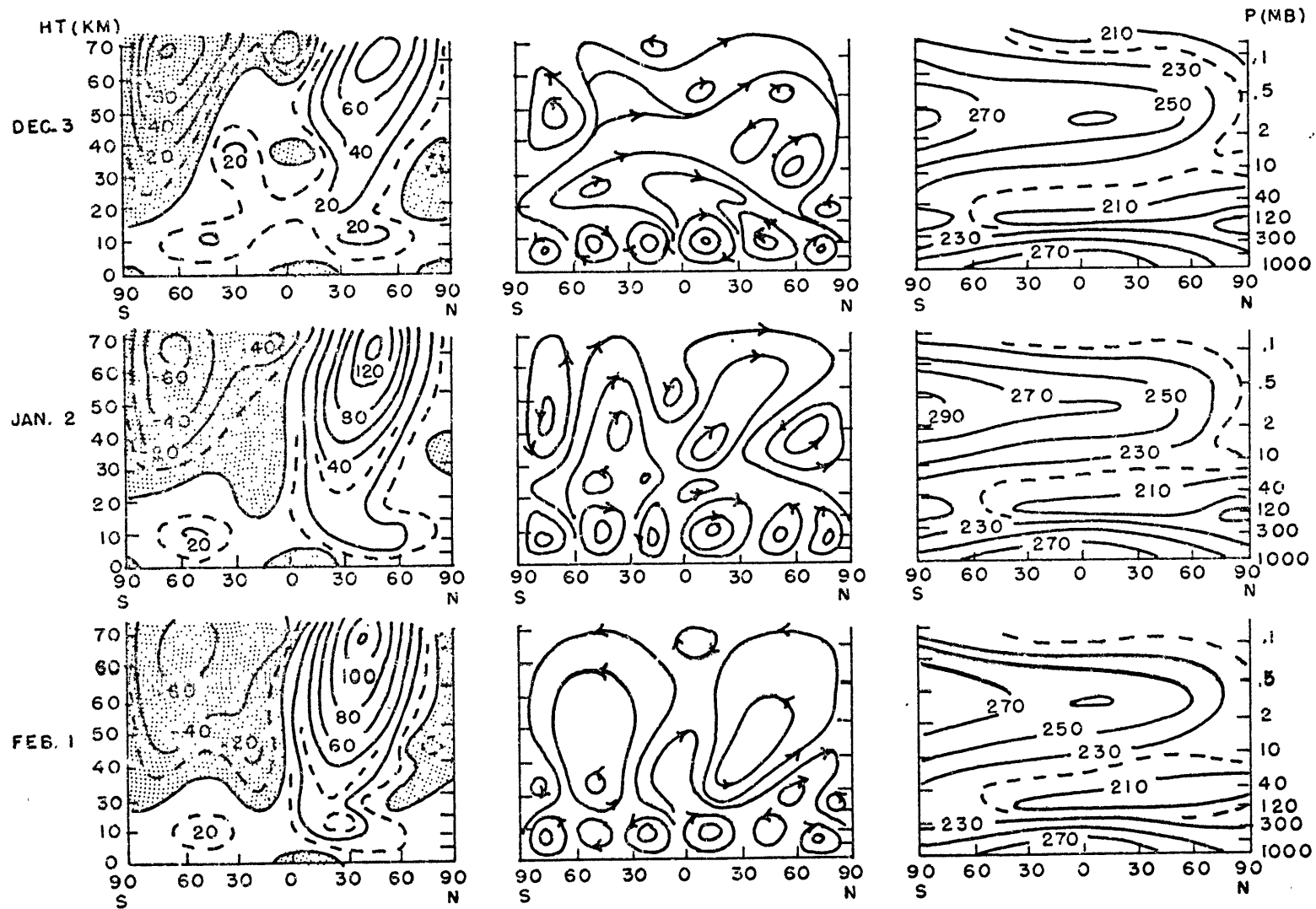
Fig. 19. (a) Zonal wind (m sec^{-1})   (b) Schematic meridional   (c) Zonal temperature
Ex. D   Easterlies are shaded   wind streamlines   (^{O}K)

149

The fields for Dec. 3 in Figs. 14 and 19 are very similar, and changes are more noticeable on the later dates.

In the N.H., the tropospheric westerly jet is slightly stronger for each day, while the stratospheric jet is about 10 m sec^{-1} weaker. At high latitudes in the stratosphere the easterlies are stronger and more extensive. Although the easterly component in low latitudes of the S.H. increased somewhat, at the equator westerlies were present to 60 km and were slightly greater than in Ex. A.

In the temperature field, the most notable difference is in the increase in N.H. polar temperatures at 10 mb by more than 20°K on both Jan. 2 and Feb. 1.

The meridional circulation shows considerably more character, although the overall features are similar. A large Hadley cell is still in existence on Jan. 2 in the stratosphere, and the cells on Feb. 1 tend to be in the opposite sense, as in Fig. 14. However, the decrease in the strength of the symmetric circulation is strongly apparent in this region. In contrast, in the troposphere, the Ferrel cells were considerably weaker.

Certain features of Fig. 19 are more realistic when compared to the observed circulation. Of particular note is the decreased westerlies in the N.H. winter, (Ex. D), compared to the S.H. winter, (Ex. A). Similarly the stronger easterlies at high latitudes in the N.H. winter lower stratosphere are an observed difference. This accompanies the much warmer temperatures in the stratospheric polar night that are observed,

and which were simulated by the model. At the pole, at 10 mb, the increase in the mean temperature from day 40 to 124 in Ex. D over Ex. A was 18°K.

The tropospheric jet in the N.H. was as much as 5 m sec^{-1} stronger in late January in Ex. D. This is also an observed difference. However the increased dominance of the direct cells in the troposphere is not observed. Both these features are closely tied to the momentum budget, see 7.3.3.

7.3.2 Energetics

Fig. 20 (a) and (b) shows the 4-box diagrams of the energetics for experiment D. This figure is the equivalent to Fig. 15 (a) and (b) except that non-zonal heating and orography have been included in the model.

The N.H. (Winter).

In the tropospheric energetics we find a number of new features. Most notable is the large increase in the intensity of the circulation in both months. This was mainly due to increased baroclinic conversions of AE to KE by large scale quasihorizontal eddies, but the increased dominance of the direct cells in the symmetric part of the circulation, AZ $\longrightarrow$ KZ, was also a factor.

As experiment C, in which only orography was included, showed a decrease in the intensity, it is obvious that the change was brought about by non-zonal heating. The increase in intensity was mainly in wave 2, although a slight increase also occurred in wave 4.

GLOBAL

2607   540
33116 (111) →1956— 5220 (6)
60← 540   1410   332
3733 (33) ←86— -4510 (21)
584   51   51   920

67   34
1687 (-8) ←71— 698 (2)
8   12   107   2
2265 (18) ←52— 1728 (9)
98   60   332   152

13.0   16.6
244 (4.7) →7.5— 106 (-1.7)
.8   7.4
689 (12.5) —5.0← 423 (-4.6)
1.7   8.4   11.9   4.1

N.H.

3450   504
45849 (272) →2460   6947 (102)
286→   2176→   ←167 ←1
1004 1081   1738 1448   249
4795 (70) →32   5695 (73)
275   129→   ←1 ←7
804   100   93   1160

104   47
1634 (-43) ←81   952 (3) ←1
19←   102←   ←26
22   0   125 139   26
3601 (56) →45   1988 (25) →2
89→   ←19
152   275   249   166

19.5   24.0
322 (4.7) →16.5   170 (-27) →1.9
2.5→   17.3→   →2.2
.8   .2   8.3 10.3
1193 (29.6) ←10.0   603 (2.1) →.7
1.7←   →5.2
2.7   22.1   25.6   5.6

S.H.

1764   576
20383 (-50) →1452   3493 (-90) →1
286←   1736→   →167
76 1   1082 1372   415
155   2671 (-4) ←204   3325 (-31) →1
301←   →7
364   2   9   670

30   21
1740 (27) ←61   444 (1) ←1
19→   40←   →26
5   25 24   89 75
929 (-21) ←149   1468 (-7) ←2
193←   →19
44   155   415   137

6.5   9.2
166 (4.7) ←1.5   42 (-.7) ←1.9
2.5←   2.3←   ←2.2
.8 1.4   6.5 4.5
180 (-4.6) ←0   243 (-11.3) ←.7
8.3←   ←5.2
.7   5.3   1.8   2.6

(i) troposphere   (ii) lower stratosphere   (iii) upper stratosphere
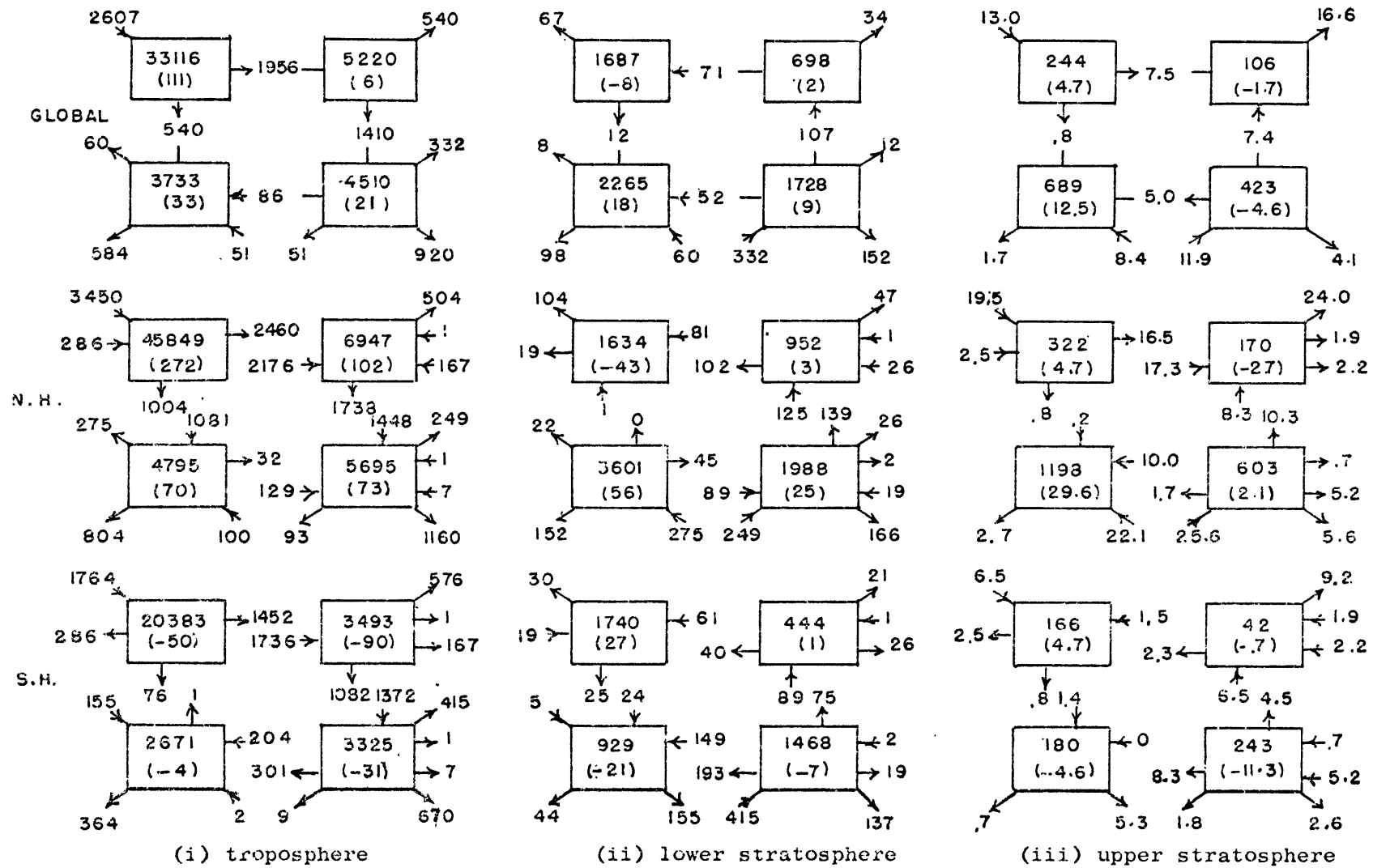
Fig. 20a.   Energetics for December in Ex. D.   Energy values are 10^5 ergs cm^{-2}, and conversions ergs cm^{-2} sec^{-1}.

(i) troposphere

GLOBAL

2797 → | 32595 (−167) | → 2333 → | 7131 (153) | → 753
64 631 ↓ | 4250 (5) | ← 67 → | 4368 (−32) | 1427 392
680 51 51 949

N.H.

.3780 → | 44564 (−306) | →3397 2964 → | 10051 (265) | → 8 ←16 | 884
364 → 1053 1217 ↓ 1903 1741 457
244 | 6236 (39) | → 2 607 → | 6210 (−45) | → 33 →22
.1031 99 .97 1303

S.H.

1814 → | 20626 (−28) | → 1269 1702 → | 4211 (41) | ← 8 → 16 | 622
364 ← 209 45 ↓ 951 1113
116 | 2364 (−29) | ← 136 194 ← | 2526 (−19) | → 327 → 33 ← 22
329 3 5 595

(ii) lower stratosphere

86 → | 2398 (−9) | — 116 ← | 492 (−2) | 2 4
6 39 ↓ | 2888 (20) | — 47 | 1706 (9) | 138 20
124 64 392 177

127 → | 2439 (−7) | ← 176 176 ← | 688 (−1) | 0 ← 5 | 37
35 ← 21 20 ↓ 207 209
11 | 5093 (42) | → 5 4 → | 2317 (19) | → 1 ← 12 | 37
206 244 457 219

45 → | 2357 (−11) | ← 56 56 ← | 296 (−3) | 0 → 5 | 11
35 ← 57 58 ↓ 69 67
1 | 683 (−2) | ← 99 98 ← | 1095 (−1) | → 3 → 1 → 12
42 116 327 135

(iii) upper stratosphere

.6.4 → | 312 (−1.6) | → 10.4 ← | 129 (3.5) | 17.2
2.4 ↑ | 964 (3.7) | ← 1.9 | 377 (4.6) | 10.3 20
2.2 6.4 20.2 3.4

12.1 → | 401 (−1.9) | → 21.2 20.7 → | 231 (6.5) | ← 1.6 ← 3.4 | 29.5
2.7 → 4.5 5.0 ↑ 10.3 12.9
| 1756 (5.1) | → 3.2 .5 → | 612 (9.8) | → 2.8 → 6.6
3.7 10.6 3 6.9 5.3

.7 → | 233 (−1.3) | ← .4 .1 → | 27 (.5) | → 1.6 → 3.4 | 4.9
2.7 ← .3 .2 ↓ 10.3 7.7
| 172 (2.3) | ← .6 4.3 ← | 142 (−.6) | ← 2.8 ← 6.6
.7 2.2 3.5 1.5

(i) troposphere   (ii) lower stratosphere   (iii) upper stratosphere
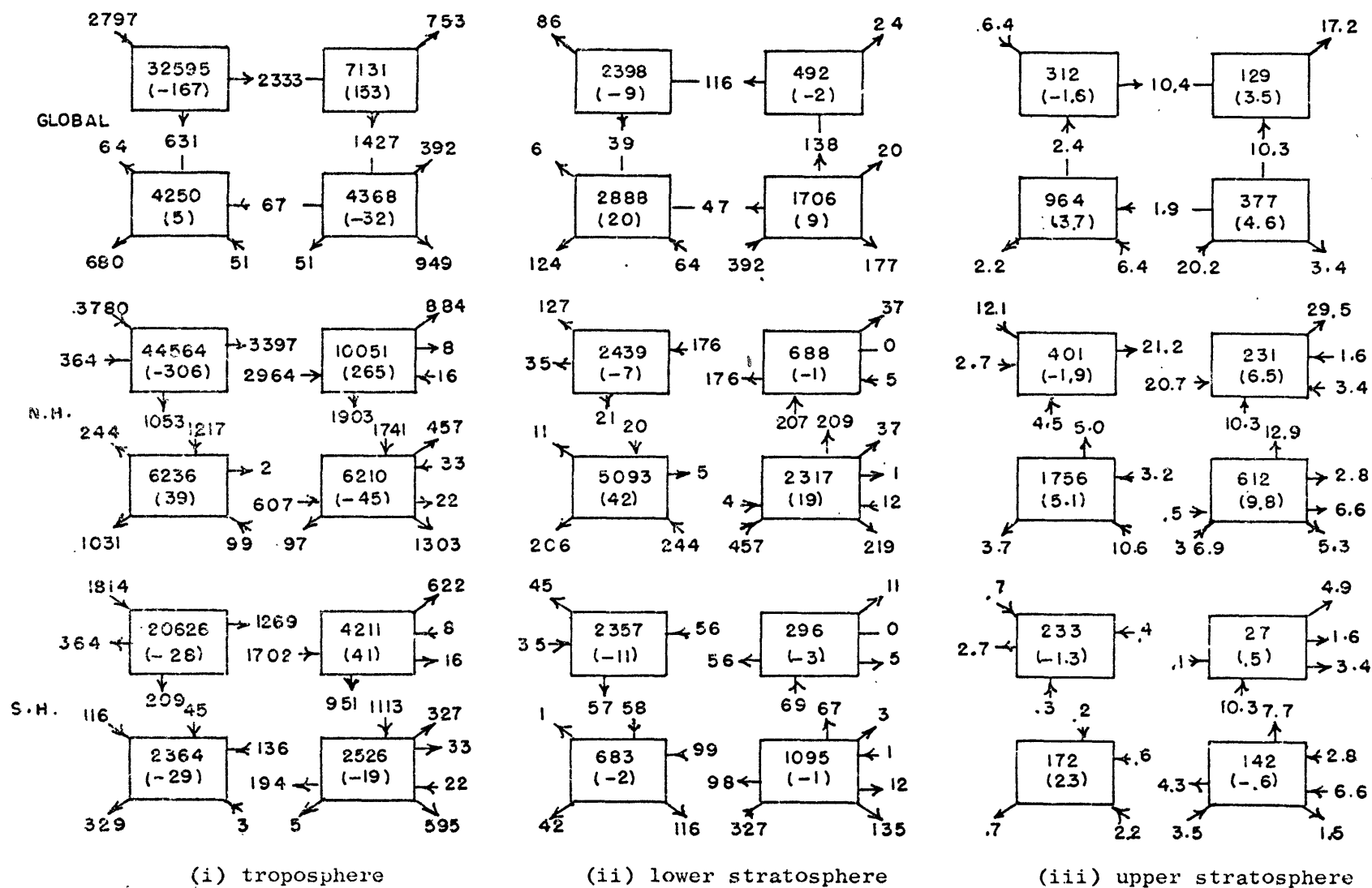
Fig. 20b. Energetics for January in Ex. D

There has been a spectacular increase in AE for both months as well as the expected decrease in GE. These values are more in line with those observed in the N.H. The change was due to the greater role of wave 2 in the circulation.

These features may be seen more clearly in Fig. 21 which shows the daily variations of the different forms of energy, averaged over the globe, and integrated in the vertical. This figure is the equivalent of Figs. 12 and 13 of Ex. A. The scale for AE has been changed and A2 is not included in order to decrease the clutter, and since it is very similar to AE in variability.

In many ways the curves are remarkably similar to those in Ex. A except in wave 2. AZ and KZ variations became quite marked. As in Ex. A, the intensity of the circulation increased going from December to January. K6 rose to a maximum in a similar manner, but four days earlier, and declined in a like fashion. AZ however, appears to reach a maximum at about the same time (when the curve is smoothed).

While the effect of orography on the energetics of experiment C was small, the mountain torque was important in the angular momentum budget. In Ex. D the presence of mountains was the cause of the other major change in the winter tropospheric energetics and resulted in a barotropic contribution to the growth of eddies. This reversal in CK is approximately offset by the loss in KE to KZ by the orography. Further detail on the reasons for this response are considered in Section 7.3.3.
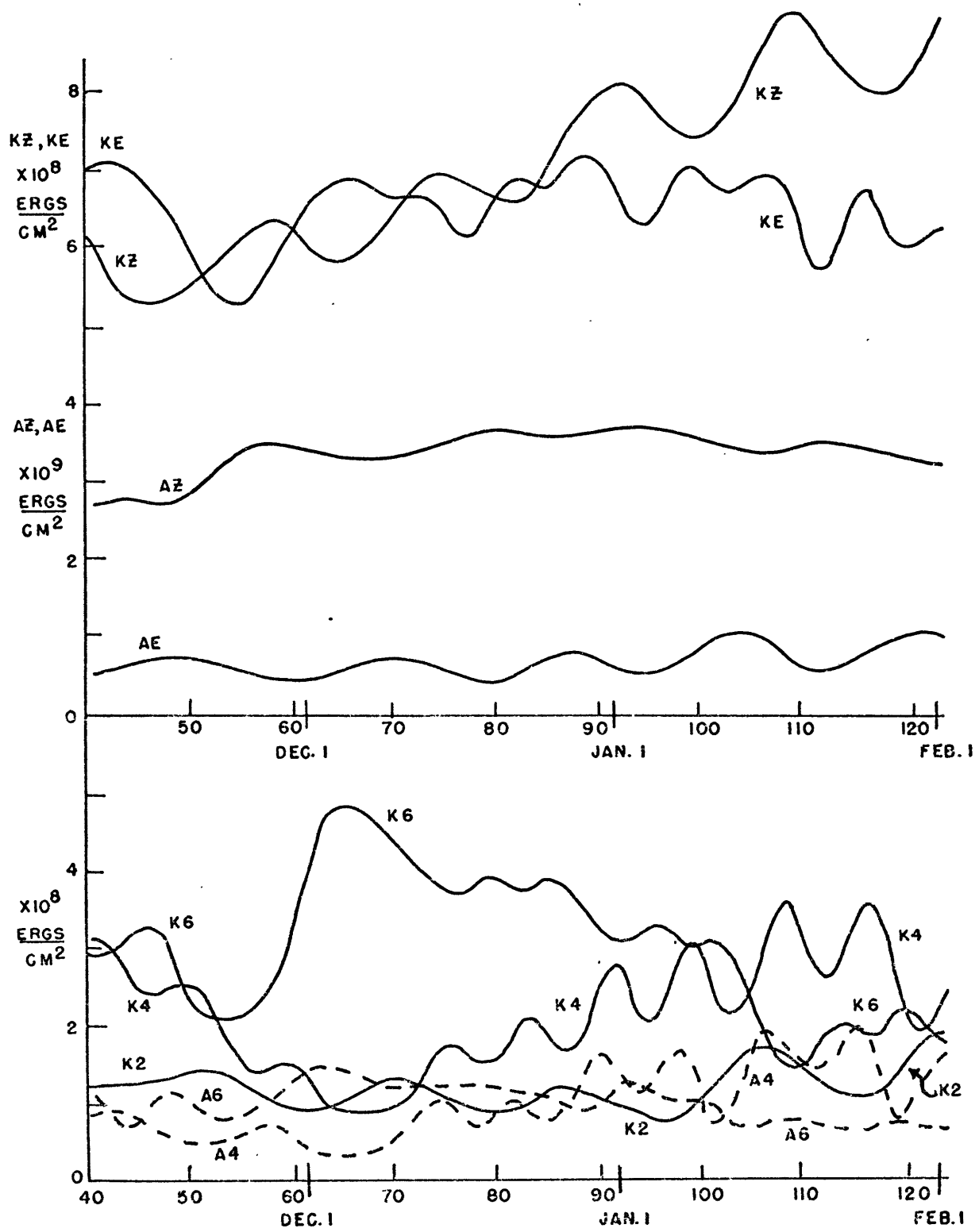
Fig. 21. Variation of Global forms of vertical integral of
energy for Ex. D.

We now briefly consider the lower stratospheric N.H. energetics. In December, the energetics are similar in Ex. A. and Ex. D. However in January, Fig. 21 shows a marked increase in the driving from below through increased vertical propagation of eddy geopotential energy. The conversions CE and CA are roughly twice those of Ex. A. Hence the increased intensity in the tropospheric circulation has increased the driven circulation aloft.

In the upper stratosphere in winter, both months have similar energetics in Ex. D. The greatest change has been an increased driving from below through the vertical propagation of energy. AE and KE increased markedly in both months. Note that associated with the increased $\nabla \phi \epsilon$ in December is an increased CA, while CE is not greatly affected. A feature of the upwards propagation of energy by stationary waves is for northward transport of heat in the N.H. (Eliassen and Palm, 1961). Then, provided there is a polewards temperature gradient, CA is positive. This will also be shown to be a feature of transient wave vertical energy propagation in westerlies for this model when we consider time series of these quantities in Chapter 8.

In summary, the introduction of orography had little effect on the energetics in agreement with comments by Mintz (1968) and Kasahara and Washington (1969, 1970). However the introduction of non-zonal heating produced a large increase in the intensity of the circulation and improved the simulation of some features of the atmosphere observed in the N.H. The transient wave 2 played an important role. Whether these kinds of effects really exist in the atmosphere for the long

transient waves is not entirely clear and will be discussed further at the end of this chapter. As a result of the changes in the troposphere, there were pronounced effects on the stratosphere and a general increase in the role of eddies in the circulation.

The S.H. (Summer).

Changes between Ex. A and Ex. D were not as great in the summer hemisphere. There was no attempt to simulate a N.H. summer in either of these integrations. KZ increased slightly as the westerlies increased at the equator, and KE decreased a little, but there was no change in the strength of the tropospheric jet. The orographic exchange was negligible. Wave 2 increased slightly in importance as is evident in slightly increased AE values in December. Generally, changes were small and do not appear to be significant.

Interhemispheric Exchange

An analysis of the total interhemispheric exchange of energy shows similar results to those of Ex. A. In January there was a small net flux into the S.H. at all levels, but only in the upper stratosphere was the flux directed into the S.H. in both months. These results generally reinforce our earlier comments on this point.

7.3.3 The Momentum Budget

The momentum budget (Fig. 22) is revealing in showing the mechanisms present in the model which produced some of these changes. The effect of the mountains has been to increase the westerly momentum of the flow in mid-latitudes of the N.H. This is contrary to that observed in this region, but is a feature of the flow across some mountain ranges, Newton (1971). It is also quite the reverse of the effect of the orography in experiment C.

Apparently this is an aspect of the flow in the model for the chosen values of phase of heating relative to orography. It signifies that in the mean geopotential pattern at 800 mb there is a high pressure cell to the east, and a trough to the west of the mountain.

Since the nonzonal heating and the baroclinicity of the wave are dominant, the analysis given in Section 7.2.1 applies. This predicts a stationary feature near $\epsilon = \gamma + 45^{\circ}$, i.e. near $\delta_{800} \sim \gamma + 115^{\circ} = 45^{\circ}$ (modulo 180°). However, the orography is acting to accelerate the wave just as the heating slows it down, so that the stationary feature should be expected further west. The analysis in 7.2.2 shows for

$$0 < \delta_{800} < \frac{\pi}{2}$$ that the eddy is cancelled by orography, (KE $\longrightarrow$ KZ), in a westerly flow, and that the atmosphere should gain momentum. Hence, given the dominance of the nonzonal heating, this response could have been expected to some extent.

The observed stationary component in the model at 800 mb is actually near $\delta_{800} \sim 35^{\circ}$ as may be seen from Fig. 23. In this figure
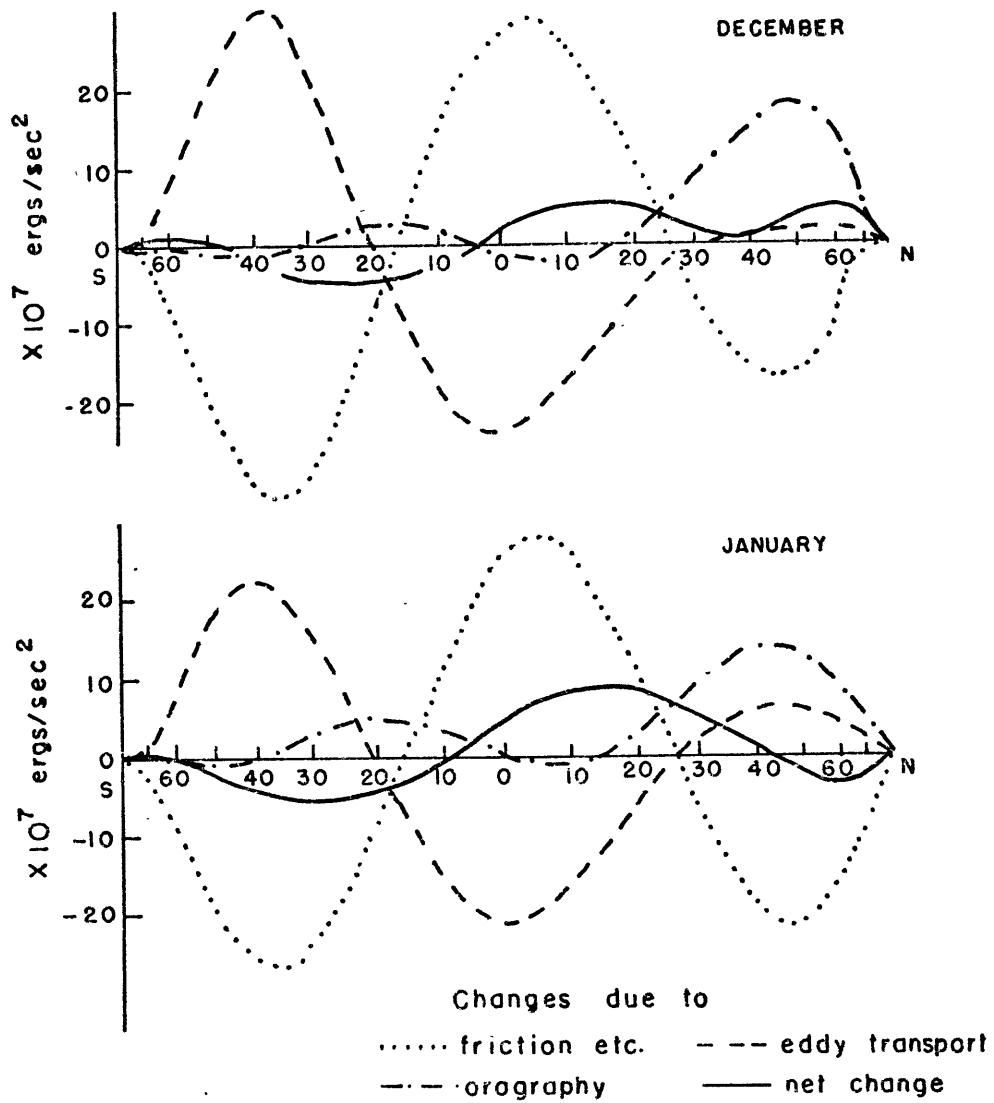
Fig. 22. Angular momentum change in 10^7 gm sec^{-2} as a function of the sine of the latitude.

the phase of wave 2 is most obvious at high latitudes. This value is in excellent agreement with the above analysis.

The response is the cause of the weakening of the Ferrel cell in the troposphere in Ex. D, since there was apparently no longer a general circulation requirement that eddies transport momentum to maintain the tropospheric jet.

The net change of angular momentum curve in Fig. 22 is similar to Fig. 17, but shows the added increase in angular momentum which was apparent in our earlier analysis of the tropospheric wind field.

With orography present in the model, it is possible for the global value of angular momentum of the atmosphere to increase and be maintained at a higher level if the orographically induced vertical motions are such the solid rotation component of the flow is increased. Ultimately however, this increase will be balanced by compensating frictional drag, and in the very long term the average changes must balance. In the model, the solid rotation component of the flow was increased in Ex. D and an exact balance does not exist for a single month.

As the mountain torque in the S.H. and in low latitudes was fairly small, the approximation used to represent the orography is probably acceptable. However, as the response in the model is unlike that observed in the region 40 to 60N, it seems that either the phase relation between the orography and nonzonal heating, or the stationary component of the wave induced by the heating is in error.

Much of the error can be assigned to the fact that only one scale and phase of orography was represented in the model. The mountains which act to produce most of the westward pressure torque are those of North East Asia, (Newton, 1971), and are located about 50° east of the Himalayas. The latter dominated the phase chosen for the model. We note that, had these mountains been included, an angular momentum sink would have resulted. The lack of a complete representation of the mountains allows air to flow through regions where mountains should be, and the dominant effect of the Himalayas as a dam, (Mintz, 1968), is not included.

However the wave structure and behavior of wave 2 are also open to question and will now be examined in more detail.
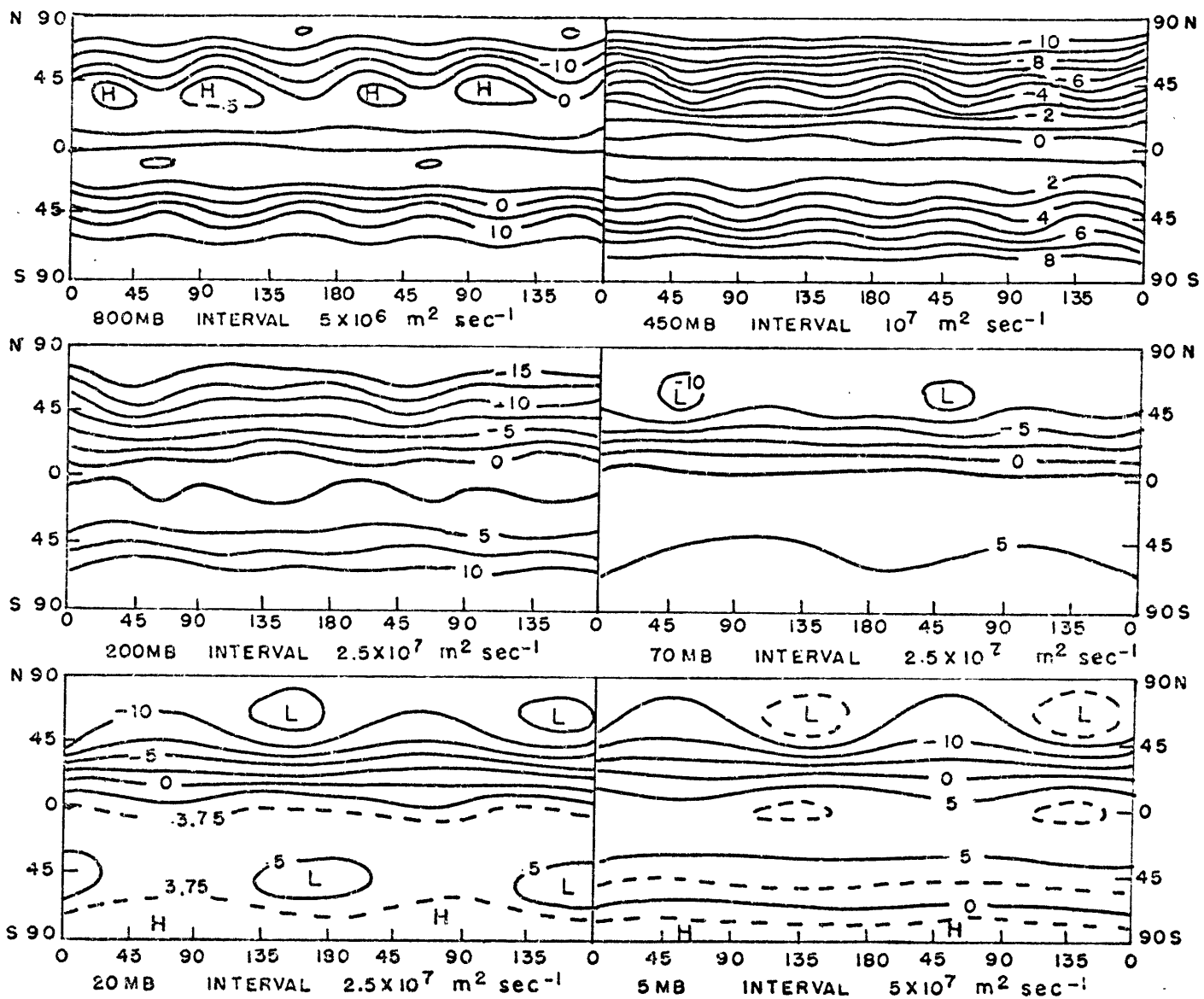
7.3.4 Behavior of waves

The model failed to produce the quasistationary features most prominent in the N.H. winter troposphere, but there was a substantial stationary component.

Fig. 23 shows the mean streamline pattern for the period December-January at the lowest six levels of the model. The mean contours were evaluated for each month separately, but as the patterns were very similar, with almost identical features and phases, they were combined. The longitude values shown are relative to our datum chosen at 35E, so that mountain peaks are at 45° and 135° in wave 2.

A curious feature of the tropospheric patterns is the appearance of a pronounced wave 4 component. This is due to the very slow movement

Fig. 23

Mean
streamlines
for period
Dec-Jan
for
Ex. D

Longitude values
are such that
0° corresponds
to 25° E.

800MB   INTERVAL 5×10^6 m^2 sec^{-1}

450MB   INTERVAL 10^7 m^2 sec^{-1}

200MB   INTERVAL 2.5×10^7 m^2 sec^{-1}

70 MB   INTERVAL 2.5×10^7 m^2 sec^{-1}

20 MB   INTERVAL 2.5×10^7 m^2 sec^{-1}

5 MB   INTERVAL 5×10^7 m^2 sec^{-1}

of wave 4 and was also apparent earlier in Fig. 11. From day 60 to 124 the total movement of wave 4 was 35° westward. This behavior is quite unlike that of the other two waves which were both progressive. As noted earlier, the linear baroclinic analysis (Section 6.3) indicated that wave 6 would be in the short wavelength region of instability, wave 2 would be in the long wavelength region, and wave 4 would be near the transition. Both wave 2 and wave 6 moved with mean speeds very close to those given in Fig. 9 for case B of the linear baroclinic study.

At the transition, a wave would be stationary and would correspond to the resonant wavelength. Thus quasiresonance may account for the oscillatory response of wave 4 apparent in Fig. 21. The fluctuations seem to be a response to nonlinear interactions between the other waves that produce a contribution to wave 4. As the interactions were almost periodic, this interpretation is not definite. The response at 600 mb is presented in Fig. 24. The gain in A4 by nonlinear interactions is shown, (AF4), along with the baroclinic conversion terms, CA and CE, as a function of time. The lag in the curves CA and CE by 1 to 2 days is most noticeable.

In Fig. 23 it may be seen that wave 2 in the N.H. is not of very great amplitude in the troposphere, but becomes increasingly marked above 200 mb. The slope of the stationary component is westward with height throughout. At 800 mb, at high latitudes in the N.H., the closed low pressure region is at 157°, i.e. near 12° longitude. This is somewhat east of the observed location in the atmosphere.
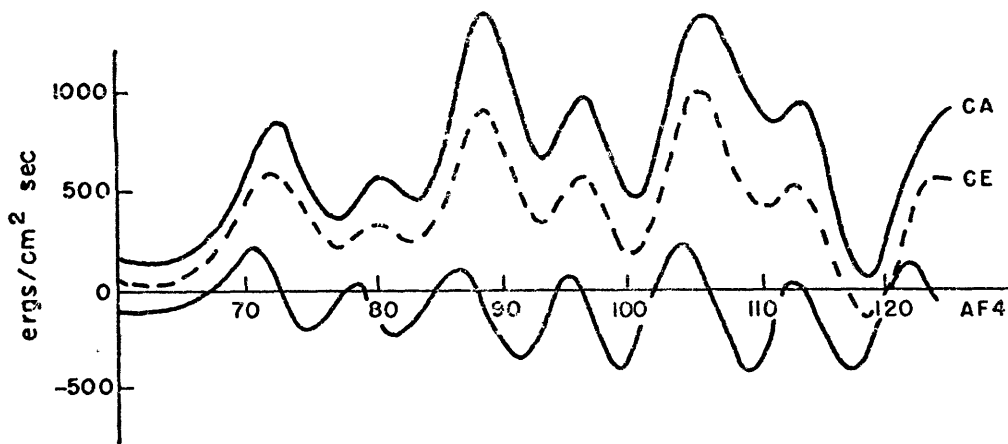
Fig. 24. Conversion terms in wave 4 for N.H. for
the layer 800-450 mb.

The primarily transient nature of wave 2 may otherwise be inter-
preted to mean that the transient component of the wave was greater in
magnitude than the stationary component. This is the case during the
S.H. winter but the reverse is true in the N.H. winter. However, the
presence of both components of the long waves in the N.H. is well estab-
lished, see Section 2.3.

Bradley and Wiin-Nielsen (1968) identified a mode of the transient
component of wave 2 in the N.H. which sloped westward with height by
about 36° longitude between 850 mb and 500 mb, while progressing east-
wards at 15° day^{-1}. Hirota (1968) found the same speed for the transient
component of wave 2 in the stratosphere. Phillpot (1969) found wave 2
to have similar movement with a pronounced amplitude at 30 mb in the S.H.
The structure and movement of these waves bears a strong resemblance to
the wave 2 performance in the model.

The performance of sophisticated general circulation models in
simulating the details of the stationary and transient very long waves

remains somewhat unsatisfactory, particularly in the low resolution models, (Manabe et al., 1970; Miyakoda et al., 1971). The problem seems to be in assigning correct amplitudes to the forced and free modes of the waves. Bradley and Wiin-Nielsen (1968) indicate the problem may also be in resolving the vertical modes of the waves.

However a question arises as to why a quasistationary wave was not produced here. Kasahara and Washington (1969, 1971) and Holopainen (1970) indicate the stationarity is due to by nonzonal heating, (see Section 2.3). In our model, we noted in Section 7.2.1 the large change in baroclinicity associated with the nonzonal heating. This appears to be caused by differential rates advection with height, which produced changes in the slope of the wave with height. Hence it seems associated with the vertical resolution of the model and the vertical distribution of the nonzonal heating.

Other factors very likely of importance are as follows:

ii) the increased westerly component in this model due to the mountain torque,

iii) the presence of westerlies at the equator which we noted in Section 6.3 (Fig. 9) increased the speed of the waves eastward.

iv) The change in static stability as a result of the linear baroclinic analysis (Section 6.3). This may have altered the response of the long wave to the heating. Fig. 9 shows it did not seem to affect the wave speed.

v) The structure of the lower stratosphere with strong winds in lower latitudes than observed.

vi) The lack of an Ekman layer in the model. Frictionally induced horizontal convergence and divergence produces significant vertical velocities at the top of the Ekman layer. Charney and Eliassen (1949) found this to be of importance for large scale quasi-geostrophic waves and derived a simple method for including it. It directly affects the baroclinicity of the wave and should have been included in the model.

vii) The lack of a variable static stability excludes the stabilizing effect of the vertical flux of heat in baroclinic systems. The quasigeostrophic formulation may have also omitted important influences on the motion.

viii) Truncation of the spectral modes restricts the number of degrees of freedom in each wave, and thus the hemispheres are not entirely independent. The effect of including an extra mode in the representation of a wave may be seen in Section 6.3 for an extreme case. The difference in the response in cases A and B, (Fig. 7) shows that the effect of the addition of one mode in representing the temperature field of a wave to be very large.

Many of the above suggestions on reasons for not obtaining a better simulation of the stationary waves can be easily implemented. Other suggestions would require an expanded model; e.g. (vi) and (vii). However in such a simple model, the improvement of one aspect of the flow may well be detrimental in other respects; e.g. (iii), or a change in heating parameterization to improve (ii) or (iv).

Some of these changes would be artificial to some degree and necessitate a certain amount of trial and error experimentation. Needless to say, the results would serve as an important guide to the design of experiments using more sophisticated models and it is somewhat surprising that more use has not been made of these highly simplified models.

The performance of the model at this stage of development has been very good in most respects and should provide results which are meaningful in the above sense.

CHAPTER VIII

DYNAMIC COUPLING BETWEEN THE TROPOSPHERE AND STRATOSPHERE

In chapter 7 the performance of the model was evaluated by comparing features of the flow with those of the observed atmosphere. Attention was centered on average properties with a view to bringing out the characteristics of the model. Some discrepancies were considered in 7.1.4 as a result of the analysis of Ex. A. Further deficiencies were evident when nonzonal forcing was introduced, most notably in the performance of individual waves. Possible reasons for this response were discussed in section 7.3.4. In general however, the model simulation of the atmosphere has been most successful and differences are chiefly in degree of response rather than in the response itself.

With this evaluation in mind we now consider the experiments with regard to the sudden warming phenomenon in all its phases, and differences between N.H. and S.H. winter circulations.

8.1   Sudden Stratospheric Warmings in the Model

In order to define the phenomenon as it occurred in the model integration, time series of the temperature at the North Pole in Ex. A and Ex. D., as a function of height, are shown in Fig. 25. The levels at which the temperatures are defined are finite, but for clarity, the presentation is continuous. The mean temperature from day 40 to 124 has been extracted.
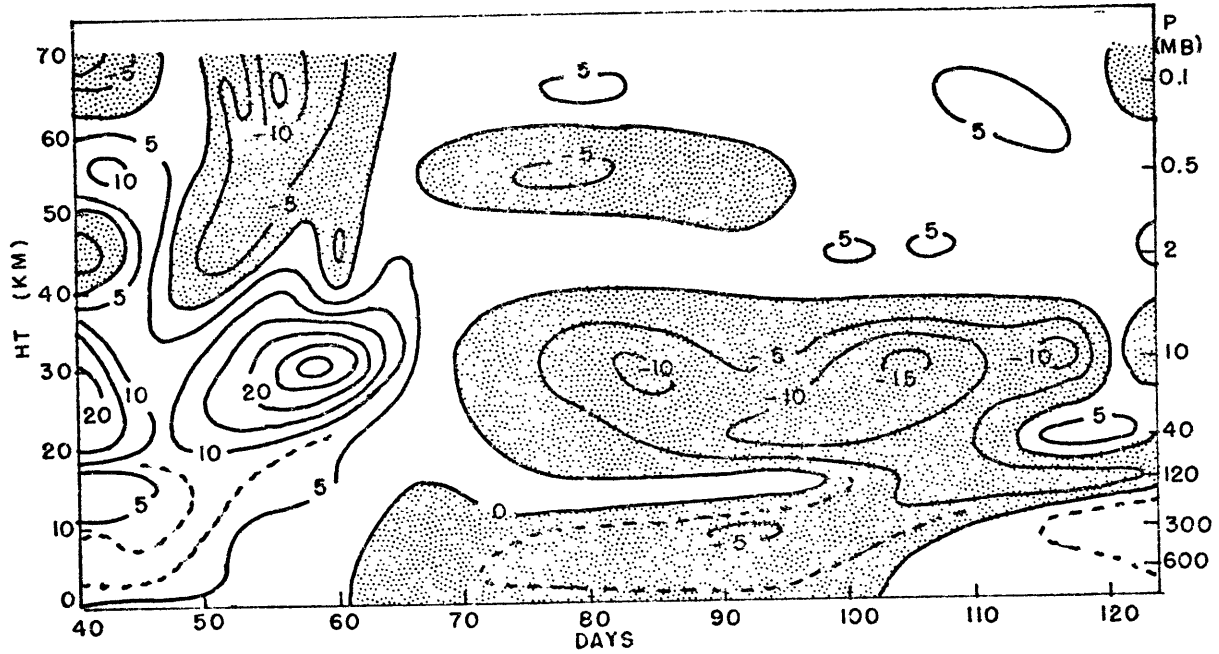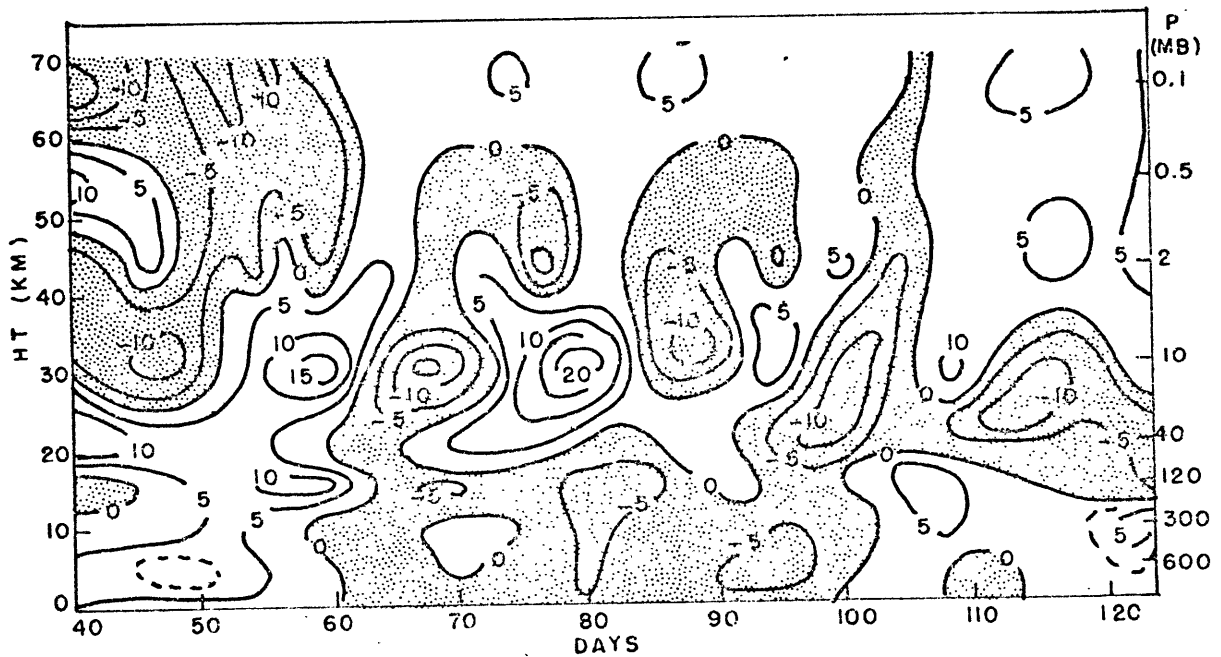
Fig. 25a.   Ex. A.

Fig. 25b.   Ex. D.

Fig. 25.   Temperature at 90N.   Deviation from mean for level.

These values are shown in table 5.

Pressure	600	300	120	40	10	2	0.5	0.1 (mb)
Ex. A	229	218	232	209	209	214	220	206
Ex. D	229	222	235	210	227	213	221	209

Table 5. Mean temperature at levels from day 110-124 in $^\circ$K at pole.

The difference between the experiments in table 5 is greatest at 10 mb, but significant increases also occurred at 300 mb, 120 mb and 0.1 mb. These are the same kinds of differences observed between the N.H. (Ex. D) and S.H. (Ex. A).

In the troposphere, the differences between the experiments in Fig. 25 are not very large. However, the heating field is acting to produce coldest polar temperatures after Jan. 12' (see section 4.6), whereas the minimum was reached during December. This was noted in the analysis of the energetics in sections 7.1.2 and 7.3.2 as a maximum in AZ at this time.

In Ex. D, at 10 mb, large fluctuations occurred in the polar temperature with a period of about 18 days, and warmings of over 40°K took place within a two week period. The patterns shown in the two experiments are almost identical until day 60, although a different mean value has been extracted. The warming on day 58 occurred in all four experiments. Otherwise the temperature in Ex. A underwent only small fluctuations until a minor warming of 15°K on day 120.
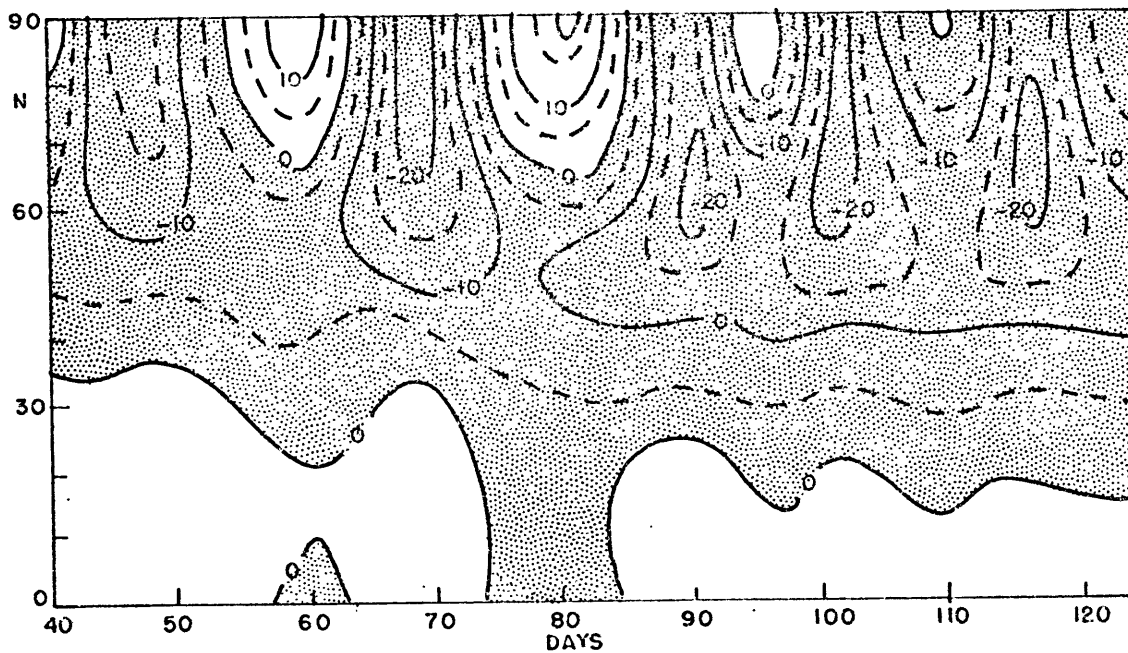
Fig. 26. Time series of zonal average temperature. Deviation from
231°K, at 10 mb in N.H. for Ex.D.

NOVEMBER ————→ I←——— DECEMBER ————→I←—— JANUARY ————————→I
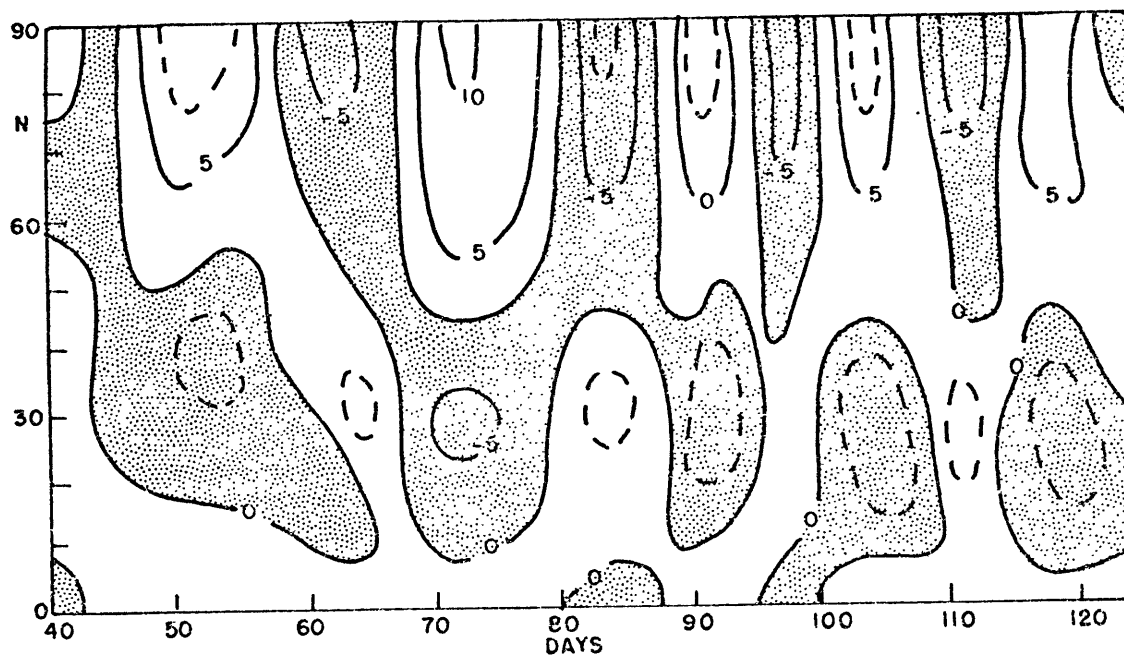

Fig. 27. Time series of change in mean zonal temperature at 10 mb
due to advection by the eddies. ° day^{-1}, for Ex. D.

In order to examine the warmings at 10 mb in greater detail, we consider the complete temperature field time series for the N.H. in Fig. 26. At 2 mb, a similar time series is not very revealing, since at all times the temperature gradient was poleward. At 10 mb however, complete reversals in the temperature gradient occurred and were accompanied by increased easterlies at high latitudes. Both these features are generally regarded as constituting a major warming. The largest warming peaked on day 80.

Coupled with the warming at high latitudes is a cooling trend at low latitudes (Fig. 26). Both these changes were being offset by an induced meridional cell, with upward motion at the pole and sinking at lower latitudes. This has been noted in warmings in the atmosphere, (Quiroz, 1969; Mahlman, 1969). It is apparently the source of the easterly acceleration of the zonal flow at high latitudes which accompanies the warming.

Clearly the warming is not caused by subsidence. Fig. 27 shows the change in temperature at 10 mb as a function of latitude due to advection of the temperature field by the eddies. Hence the warming is produced by the northward flux of heat by the eddies. Diabatic effects were continually acting to cool the high latitude region, but Fig. 27 also shows most of the cooling to have a dynamic source.

At 2 mb, the polar temperature fluctuated more than at the lower level but warmings of 10°K over 4 or 5 days were common. Most of these changes were due to the eddies, but the meridional cell induced by the

warming at 10 mb was also of significance.

An example of the streamlines and temperature field at 10 mb in the midst of a warming is given for day 74 in Fig. 28. Temperatures are deviation: from the mean for the globe (231°K).

The northward heat flux is the source of the warmings, and in a quasigeostrophic model it is directly related to the conversion of AZ to AE (CA). Therefore in the following sections the energetics are examined in detail in order to find the antecedent of the flux.

8.2 Energetics Time Series

In this section, a brief presentation is made of the variation in the eddy energy terms for Ex. D. Fig. 29 shows time series of the vertical integral of AE and KE for the N.H. troposphere (1000-200 mb), lower stratosphere (200-20 mb), and upper stratosphere (above 20 mb) values. Note the different scale for each quantity, given at left.

The very regular oscillation in AE in the troposphere is quite striking. The lack of any such feature in the tropospheric KE is an indication that it is in the very long wave, (wave 2), in which the ratio of AE:KE is much greater than unity. In the lower stratosphere the fluctuation is not as regular, and the two maxima in January are much less than those of December. Most of the variability of the total KE is present in the lower stratosphere. In this region each maximum in the AE curve corresponds to a double maximum in KE and lags slightly behind the first. AE in the upper stratosphere has no major character-
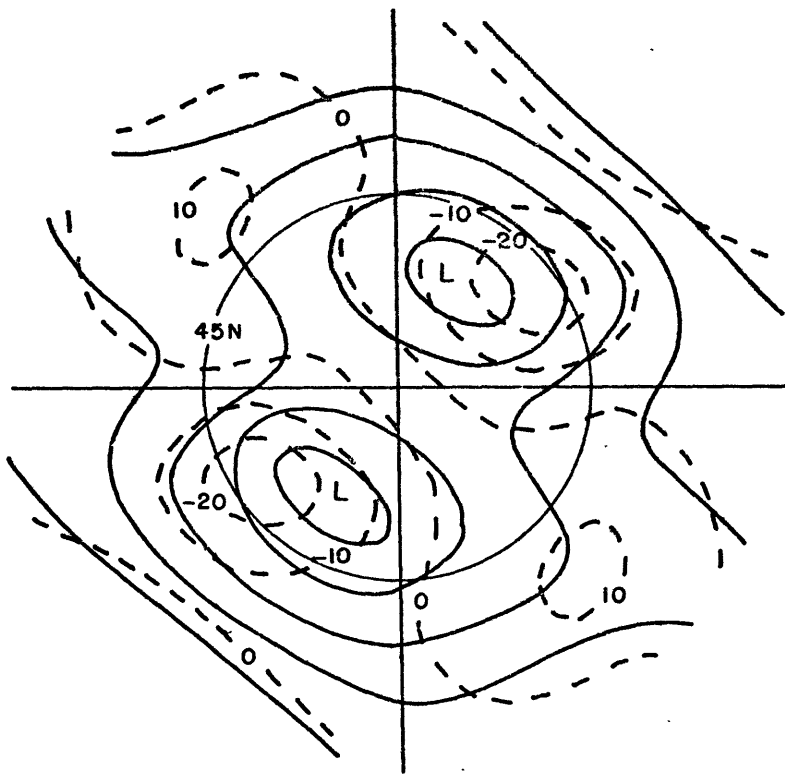
Fig. 28.   Streamline and temperature field at 10 mb on day 74.
Temperatures are deviation from 231°K, streamline
interval is 5×10^7 m^2 sec^{-1}.

istics although KE still shows similar features to the lower strato-

spheric curve but with a lag of a few days.

In Fig. 30 the corresponding curves for the S.H. are presented

for comparison and completeness. Note the different scales at left.

These time series show little character, particularly in the strato-

sphere. KE has a small cyclic response in the troposphere but is due

to variations in K6 and to a lesser extent K4. Apparently the existence

of nonzonal forcing which affects a progressive wave with a certain

period, has induced a cyclic response in the other waves. This is most

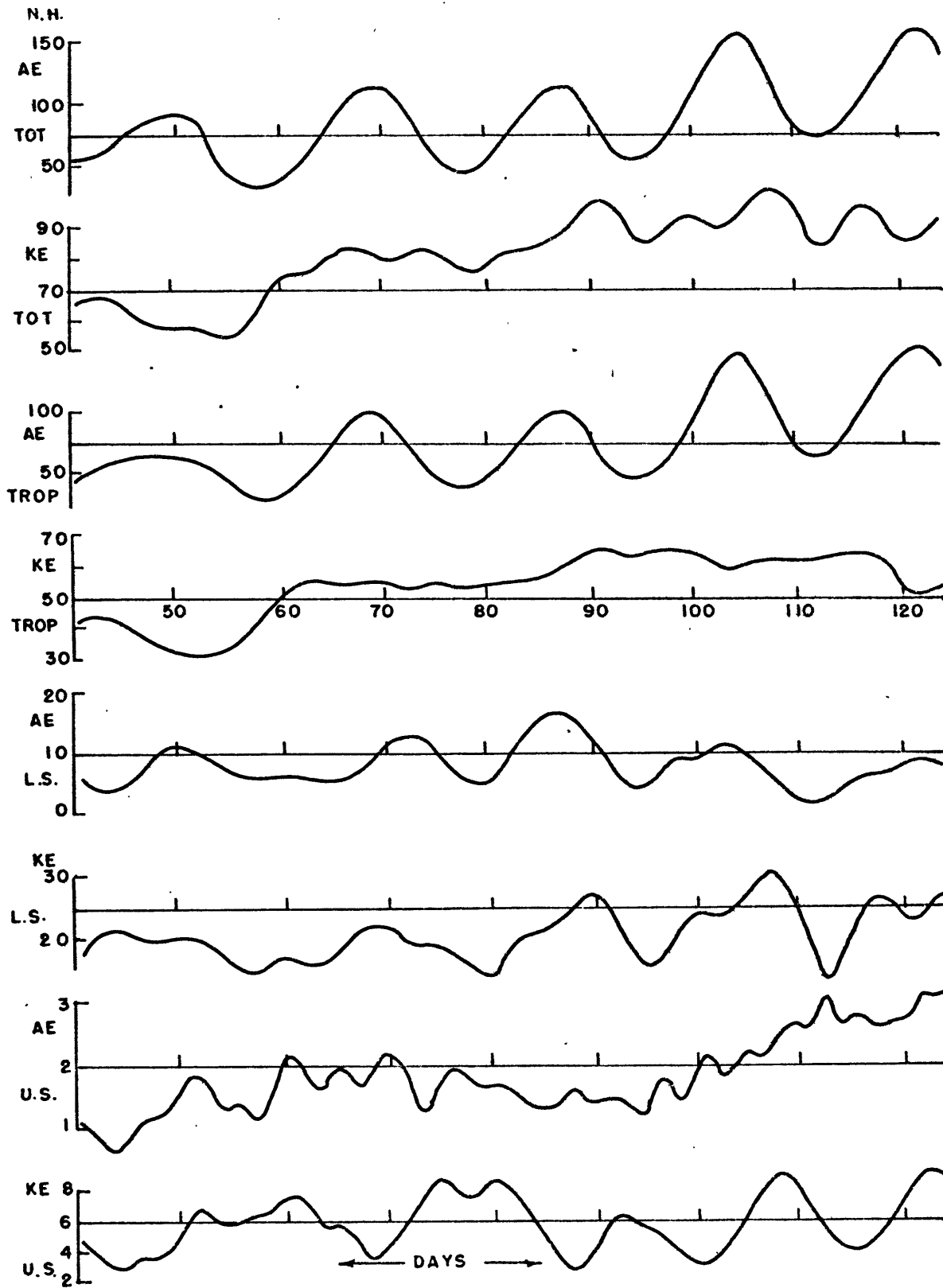likely caused by the limited number of waves represented in the model.

Fig. 29. N.H. eddy energy terms for Ex.D. Total, troposphere, lower and upper stratosphere values in 10^7 ergs cm^{-2}.
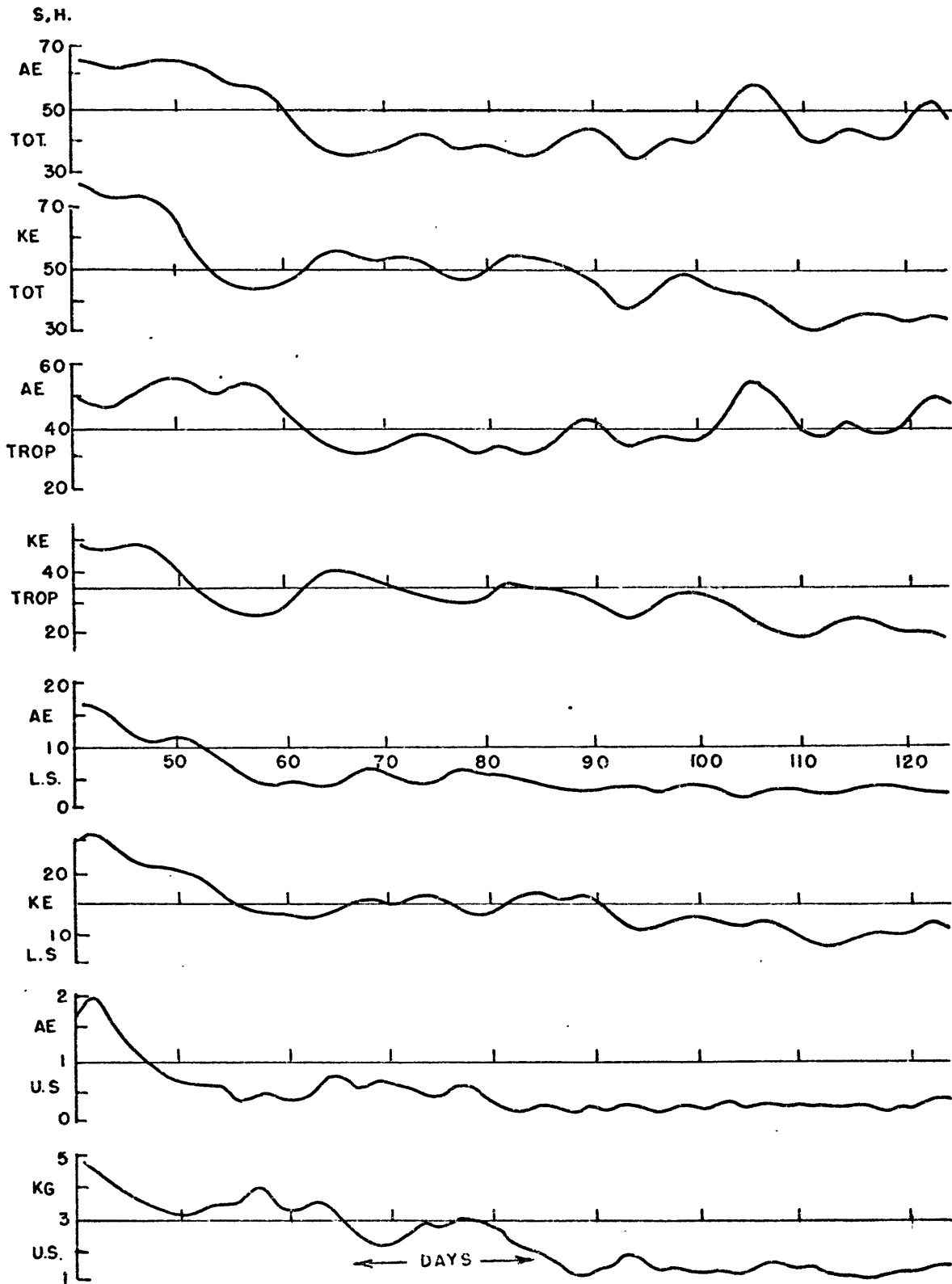
Fig. 30. As for Fig. 29 but for S.H.

The variability of the energy components in the atmosphere has not been studied in great detail. Krueger et al. (1965) presented 10-day mean values for the lower part of the troposphere and computed standard deviations of the quantities. The model values are not unreasonable in comparison. Dopplick (1971) considered daily values of zonal and eddy forms of energy in the lower stratosphere for 1964. His computations reveal an almost cyclic oscillation in AE throughout the first three months of 1964 with a period of roughly two weeks and a range of values comparable to those in Fig. 29. Holloway and Manabe (1971) presented time series for the rate of change of eddy kinetic energy for the N.H. of their global model. This also showed a very marked cyclic oscillation with a period of roughly two weeks and a range greater than found here. Therefore the model energy terms show similar large scale variability to that observed and found in more sophisticated models.

In order to determine the relation between the variations in the troposphere and the higher levels, we consider the vertical flux of eddy energy through 200 mb and 20 mb in Fig. 31. Global, N.H. and S.H. values are shown.

In the S.H. the flux through 200 mb is reasonably constant, and, as expected from the theory (section 2.4), is very small through 20 mb. Dopplick (1971) presented values of this flux through 100 mb and 10 mb for 1964. The model shows excellent agreement with his summer values once allowance is made for the different levels.
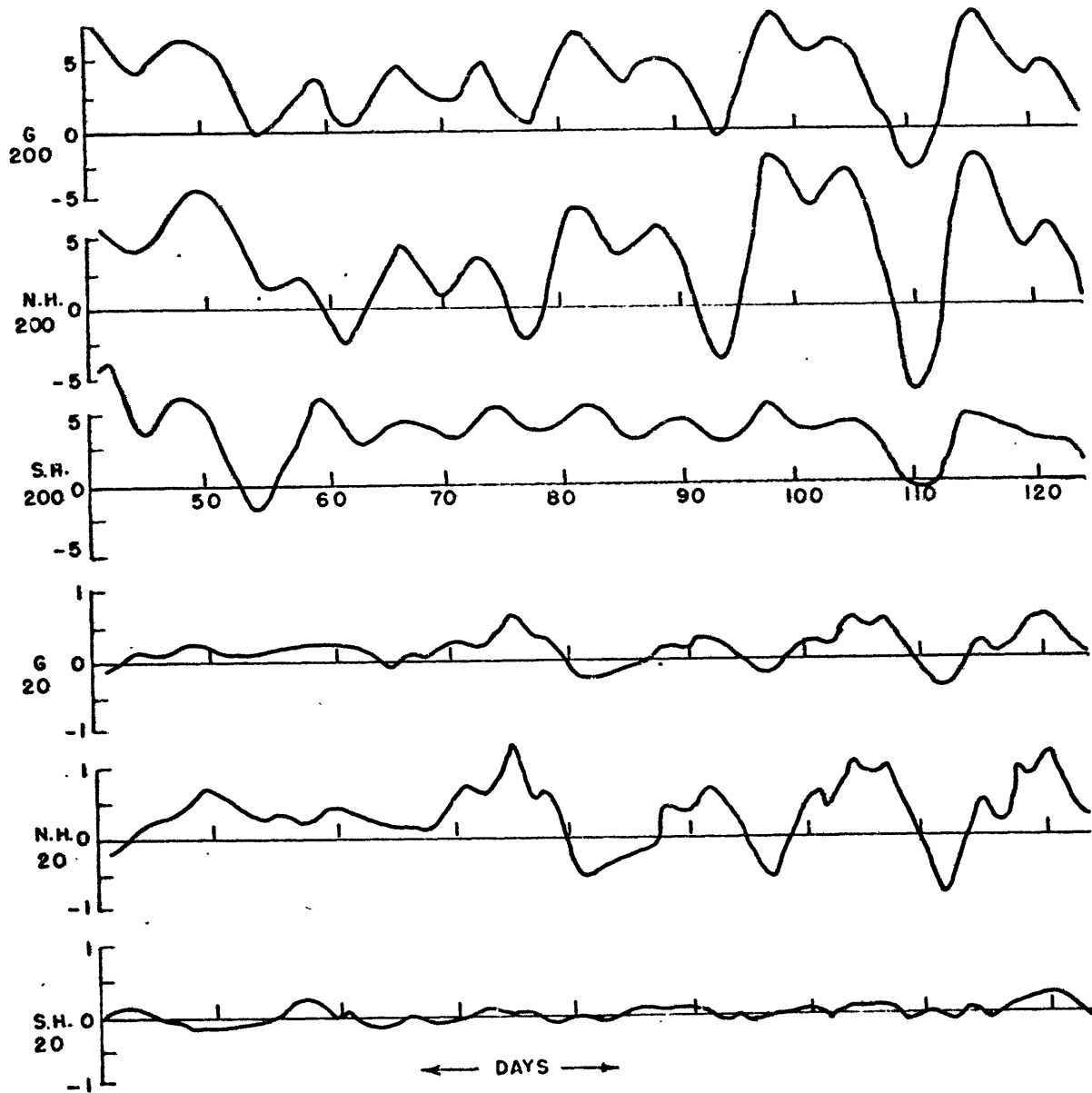
Fig. 31. $\nabla \mathcal{E}_E$, the vertical propagation of eddy geopotential energy in 10^2 ergs cm^{-2} sec^{-1} for the globe (G), N.H. and S.H. through 200 mb and 20 mb, for Ex. D.

However, Fig. 31 shows the flux through 200 mb in the N.H. is extremely variable. At 20 mb the variations are also quite marked and appear to correspond to fluctuations at the lower level with a lag of a few days. This point will be expanded and clarified later.

Dopplick's calculations for winter indicate that the atmospheric values are slightly larger and have greater range than those in Fig. 31. Nevertheless the overall features were rather similar, and Dopplick's values also showed the largest surges to be regularly spaced at two to three week intervals.

The excellent resemblance between the model and the atmosphere in the character of the time series of the lower stratospheric energy and the flux of geopotential into and out of the region shows that in spite of the appearance of a number of discrepancies in the tropospheric circulation, the forcing of the upper atmosphere in the model, and hence perhaps its response, may be quite realistic.

8.3 The Stationary Features

Orographically induced disturbances have little or no phase change with height, whereas nonzonal heating may maintain stationary disturbances with either westward or eastward slope with height, (Saltzman, 1965; Murakami, 1967). Mean tropospheric charts for the N.H. in January (e.g. Willett and Sanders, 1959) reveal the Aleutian low to slope very strongly westward with height. The Aleutian anti-cyclone is a prominent stationary perturbation which extends to very

high levels in the stratosphere (e.g. Finger, Woolf and Anderson, 1966), and has been related to tropospheric cyclogenesis by Boville (1960). Since the Aleutian low seems to be maintained primarily by nonzonal heating (Holopainen, 1970), the evidence suggests a direct association with the Aleutian high aloft.

Although the Aleutian system has a large wave 1 component, the stationary component in the model in Ex. D has a similar structure, but with an even greater slope with height, see Fig. 23. Both are baroclinic systems maintained by nonzonal heating and propagate energy to higher levels. Associated with these features is the considerably warmer temperatures which exist in the winter N.H. stratosphere (Ex.D) compared to the S.H. stratosphere (Ex. A), see table 5.

8.4 Energetics of Sudden Warmings

In chapter 1 we subdivided the problem of sudden warmings into three stages.

i) the mechanism of the production of the long wave energy which is propagated upwards and ultimately produces the warming

ii) the mechanisms of the propagation of this energy

iii) the absorption of this energy and the mechanism of the warming itself.

In order to evaluate the role of the vertical flux of energy we consider these in reverse. The remainder of this chapter will be concerned only with the N.H. (winter), unless otherwise stated.

8.4.1   States II and III

The manifestations of stage III of the sudden warming were pre-
sented in section 8.1, but an explanation of the mechanism was not made.
This will be done here.

In Fig. 32 a time series of the vertical flux of eddy geopotential
energy is shown as a function of height for the N.H. in Ex. D . Fig. 32a
shows the wave 2 component and Fig. 32b shows the total for all waves.
The levels at which this quantity was evaluated are shown at right. At
1000 mb, the value shown is the contribution to KE by the orographic
distortion of the flow. Values are in 10^2 ergs cm^{-2} sec^{-1}, and between
levels the isolines were subjectively analysed. Upward propagation is
positive. The vertical gradient of this quantity shows the net contri-
bution of this form of energy to a given layer.

We first note the very strong resemblance between the patterns
in the stratosphere above 20 km showing the overwhelming dominance of
wave 2 in this region. This was true in all energetics terms so that
only the contribution of the wave 2 component was of significance there.

In Fig. 33 a similar presentation to that in Fig. 32b is shown
for the conversion CA (actually CAZ), and Fig. 34 shows that for CE
(actually CEK). In these two figures the conversion takes place in
the layer centered on the level given at right, and the units are
ergs cm^{-2} sec^{-1} mb^{-1} . These units are somewhat misleading in inter-
preting the meaning of these diagrams owing to the different scale
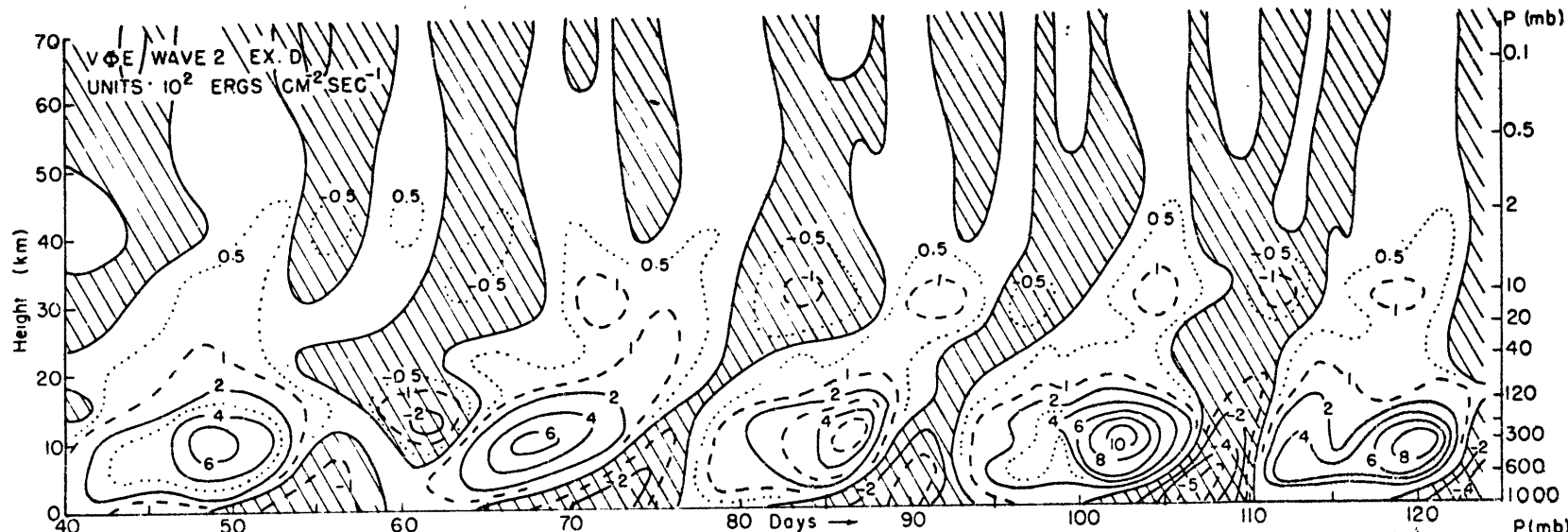1 mb occupies at high and low levels.
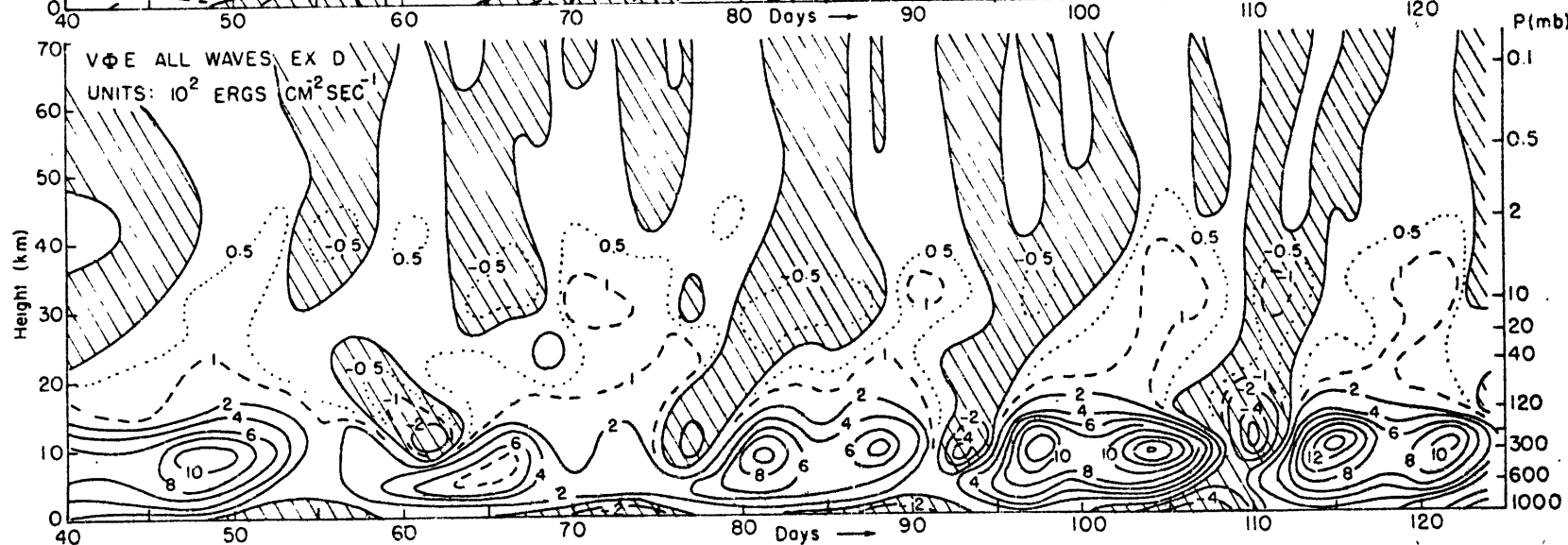
Fig. 32a.

Fig. 32b.

Fig. 32.   Vertical propagation of eddy geopotential energy ($v\bar{\Phi}\epsilon$); above: wave 2 component
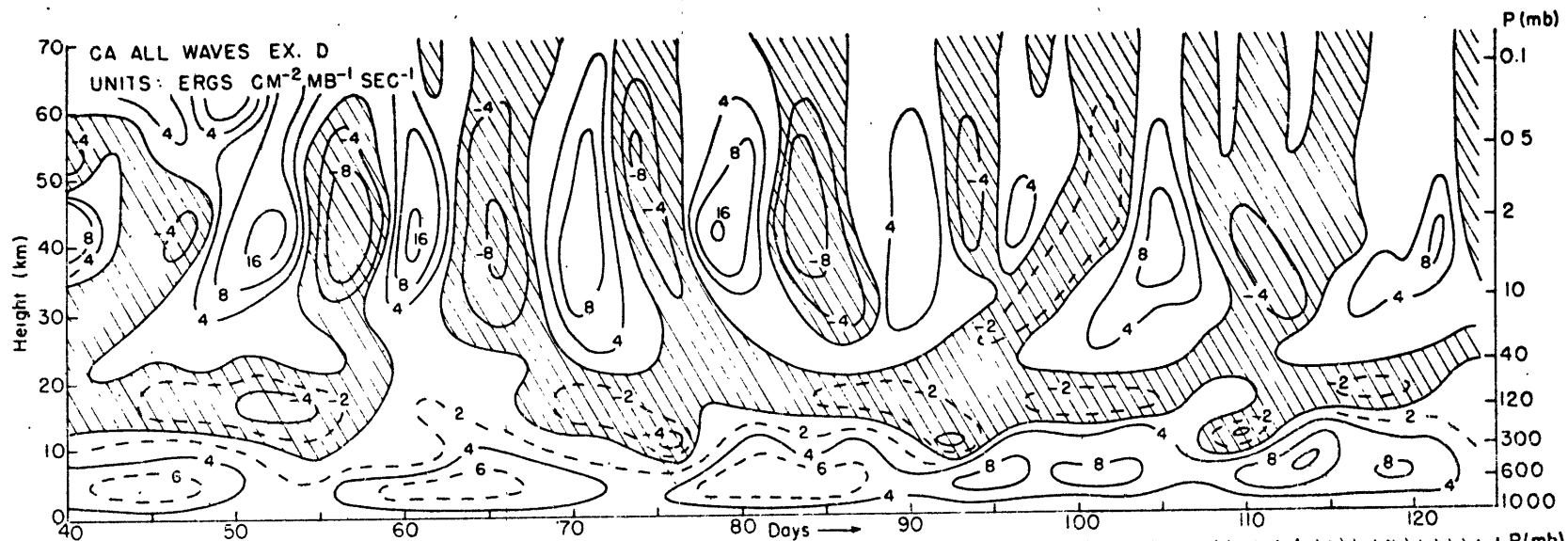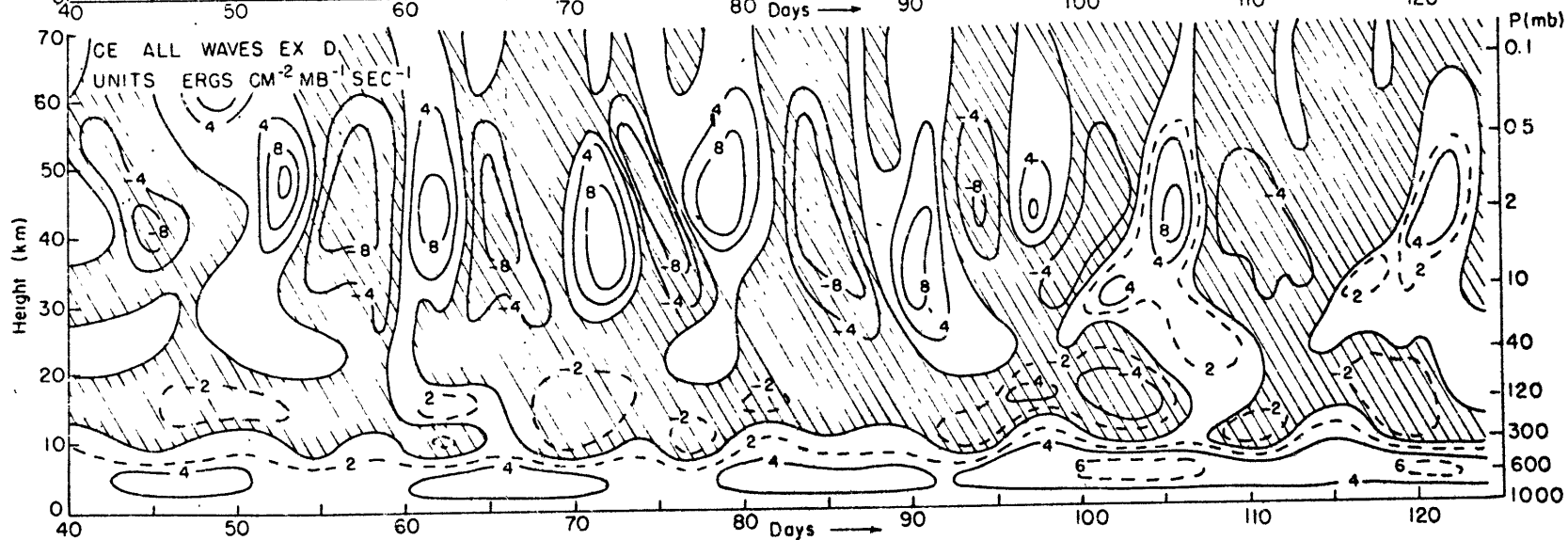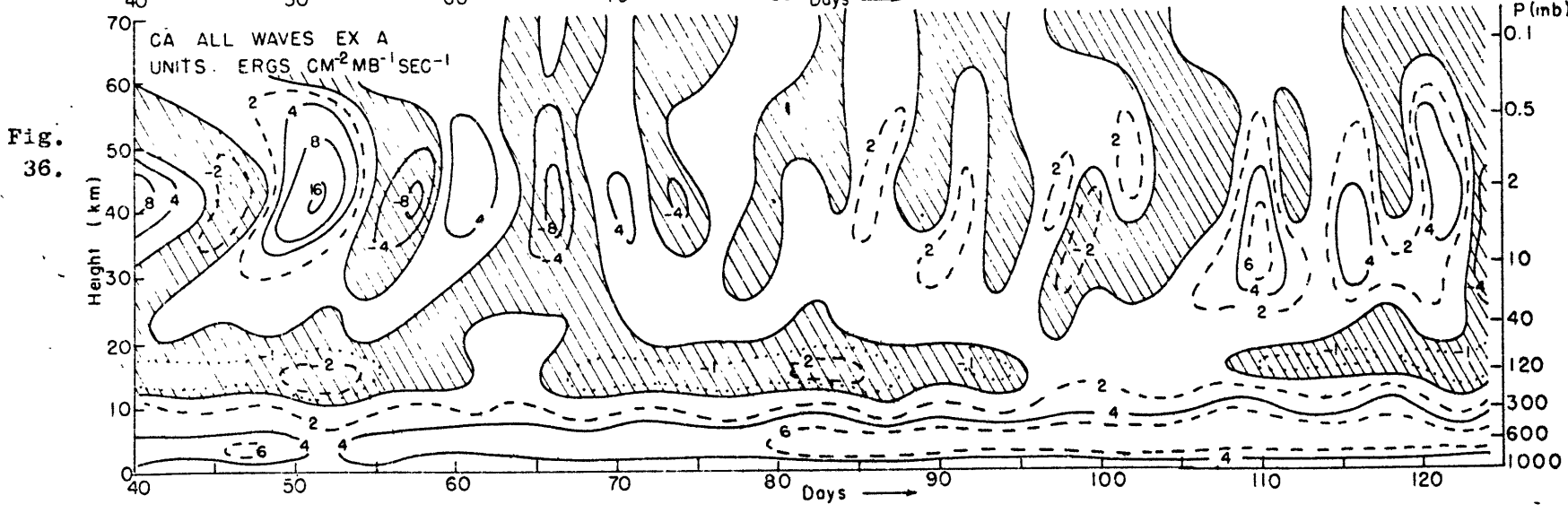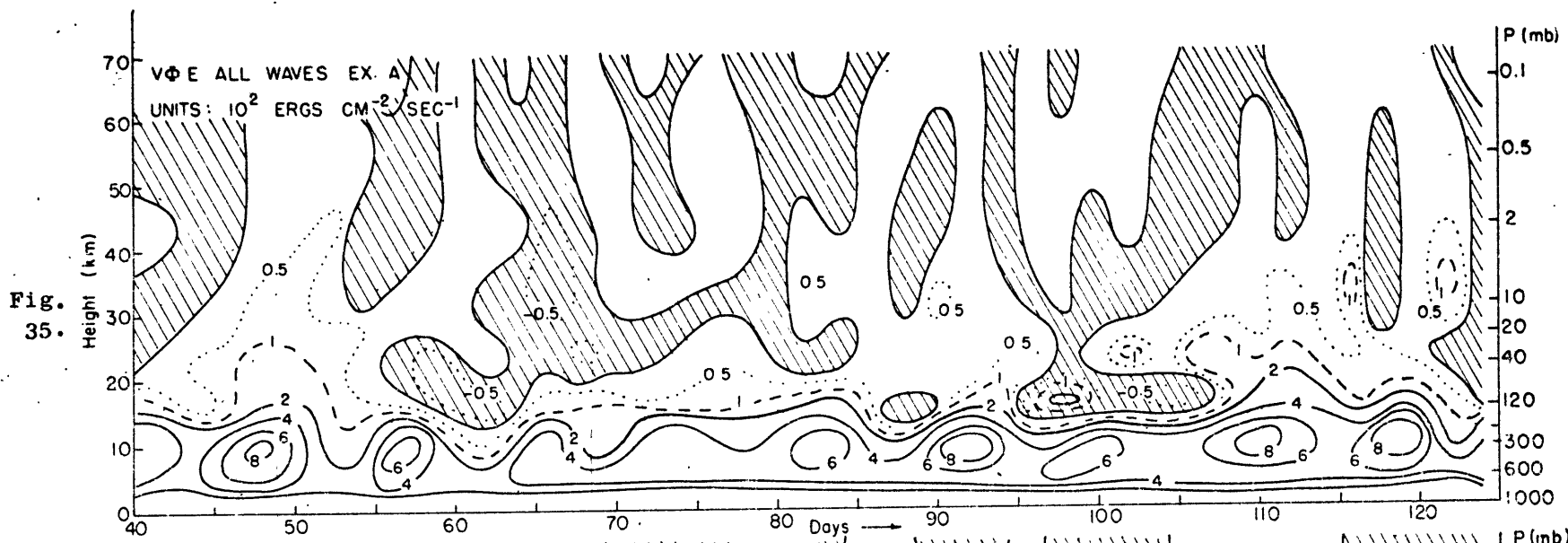below: all waves, for Ex. D.

Figs. 33 and 34. Baroclinic conversions, CA (above) and CE (below) for Ex. D.

Figs. 35 and 36. As for Fig. 32b and 33, but for Ex. A.

Both figures 33 and 34 reveal the existence of a double maximum in the values, in the troposphere and in the 10-2 mb region.

For comparison, the diagrams corresponding to Figs. 32b and 33 are shown for Ex. A in Figs. 35 and 36.

In section 7.3.2 we noted the increase in CA and $\overline{v'\phi'}$ in Ex. D in the upper stratosphere, while CE did not change a great deal. Figures 32 to 36 show the interrelation of these quantities and how they relate to sudden warmings.

Eliassen and Palm (1961) showed that stationary waves which propagate energy upwards are accompanied by a poleward heat transport and a westward slope with height. In a poleward temperature gradient, for quasigeostrophic motion, this implies for $\overline{v'\phi'}$ positive, that CA is also positive. Figures 27 and 32 to 36 show this also to be true for transient wave propagation.

In Ex. D, at 2 mb, the temperature gradient remained polewards so that CA had the same sign as the northward flux of heat. This was also true at 10 mb till day 54, and from day 62 to 75, but at other times the coldest temperatures were in mid-latitudes, see Fig. 26. Then, the hemispheric value of CA for a poleward heat flux will be composed of upgradient heat transports, (negative CA) at high latitudes, and down-gradient heat transports, (positive CA) in low latitudes. A comparison of Fig. 27 with Fig. 33 at 10 mb shows the high latitude region to dominate the hemisphere from days 54 to 62 and 75 to 84.

A major sudden warming is thus revealed to consist of two phases:

(a) In a poleward temperature gradient with westerly winds, a large surge in upwards propagating energy is accompanied by a northward flux of heat; so that for $\nabla \overline{\Phi E}$ upwards, CA is positive. The relation with CE is not as distinct, but positive values generally follow positive CA with a slight lag. The induced meridional circulation opposes the high latitude warming trend and produces an easterly acceleration of the zonal winds in this region. In general the vertical flux of energy does not modify the zonal flow to the second order, (Charney and Drazin, 1961), but transient wave propagation of energy is accompanied by a vertical gradient of northward heat flux which produces a net warming at high latitudes, (Matsuno, 1971). This phase of the warming is the same as the first stage described by Matsuno.

If this upward flux is sustained for any period a reversal in the temperature gradient will result from this process.

(b) At this point CE and CA become negative and the upward flux of geopotential drives upgradient heat transports in the manner akin to the forcing of the lower stratosphere. The formation of a critical layer follows shortly thereafter. Then, the existence of an upward flux of energy is sufficient to continue the warming. The energy is absorbed and the warming becomes localized and may begin to propagate downwards. Matsuno (1971) considers the second stage to begin once the critical layer has formed, but the energetics change prior to that point.

Phase (a) would constitute a minor warming, and the upward flux of energy is not absorbed but instead induces baroclinic growth of the eddy,

$$KZ \longrightarrow AZ \longrightarrow AE \longrightarrow KE.$$

This in turn results in a divergence of the upward energy flux in the layer. Many examples of this exist in the model, as may be seen in Fig. 32 where the flux through 10 mb was generally greater than that through 40 mb.

Phase (b) constitutes a major warming, and the source of energy for the warming is a convergence of the upward propagating energy into the layer,

$$KE \longrightarrow AE \longrightarrow AZ.$$
$$\uparrow$$
$$V \overline{\Phi} E$$

We have described phase (b) as it probably pertains to the atmosphere, but owing to the unrealistic structure of the lower stratosphere the model did not behave in quite this manner. The lack of sustained upward energy flux also meant that the warming did not extend over the entire hemisphere of the model.

Eliassen and Palm (1961) discussed the nature of the vertical flux of energy as a function of the zonal wind field, and in particular with regard to the change from divergence to convergence of the flux where the vertical shear of the wind reverses above the tropospheric jet. In both phases of the warming described above energy may still propagate, but will be either enhanced (phase a) or damped (phase b). It will be

unable to propagate only when a critical layer is formed. These aspects of stage II of the warming, i.e. the theory of the vertical propagation of energy, seem to be explained by the theory as outlined in section 2.4.

In the model, major warmings where both phases were enacted occurred on days 58 and 80. At other times, the temperature gradient had already reversed so that phase (a) did not occur. The study by Dopplick (1971) indicates that both phases are found in the atmosphere.

The manner in which we have delineated the warming is somewhat different from the aspects stressed by Matsuno (1971). His description required the first stage to continue until a 'critical layer interaction' took place.

The critical layer concept arises from a singularity in linear theory, where u (the zonal wind speed) equals c (the phase speed of the wave), see for example Charney and Drazin (1961). In our model it is not well defined owing to the transient nature of the waves, so that c is complex. Because of the unrealistic structure of the model winter lower stratosphere, easterlies were frequently present at high latitudes in the stratosphere, see Fig. 19. Therefore the real part of c did equal u at some part of the atmosphere. However, this did not seem to play a major role in the model.

The division used above not only distinguishes minor from major warmings but also separates the role of the vertical flux of energy into two phases and divides the baroclinically direct energy cycle prior to

the warming from the driven energy cycle during the latter stage. However, the formation of a critical layer is undoubtedly important for a complete changeover and downwards propagation of the warming.

8.4.2 Stage I

In the model the lower stratosphere did not include a baroclinic region at high latitudes, and as such, acted as a sink to the upward flux of energy emanating from the troposphere, see Figs. 32 and 35. For this reason, as noted in section 8.2, the vertical flux of energy at higher levels was less than found in the atmosphere.

The importance of the transient wave, and in particular the transient component in time of the very long wave, in the sudden warming has been brought out in the previous section. Matsuno (1971) established the reason being in the resulting modification it causes in the zonal flow. In anticipation of this, at the inception of this study, we established a number of hypotheses in chapter 3 which considered possible sources of rapid changes in the intensity of the circulation in the troposphere. These changes in activity were regarded as being part of the familiar index cycle. We therefore consider the tropospheric activity, its relation to the index cycle of the model and reasons for its existence.

Tropospheric Activity in N.H.

The tropospheric energetics conversion terms reveal the source of the energy which is propagated in wave 2. These are shown in Fig. 37, excluding horizontal boundary terms, D2 which was similar to K2 varia-
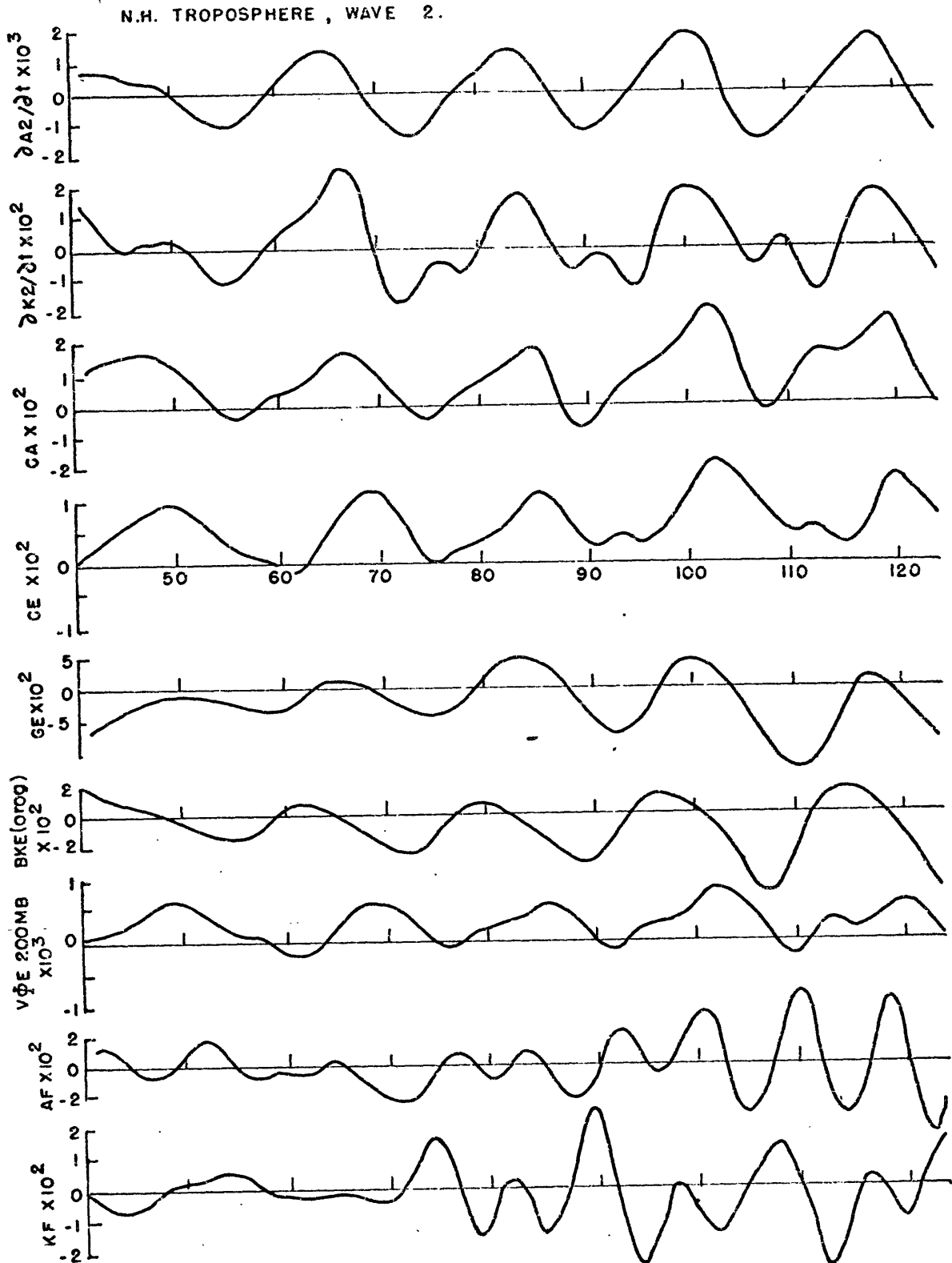
Fig. 37. N.H. tropospheric conversions for wave 2 component (ergs cm^{-2} sec^{-1}) for Ex. D.

tions, and CK which was small and changed very little in time compared to the other terms. The major source of the change in baroclinic activity in the troposphere was in the nonlinear response to the nonzonal heating by the traveling wave, as already mentioned in sections 7.2.1 and 7.3.4. In Fig. 37 it may be seen as a regular fluctuation in GE, increasing in amplitude as the winter season progressed. The major part of the variation in CA, CE and $\nabla \vec{\phi} E_{200\,mb}$ was associated with this, with a lag of a few days in CA, and a further lag in CE and $\nabla \vec{\phi} E_{200}$.

However, Fig. 32a reveals a tendency for a double maximum in the wave 2 component of $\nabla \vec{\phi} E$ in the troposphere. In Fig. 32b the second maximum was further emphasized with all waves considered. Apparently this reflects the limited number of waves in the model and the nature of the response in wave 4 noted in section 7.3.4. Thus the secondary maximum may be associated with a nonlinear gain in A2 by interactions of other waves (AF).

The $\partial K2/\partial t$ curve exhibits a marked secondary maximum that seems related to the nonlinear gain (KF), and the orographic term (BKE orog). These two terms are of the same order. As anticipated in section 7.2.3 the orographic reinforcement took place about 5 days prior to the nonzonal heating reinforcement.

The level of activity in Ex. A was much more nearly constant, see Figs. 35 and 36. The most notable change occurred with an increase in circulation intensity in early January (see section 7.1.2), mainly in the wave 2 component. This resulted in a minor warming at 40 mb and

10 mb from day 112-121, see Fig. 25a.

Index Cycle

In chapter 3, we attempted to relate the concept of an index cycle to changes in the intensity of the baroclinic energy cycle in the troposphere. Fig. 38 compares the intensity of the eddy conversion (CE) in the troposphere with parameters normally used to measure the index cycle. Shown is the latitude and strength of the N.H. tropospheric jet at 200 mb. This level is somewhat higher than that used in most measures of the index cycle. The latitude and strength were estimated from values calculated each day every 10° of longitude.

While the overall seasonal trend of these two quantities is opposite in Fig. 38, the modulations are in phase with one another and with those in CE. In the model, a decrease in strength is therefore associated with an equatorwards movement of the jet and increased eddy activity. These patterns are also found in the atmosphere when a high index situation changes to low index, Willett and Sanders (1959).

In Ex. A there were no marked short term fluctuations such as those in Fig. 38. The difference is also apparent between KZ variations in Fig. 12 and Fig. 21. KE showed only small fluctuations in Fig. 12, but Fig. 13 reveals each wave component of KE to undergo marked undulations, roughly compensating one another. Thus while no marked index cycle exists, a distinct baroclinic energy cycle may occur on a given scale.
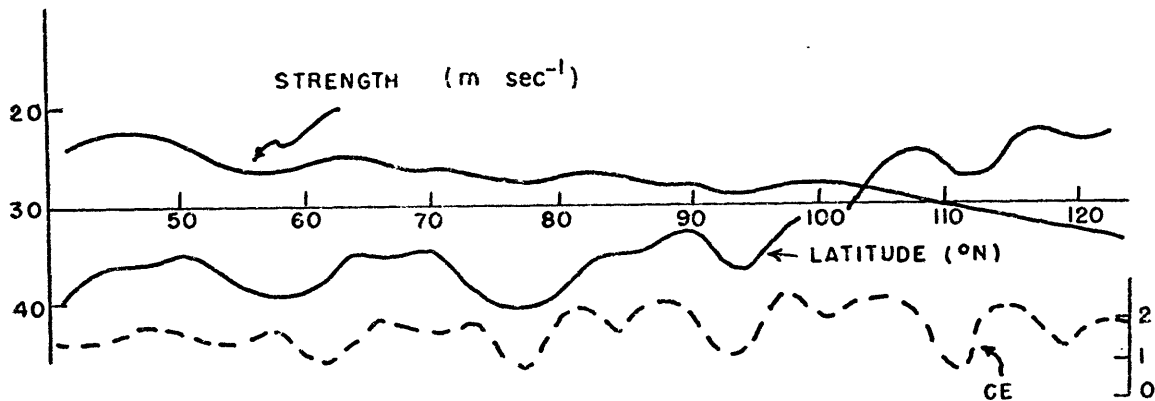
Fig. 38. Variation of latitude and strength of tropospheric jet
in N.H. for Ex. D., scale at left.
Dashed curve is the intensity of the eddy circulation (CE)
in the N.H. troposphere, (10^3 ergs cm^{-2} sec^{-1}), scale at
right.

In Ex. D the existence of a marked index cycle was associated

with the periodic response of wave 2, as the traveling wave interacted

with the stationary forcing. We have already noted the existence of a

similar traveling wave in the atmosphere and a fluctuation of a similar

period in observed N.H. energetics. However we can only speculate as

to whether these are associated. This period of two to three weeks is

also less than that generally associated with the index cycle.

Tropospheric Source of Warming

By relating sudden stratospheric warmings, and the vertical flux

of energy which causes them, to large changes in the level of activity

of the tropospheric very long waves, we may be able to establish a means

of predicting the events. Fig. 32 indicates that the lag in time be-

tween the tropospheric activity and the resulting modification of the

upper atmosphere may be from three days to a week. The actual response

of the upper atmosphere is dependent upon its initial state, but either

phase (a) or phase (b) kinds of events should be expected. Once these begin however, the induced meridional circulation must also be considered in determining the net effect at a given level. The level at which the warming is a maximum, and therefore the level which dominates those above, may be difficult to determine as it is dependent upon many factors. In our model it was reasonably clearcut owing to the finite resolution in the vertical. This aspect will not be considered further here.

However, we shall consider the events in the troposphere which ultimately result in the warming. We have found the source of the changes in activity in the long waves in the model and have related these changes to the index cycle. Therefore we have shown the relevance of the discussion in chapter 3. We shall now reconsider the hypotheses.

As we have seen, all events which affect the long waves may be important, and variations in their degree of importance may account for the variations in the sudden warmings which are observed from year to year. The effect of orography, $H(1)$, and the contribution from the interactions between other waves, $H(4)$, seem to be of secondary importance and may play this subsidiary role. On the basis of the performance of the waves in our model, it was not considered worthwhile carrying out the experiment outlined in section 3.5, experiment (f), without incorporating some improvements.

The primary source of the long wave activity in the model was a nonlinear response of the traveling wave to the nonzonal heating. Thus

a combination of H(2) and H(3) is the cause of stage III of the sudden warming. However, as noted in section 7.3.4, there is some doubt about the applicability of the events in the model to those in the atmosphere. Nevertheless in section 8.2 we noted observations which show similar kinds of periodicities to exist in the atmosphere, and in more sophisticated models. The existence of the transient and stationary components of the long waves has also been established (see sections 2.3.2 and 7.3.4).

Hence there does seem to be a good possibility that the atmosphere exhibits a response to nonlinear interactions between the stationary and transient wave component. A possible alternative is an interaction between the wave and transient forcing. As noted in chapter 3, H(2), the nonzonal heating may be particularly susceptible to a transient component if the shorter cyclone waves release latent heat on a scale which affects the long wave as they are steered by the larger scale.

However the model does indicate another possibility. The existence of an index cycle on the scale of the long wave, H(3), may be an important mechanism in the atmosphere.

In section 3.1 we noted the change in the dominant wave in the circulation as the seasons progress. It is revealed to be caused by the seasonally increasing meridional temperature gradient producing an increase in the intensity of the circulation. This augments the upwards heat flux thereby increasing the static stability. While the latter effect was precluded in the model, the increase in the intensity of the circulation during January was most noticeable in Ex. A, and it

also occurred in Ex. D. In the former case it was directly associated with a minor warming.

Apparently it is a common feature of the observed circulation, Krueger et al. (1965). Their computations were for October 1958 to July 1963 and showed the most marked change of this sort to occur in the first week of January 1963. At this time a large increase in baroclinic conversion terms produced a marked decrease in AZ while KE increased, in the 850-500 mb layer. This was apparently the source of the vertically propagating energy which produced the major sudden stratospheric warming that followed a week or so later, (Finger and Teweles, 1964; Miyakoda, 1963).

Tropospheric blocking was not present in the model owing to the truncation of modes (Kikuchi, 1969), but it may follow the intense tropospheric activity as a part of the index cycle, as noted in section 3.4.

If this is the primary cause of sudden warmings in the atmosphere, it should also be observed in the S.H. However, owing to the presence of large scale stationary features in the N.H. the initial state of the stratosphere in each hemisphere is quite different, and phase (a) would need to persist much longer in the S.H. in order to overcome the much colder polar temperatures. This may result in only a minor warming, as occurred in Ex. A, and which has been found in the S.H. Nevertheless it is also very likely that the seasonally increasing land-sea contrast is also a major factor in the N.H.

Other possible effects mentioned in chapter 3 were not of great importance in the model but cannot be entirely ruled out. Quasiresonance was important for wave 4 and as such served to enhance wave 2 at times through nonlinear interactions. A major source of wave 1 energy appears to come from nonlinear interactions in the atmosphere (Saltzman and Teweles, 1964), and in the G.F.D.L. model, (Manabe et al., 1970). Hence while these studies show this to be unimportant in wave 2, it may be of significance in wave 1.

8.5 The S.H. Spring Warming

Recent satellite soundings have been processed to produce an untold wealth of new information on the higher levels of the atmosphere in both hemispheres. In particular Barnett et al. (1971b) have produced mean meridional temperature cross sections of latitude versus height for the globe, extending to 0.5 mb, on a daily basis since mid 1970 from Nimbus 4 data.

An aspect of this information which has relevance to the S.H. spring warmings is the very large difference in the time at which the coldest temperatures are observed at different levels. Table 6 shows the mean meridional temperature $^\circ$K at levels 2, 10 and 50 mb.

We note that at 2 mb, the coldest temperatures occur about the time of the solstice. At 10 mb there is some lag, but at 50 mb, there was little change until October. The temperatures at 80°S are generally warmer than at 60°S at 2 mb. By October this is

P. mb		19 May	15 June	16 July	16 August	18 Sept	15 Oct	21 Nov	1970
2	80S	246	236	240	262	272	282	285	
	60S	240	230	240	259	259	261	280	
10	80S	215	214	202	218	228	244	254	
	60S	216	214	211	224	232	237	246	
50	80S	195	193	185	185	192	207	234	
	60S	208	208	203	208	212	222	227	

Table 6. Meridional temperatures at 80S and 60S for dates and levels as shown. From Barnett et al. (1971b) and extra profiles furnished by C.D. Rogers (private communication).

also true at 10 mb. Therefore the spring warming which occurs at 50 mb is preceded by a marked change in the temperatures and temperature gradients at higher levels. Solar heating is of significance during the later months, but the temperature increases in polar regions at 2 mb tended to take place in surges spaced at roughly two week intervals, beginning late June (C.D. Rogers, private communication).

Therefore, even in the S.H., the spring warming is most likely a result of vertically propagating energy out of the troposphere, which modifies the upper stratosphere, and with the aid of solar heating progressively affects lower levels by lowering the trapping layer.

CHAPTER IX

CONCLUDING REMARKS

In this thesis we studied the tropospheric-stratospheric inter-action with particular attention given to the sudden stratospheric warmings. Some byproducts emerged from the numerical model which was used as the primary tool. The model is a quasigeostrophic spectral model but has many features not included in previous investigations. It is global and is very extensive in the vertical with the highest level in the mesosphere at 0.05 mb ($\sim$ 71 km), and about 10 km resolution in the stratosphere. The model also incorporates an annual heating cycle, so that each hemisphere exhibits opposite seasonal circulations and trends.

In order to help establish the characteristics of the model, a linear baroclinic analysis was made using a similar model. This considered single modes of each wave imbedded in a realistic basic flow and was formulated on a sphere with similar vertical resolution in the troposphere. The study not only proved to be a useful guide in evaluating the model, but it also revealed some new features in this problem with regard to the spherical geometry. In particular, the long wave region of instability is shown to contain significant growth rates.

While the model is clearly deficient in a number of ways, (see sections 7.1.4 and 7.3.4), it appears suitable for the problem chosen for investigation here, and provides some insight into other aspects

of the upper atmospheric circulation which to date have been largely speculative.

The manner in which the symmetric version (i.e. no eddies) of the model responded to the annual heating cycle is of considerable interest, as is the response of this circulation to the introduction of an eddy perturbation. In our initialization, the perturbation was introduced only in the troposphere and the model responded with sudden warming type of events in each hemisphere. It would also be of interest to determine the response to perturbations introduced at other levels, although the limited vertical resolution of the model may restrict the value of such an experiment. For example, for predictability purposes, it is of interest to determine the growth rates and the degree to which a lack of knowledge of the initial state in the stratosphere may affect a forecast at lower levels.

The general features of the simulation of months December and January were extremely good for the most part, in both hemispheres and at all levels. Although the effects of eddies on the model stratosphere in Ex.A were probably less than exists in the atmosphere, the model indicated their importance, especially in winter, and showed them to be at least partly responsible for the observed temperature distribution in the mesosphere.

Our other experiments indicate that while the mountains are of significance in the angular momentum budget, they play only a minor role in the energy budget. In contrast, the effect of nonzonal heating

on the model atmosphere energetics was very marked. This was included in order to simulate the land-sea heating contrast, and its addition increased the role of the longer wave, and increased the intensity of the circulation. To date, no detailed energetics analysis has been made of a sophisticated general circulation model which includes this effect.

Experiment D, in which both orography and nonzonal heating were incorporated, when compared to the integration without these effects, successfully reproduced the same kinds of differences observed between the northern and southern hemisphere winter circulations. The stationary component of the flow exhibited a marked wave 2 component in the model stratosphere. This feature was primarily maintained by the baroclinic production of eddy energy in conjunction with the nonzonal heating in the troposphere, and it sloped strongly westward with height throughout the model atmosphere. Thus it bears some resemblance to the Aleutian system in the N.H. winter. Associated with this feature were generally warmer temperatures in the polar night stratosphere and a weaker stratospheric jet, as found in the N.H.

The model atmosphere failed to produce quasistationary features in the N.H. troposphere and the progressive wave interacted periodically with the stationary forcing. In this way, large changes in tropospheric activity produced large changes in the forcing of the stratosphere through the vertical flux of energy, and events of a sudden warming nature were produced. Therefore changes in the intensity of a wave

(i.e. the transient component in time), were confirmed to be of major importance in producing a modification of the zonal flow.

The mechanism of the warming was found to be much the same as that outlined by Matsuno (1971), although different aspects were stressed here. In particular, the vertical propagation of transient wave energy and the stratospheric energetics as a whole were divided into two phases. The first phase takes place in a poleward temperature gradient and upward propagating energy stimulates baroclinic growth of the wave, thereby enhancing the upward flux. The associated northward heat flux warms the polar regions and induces a meridional circulation which modifies the zonal flow. The second phase begins when the temperature gradient has reversed as a result of the above process. The energy may still propagate, but some is absorbed and drives upgradient heat transports in the manner normally present in the lower stratosphere. This reverses the baroclinic energy cycle present in the first phase. If this process continues a critical layer may form, at which time the energy will no longer be able to propagate and will be absorbed. There is no change in the energetics with the critical layer formation, but this step is probably important in the atmosphere for localizing the warming and for the ensuing downward propagation.

With regard to the events in the troposphere which preceded the stratospheric warming, two likely mechanism emerged from the model as being responsible for the upward flux of transient wave energy in the atmosphere. Nonlinear interactions between the traveling wave with the

stationary component appear capable of producing periodic surges of energy into the stratosphere. These were very marked in the model owing to the primarily transient nature of the long wave interacting with the stationary forcing by nonzonal heating. These changes were identified with the atmospheric index cycle in the model N.H. The release of latent heat by small scale waves which are steered by the planetary scale waves may introduce a transient component of nonzonal heating that would produce a similar effect.

The most likely alternative stems from the increasing intensity of the tropospheric circulation as the winter season progresses. The existence of an index cycle in the very long waves, perhaps tied to the progress of the seasons, was found in the model and has also been found in the atmosphere.

Other effects were smaller, but the manner in which they reinforce the larger effects from year to year, may well be the source of the observed variability in sudden warming occurrence. Further experiments of the nature of that proposed in section 3.5, experiment (f), are desirable if the model can be sufficiently improved to produce a quasistationary wave. The importance of the relative phase of the heating and the orography may then be determined, particularly if it varies with the season.

A detailed knowledge of the kind of events in the troposphere which causes a large flux of energy to propagate into the stratosphere may enable some form of prediction scheme to be setup which will allow

large scale changes, and particularly sudden stratospheric warmings to be anticipated. This study indicates that we should look for increases in the intensity of very large scale systems such as the Aleutian low or Icelandic low.

We have also made a first attempt to evaluate the role of shorter scale waves, orography, the land-sea heating contrast, seasonal cycles and combinations of these in producing such changes. Other effects such as the vertical structure of the atmosphere and the upper boundary condition, particularly with regard to the location of a trapping layer at some high level perhaps changing because of extraterrestrial heating, may be very important in determining the exact location and degree of response. Only a knowledge of the importance of each factor will enable an explanation to be made of the variability in the sudden warmings from year to year. Such variability is perhaps a sign of sensitivity to certain factors in the atmospheric circulation, and thus perhaps the activity of man may eventually become a significant factor.

In establishing the characteristics of the model the deficiencies were analysed in detail and likely causes suggested. Some of these defects may be easily removed without major changes in the model. Other improvements may require an expanded model. However it is felt that the results given by this model should be of considerable value in designing further such models and in designing experiments for more sophisticated models. Indeed, this approach seems most useful in bridging the gap between linear theory and the extremely complex primitive equation models.

APPENDIX

The normalized surface spherical harmonics are defined as

$$Y_n^m = P_n^m(\mu)\, e^{im\lambda} \qquad\qquad \text{A-1}$$

where $\mu = \sin\phi$, and P_n^m is the normalized associated Legendre function of order m and degree n. The unnormalized function (also known as Ferrer's Associated Legendre Function) is given by

$$T_n^m = P_n^m\, N_n^m \qquad\qquad \text{A-2}$$

where

$$N_n^m = \left(\frac{1}{(2n+1)}\, \frac{(n+m)!}{(n-m)!} \right)^{1/2} \qquad\qquad \text{A-3}$$

and

$$T_n^m(\mu) = \frac{(1-\mu^2)^{m/2}}{2^n\, n!} \left(\frac{d}{d\mu}\right)^{m+n} (\mu^2-1)^n \qquad\qquad \text{A-4}$$

so that

$$\frac{1}{4\pi} \int_0^{2\pi} \int_{-1}^{+1} P_i^m(\mu)\, P_j^m(\mu)\, d\mu\, d\lambda = \delta_{ij} \qquad\qquad \text{A-5}$$

where δ is the kronecker delta; $\quad \delta_{ij} = 0 \;$ if $\; i \neq j$

$$= 1 \;\; \text{if} \;\; i = j \quad .$$

P_n^m for negative m is given by

$$P_n^{-m} = (-1)^m\, P_n^m \qquad\qquad \text{A-6}$$

and P_n^m vanishes unless $n \geqslant |m|$.

$Y_n^m(\mu, \lambda)$ satisfies the equation

$$\frac{d}{d\mu}\left((1-\mu^2)\frac{dF}{d\mu}\right) + \frac{1}{(1-\mu^2)}\frac{d^2F}{d\lambda^2} = -(n+1)nF$$

i.e. $\qquad\qquad a^2 \nabla^2 F \qquad\qquad = -(n+1)nF \qquad$ A-7

The following recurrence relations hold

$$(2n+1)\mu T_n^m = (n-m+1)T_{n+1}^m + (m+n)T_{n-1}^m \qquad\text{A-8}$$

$$(\mu^2-1)\frac{dT_n^m}{d\mu} = -(n+m)T_{n-1}^m + n\mu T_n^m \qquad\text{A-9}$$

We have made the following spectral representation

$$\nabla^2\psi(\lambda,\mu) = \sum_{n=|m|}^{\infty}\sum_{m=-\infty}^{\infty} \zeta_n^m Y_n^m \qquad\text{A-10}$$

$$\theta(\lambda,\mu) = \sum_{n=|m|}^{\infty}\sum_{m=-\infty}^{\infty} \theta_n^m Y_n^m \qquad\text{A-11}$$

$$\nabla^2 X(\lambda,\mu) = \sum_{n=|m|}^{\infty}\sum_{m=-\infty}^{\infty} \omega_n^m Y_n^m \qquad\text{A-12}$$

and we wish to find expressions for the following. We put

$$J(\psi,\nabla^2\psi) = \sum_{n=|m|}^{\infty}\sum_{m=-\infty}^{\infty} A_n^m Y_n^m \qquad\text{A-13}$$

$$J(\psi,\theta) = \sum_{n=|m|}^{\infty}\sum_{m=-\infty}^{\infty} B_n^m Y_n^m \qquad\text{A-14}$$

$$\nabla\cdot\mu\nabla\psi = \sum_{n=|m|}^{\infty}\sum_{m=-\infty}^{\infty} C_n^m Y_n^m \qquad\text{A-15}$$

$$\nabla\cdot\mu\nabla X = \sum_{n=|m|}^{\infty}\sum_{m=-\infty}^{\infty} D_n^m Y_n^m \qquad\text{A-16}$$

and find A_n^m, B_n^m, C_n^m and D_n^m in terms of ζ_n^m, θ_n^m and ω_n^m .

From A-7

$$\psi = -a^2 \sum_{n=|m|}^{\infty} \sum_{m=-\infty}^{\infty} \frac{\zeta_n^m}{n(n+1)} Y_n^m \qquad \text{A-17}$$

and similarly for X . The Jacobian is defined as

$$J(u,v) = \frac{1}{a^2} \left(\frac{\partial u}{\partial \lambda} \frac{\partial v}{\partial \mu} - \frac{\partial v}{\partial \lambda} \frac{\partial u}{\partial \mu} \right) \qquad \text{A-18}$$

From A-13, A-10 and A-17

$$\sum_{g=|h|}^{\infty} \sum_{h=-\infty}^{\infty} A_g^h P_g^h e^{ih\lambda} = i \sum_{\substack{\ell=|k| \\ s=|r|}}^{\infty} \sum_{\substack{k=-\infty \\ r=-\infty}}^{\infty} \frac{\zeta_\ell^k \zeta_s^r}{\ell(\ell+1)} e^{i(k+r)\lambda} \left[r P_s^r \frac{dP_\ell^k}{d\mu} - k P_\ell^k \frac{dP_s^r}{d\mu} \right]$$

Multiply both sides by $P_n^m e^{-im\lambda}$ and integrate over the whole sphere, then

$$A_n^m = i \sum_{\substack{\ell=|k| \\ s=|r|}}^{\infty} \sum_{\substack{k=-\infty \\ r=-\infty}}^{\infty} \frac{\zeta_\ell^k \zeta_s^r}{\ell(\ell+1)} L_n^{\bar{m}} {}_s^r {}_\ell^k \qquad \text{A-19}$$

where $k + r = m$,

$$L_{n_1}^{m_1} {}_{n_2}^{m_2} {}_{n_3}^{m_3} = \frac{1}{2} \int_{-1}^{+1} P_{n_1}^{m_1} \left(m_2 P_{n_2}^{m_2} \frac{dP_{n_3}^{m_3}}{d\mu} - m_3 P_{n_3}^{m_3} \frac{dP_{n_2}^{m_2}}{d\mu} \right) d\mu \qquad \text{A-20}$$

and use has been made of A5 and A6. Similarly, from A-14, A-11 and A-18, we find

$$B_n^m = i \sum_{\substack{\ell=|k| \\ s=|r|}}^{\infty} \sum_{\substack{k=-\infty \\ r=-\infty}}^{\infty} \frac{\zeta_\ell^k \theta_s^r}{\ell(\ell+1)} L_n^m {}_s^r {}_\ell^k \qquad \text{A-21}$$

where $k + r = m$.

Now consider

$$\nabla \cdot \mu \nabla \psi = \mu \nabla^2 \psi + \nabla \mu \cdot \nabla \psi$$

$$= \mu \nabla^2 \psi + \frac{1}{a^2} (1 - \mu^2) \frac{\partial \psi}{\partial \mu}$$

From A-15, A-10 and A.17

$$\sum_{g=|h|}^{\infty} \sum_{h=-\infty}^{\infty} C_g^h P_g^h e^{ih\lambda} = \sum_{d=|k|}^{\infty} \sum_{c=-\infty}^{\infty} \left(\mu P_d^c - \frac{(1-\mu^2)}{d(d+1)} \frac{dP_d^c}{d\mu} \right) \zeta_d^c e^{ic\lambda}$$

Multiply both sides by $P_n^{-m} e^{-im\lambda}$ and integrate over the entire sphere, then using A-5 and A-6

$$C_n^m = \frac{1}{2} \sum_{d=|m|}^{\infty} \zeta_d^m \int_{-1}^{+1} P_n^m \left(\mu P_d^m - \frac{(1-\mu^2)}{d(d+1)} \frac{dP_d^m}{d\mu} \right) d\mu$$

Now using A-2, A-3, A-8 and A-9

$$C_n^m = \frac{1}{2} \sum_{d=|m|}^{\infty} \zeta_d^m \left[\frac{(d-m+1)(d+2)}{(d+1)(2d+1)} \frac{N_{d+1}^m}{N_d^m} \int_{-1}^{+1} P_{d+1}^m P_n^m \, d\mu + \frac{(d+m)(d-1)}{d(2d+1)} \frac{N_{d-1}^m}{N_d^m} \int_{-1}^{+1} P_{d-1}^m P_n^m \, d\mu \right]$$

$$= \frac{n+1}{n} \left[\frac{(n+m)(n-m)}{(2n-1)(2n+1)} \right]^{\frac{1}{2}} \zeta_{n-1}^m \quad \frac{n}{n+1} \left[\frac{(n+m+1)(n-m+1)}{(2n+3)(2n+1)} \right]^{\frac{1}{2}} \zeta_{n+1}^m$$

$$= (n+1) a_n^m \zeta_{n-1}^m + n a_{n+1}^m \zeta_{n+1}^m \qquad \text{A-22}$$

where the a_n^m were defined in (4.37).

Similarly using A-16, A-12, A-2, A-3, A-7, A-8, A-9.

$$D_n^m = (n+1) a_n^m \omega_{n-1}^m + n a_{n+1}^m \omega_{n+1}^m \qquad \text{A-23}$$

The coefficients $L_{n_1 \ n_2 \ n_3}^{m_1 \ m_2 \ m_3}$, where $m_1 = m_2 + m_3$ are

variously known as the interaction coefficients or the coupling integrals,

since pairs of waves degree m_2 and m_3 are capable of interacting to modify wave degree m_1. The symmetry of A-20 gives rise to certain redundancies

$$L_{\substack{m_1 \ m_2 \ m_3 \\ n_1 \ n_2 \ n_3}} = -L_{\substack{-m_1 \ -m_2 \ -m_3 \\ n_1 \ n_2 \ n_3}} = -L_{\substack{m_1 \ m_3 \ m_2 \\ n_1 \ n_3 \ n_2}} \quad \text{and by}$$

integrating by parts it may be shown that

$$L_{\substack{m_1 \ m_2 \ m_3 \\ n_1 \ n_2 \ n_3}} = (-1)^{m_2} L_{\substack{m_3 \ -m_2 \ m_1 \\ n_3 \ n_2 \ n_1}} = (-1)^{m_3} L_{\substack{m_2 \ m_1 \ -m_3 \\ n_2 \ n_1 \ n_3}}$$

and thus without loss of generality, the expression need be evaluated only for non-negative m_1, m_2, m_3 . The method used is that given by Ellsaesser (1966).

Along with the above symmetries and antisymmetries, certain rules must be satisfied in order to select components capable of interacting. These rules may be derived from the mathematical properties of the integral and are summarized below.

$$m_1 = m_2 + m_3 \tag{A-24}$$

$$m_2^2 \neq m_3^2 \neq 0 \tag{A-25}$$

$$n_1 n_2 n_3 \neq 0 \tag{A-26}$$

$$(m_2, n_2) \neq (m_3, n_3) \tag{A-27}$$

$$(m_1, n_1) \neq (-m_2, n_2) \tag{A-28}$$

$$(m_1, n_1) \neq (-m_3, n_3) \tag{A-29}$$

$$(|m_2| - n_2)^2 + (|m_3| - n_3)^2 \neq 0 \tag{A-30}$$

$$|n_2 - n_3| < n_1 < n_2 + n_3 \tag{A-31}$$

$$n_1 + n_2 + n_3 = \text{odd integer} \tag{A-32}$$

Physical interpretation of the rules is as follows. Two components may interact provided neither is of zero degree (A-26), they are not both zonal (A-25) or sectional (A-30) and they are not identical (A-27). Through mutual interaction they may contribute to any component whose order is the sum or difference of their order (A-24), and whose degree is such as to form with their degrees a triangle of non-zero area (A-31) and odd perimeter (A-34), and may not contribute to either of their image components (A-28), (A-29). Thus a wave may contribute to itself, only by interacting with a zonal component of odd degree (A-24) and (A-32) and in so doing, change its phase speed but not its amplitude, Ellsaesser (1966).

The evaluated coefficients were hand checked using calculations described by Baer and Platzman (1961).

REFERENCES

Baer, F., and G.W. Platzman, 1961: A procedure for numerical integrations of the spectral vorticity equation. J. Meteor., 18, 393-401.

Barnett, J.J., R.S. Harwood, J.T. Houghton, C.G. Morgan, C.D. Rogers, E.J. Williamson, G. Peckham, S.D. Smith, 1971a: Stratospheric warming observed by Nimbus 4. Nature, 230, March 5, 1971, 47-48.

——————— , M.J. Cross, R.S. Harwood, J.T. Houghton, C.G. Morgan, G.E. Peckham, C.D. Rogers, S.D. Smith, E.J. Williamson, 1971b: The first year of the selective chopper radiometer on Nimbus 4. Nimbus Satellite Experiments, Ref.: 21/71. Clarendon Lab., University of Oxford.

Boville, B.W., 1960: The Aleutian stratospheric anticyclone. J. Meteor. 17, 329-336.

Bradley, J.H.S., and A. Wiin-Nielsen, 1968: On the transient part of the atmospheric planetary waves. Tellus, 20, 533-544.

Brown, J.A., 1969: Numerical investigation of hydrodynamic instability and energy conversions in the quasi-geostrophic atmosphere. Part I and Part II. J. Atmos. Sci., 26, 352-375.

Bryan, K., 1959: A numerical investigation of certain features of the general circulation. Tellus, 11, 163-174.

Burger, A., 1958: Scale considerations of planetary motions of the atmosphere. Tellus, 10, 195-205.

Byron-Scott, R., 1967: A stratospheric general circulation experiment incorporating diabatic heating and ozone chemistry. Pub. in Meteor. No. 87, Arctic Meteor. Res. Group, McGill University, 201 pp.

Charney, J.G., 1949: On the physical basis for numerical prediction of large-scale motions in the atmosphere. J. Meteor., 6, 371-385.

——————— , 1959: On the general circulation of the atmosphere. Rossby Memorial Volume. N.Y. Press. Rockefeller Inst., 178-193.

——————— , 1962: Integration of the primitive and balance equations. Proc. of the Inter. Symp. on N.W.P. in Tokyo. Pub. Met. Soc., Japan. 131-152.

Charney, J.G., and P.G. Drazin, 1961: Propagation of planetary-scale disturbances from the lower into the upper atmosphere. J. Geophys. Res., 66, 83-109.

——————— , and A. Eliassen, 1949: A numerical method for predicting the perturbations of the middle-latitude westerlies. Tellus, 1, 38-54.

——————— , and M. Stern, 1962: On the stability of internal baro-clinic jets in a rotating atmosphere. J. Atmos. Sci., 19, 159-172.

——————— , and J. Pedlosky, 1963: On the trapping of unstable planetary waves in the atmosphere. J. Geophys. Res., 68, 6441-6442.

Clapp, P.F., 1961: Normal heat sources and sinks in the lower troposphere in winter. Mon. Wea. Rev., 89, 147-162.

Clark, J.H., 1969: A spectral model of the winter stratosphere, Rep. No. 69-7, Dept. of Meteor., Florida State University, Tallahassee. 155 pp.

——————— , 1970: A quasigeostrophic model of the winter stratospheric circulation. Mon. Wea. Rev. 98, 443-461.

Deland, R.J., 1964: Travelling planetary waves. Tellus, 16, 271-273.

——————— , 1965: Some observations of the behaviour of spherical harmonic waves. Mon. Wea. Rev., 93, 307-312.

——————— , and K.W. Johnson, 1968: A statistical study of the vertical structure of travelling planetary-scale waves. Mon. Wea. Rev. 96, 12-22.

——————— , and Y-J. Lin, 1967: On the movement and prediction of travelling planetary-scale waves. Mon. Wea. Rev., 95, 21-31.

Derome, J. and A. Wiin-Nielsen, 1971: The response of a middle-latitude model atmosphere to forcing by topographical and stationary heat sources. Mon. Wea. Rev., 99, 564-576.

Dickinson, R.E., 1968a: On planetary Rossby waves propagating vertically through weak westerly wind wave guides. J. Atmos. Sci., 25, 984-1002.

Dickinson, R.E., 1968b: On the exact and approximate linear theory of vertically propagating planetary Rossby waves forced at a spherical lower boundary. Mon. Wea. Rev., 96, 405-415.

_____ 1968c: On the excitation and propagation of zonal winds in an atmosphere with Newtonian cooling. J. Atmos. Sci., 25, 269-279.

_____ , 1969a: Vertical propagation of planetary Rossby waves through an atmosphere with Newtonian cooling. J. Geophys. Res., 74, 929-938.

_____ , 1969b: Theory of planetary wave-zonal flow interaction. J. Atmos. Sci., 26, 73-81.

Dopplick,T.G., 1971: The energetics of the lower stratosphere including radiative effects. Quart. J. Royal Meteor. Soc., 97, 209-237.

Eady, E.T., 1949: Long waves and cyclone waves. Tellus, 1, 33-52.

Eliasen, E. and B. Machenhauer, 1965: A study of the fluctuations of the atmospheric planetary flow patterns represented by spherical harmonics. Tellus, 17, 220-238.

_____ 1969: On the observed large-scale atmospheric wave motions. Tellus, 21, 149-166.

Eliassen, A. and E. Palm, 1961: On the transfer of energy in stationary mountain waves. Geofys. Publikasjoner, Norske Videnskaps-Akad. Oslo, 22(3), 1-23.

Ellsaessar, H.W., 1966: Evaluation of spectral versus grid methods of hemispheric numerical weather prediction. J. App. Meteor., 5, 246-262.

Finger, F.G. and S. Teweles, 1964: The mid-winter 1963 stratospheric warming and circulation change. J. App. Met., 3, 1-15.

_____ , H.M. Woolf and C.E. Anderson, 1966: Synoptic analyses of the 5, 2 and 0.4 mb surfaces for the IQSY period. Mon. Wea. Rev., 94, 651-661.

Fleagle, R.G., 1957: On the dynamics of the general circulation. Quart. J. Royal Meteor. Soc., 83, 1-20.

_____ , 1958: Inferences concerning the dynamics of the mesosphere. J. Geophys. Res., 63, 137-145.

Green, J.S.A., 1960: A problem in baroclinic stability. Quart. J. Royal Meteor. Soc., 86, 237-251.

Hare, F.K., 1960: The disturbed circulation of the Arctic stratosphere. J. Meteor., 17, 36-51.

Hines, C.O., 1963: The upper atmosphere in motion. Quart. J. Royal Meteor. Soc., 89, 1-42.

Hirota, I., 1967a: The vertical structure of the stratospheric sudden warming. J. Meteor. Soc. Japan, 45, 422-435.

——————— , 1967b: Dynamic instability of the stratospheric polar vortex. J. Meteor. Soc. Japan, 45, 409-421.

——————— , 1968: Planetary waves in the upper stratosphere in early 1966. J. Meteor. Soc. Japan, 46, 418-430.

——————— , 1971: Excitation of planetary Rossby waves in the winter stratosphere by periodic forcing. N.C.A.R. Ms. No. 71-51.

——————— , and Y. Sato, 1969: Periodic variation of the winter stratospheric circulation and intermittent vertical propagation of planetary waves. J. Meteor. Japan, 47, 390-402.

Holloway, J.L. and S. Manabe, 1971: Simulation of climate by a global general circulation model. 1. Hydrologic cycle and heat balance. Mon. Wea. Rev., 99, 335-370.

Holopainen, E.O., 1970: An observational study of the energy balance of the stationary disturbances in the atmosphere. Quart. J. Royal Meteor. Soc., 96, 626-644.

Johnson, K.W., 1969: A preliminary study of the stratospheric warming of December 1967-January 1968. Mon Wea. Rev., 97, 553-564.

Julian, P.R., 1965: Some aspects of tropospheric circulation during mid-winter stratospheric warming events. J. Geophys. Res., 70, 757-767.

——————— , 1966: The index cycle: A cross-spectral analysis of zonal index data. Mon. Wea. Rev., 94, 283-293.

——————— , 1967: Mid-winter stratospheric warmings in the southern hemisphere: General remarks and a case study. J. App. Meteor., 6, 557-563.

Julian, P.R. and K.B. Labitzke, 1965: A study of atmospheric energetics during Jan. and Feb. 1963 stratospheric warming. J. Atmos. Sci., 22, 597-610.

Kasahara, A. and W.M. Washington, 1969: Thermal and dynamical effects of orography on the general circulation of the atmosphere. Proc. of the W.M.O/IUGG Symp. on N.W.P., Tokyo, Japan, Nov. 26-Dec. 4., 1968. Japan Meteor. Agency, Tokyo, March 1969. pp IV, 47-56.

———————————————————, 1971: General circulation experiments with a six-layer NCAR model, including orography, cloudiness and surface temperature calculations. J. Atmos. Sci., 28, 657-701.

Katayama, A., 1964: On the heat budget of the troposphere over the northern hemisphere. Doctoral Dissertation, Tohoku University.

Kidson, J.W. and R.E. Newell, 1969: Exchange of atmospheric angular momentum between the hemispheres. Nature, 221, 352-353.

Kikuchi, Y., 1969: Numerical simulation of the blocking process. J. Meteor. Soc. Japan, 67, 29-53.

Krueger, A.F., J.S. Winston and D.A. Haines, 1965: Computation of atmospheric energy and its transformation for the northern hemisphere for a recent five-year period. Mon. Wea. Rev., 93, 227-238.

Kuhn, W.R. and J. London, 1969: Infrared radiative cooling in the middle atmosphere (30-110 km). J. Atmos. Sci., 26, 189-204; and corrigenda, 26, p 620.

Labitzke, K., 1965: On the mutual relation between stratosphere and troposphere during periods of stratospheric warmings in winter. J. App. Meteor., 4, 91-99.

Leovy, C., 1964: Simple models of thermally driven mesospheric circulation. J. Atmos. Sci., 21, 327-341.

Lindzen, R.S., 1966: Radiative and photochemical processes in mesosphere dynamics: Part IV, Stability of a zonal vortex at mid-latitudes to baroclinic waves. J. Atmos. Sci., 23, 350-359.

———————————, 1967: Planetary waves on beta-planes. Mon. Wea. Rev., 95, 441-451.

———————————, E.S. Batten and J.W. Kim, 1968: Oscillations in atmospheres with tops. Mon. Wea. Rev., 96, 133-140.

Lorenz, E.N., 1955: Available potential energy and the maintainence of the general circulation. Tellus, 7, 157-167.

Lorenz, E.N., 1960a: Maximum simplification of the dynamic equations.
   Tellus, 12, 243-254.

———————— , 1960b: Energy and numerical weather prediction. Tellus,
   12, 364-373.

———————— , 1962: Simplified dynamic equations applied to rotating-
   basin experiments. J. Atmos. Sci., 19, 39-51.

———————— , 1963: The mechanics of vacillation. J. Atmos. Sci., 20,
   448-464.

———————— , 1971: An N-cycle time-differencing scheme for stepwise
   numerical integration. Mon. Wea. Rev., 99, 644-648.

Mahlman, J.D., 1969: Heat balance and mean meridional circulations in
   the polar stratosphere during the sudden warming of January 1958.
   Mon. Wea. Rev., 97, 534-540.

Manabe, S. and B.G. Hunt, 1968: Experiments with a stratospheric general
   circulation model Part I. Mon. Wea. Rev., 96, 477-502.

———————— , and F. Moller, 1961: On the radiative equilibrium and heat
   balance of the atmosphere. Mon. Wea. Rev., 89, 503-532.

———————— , J. Smagorinsky and R.F. Strickler, 1970: Simulated climato-
   logy of a general circulation model with a hydrologic cycle, III.
   Effects of increased horizontal computational resolution. Mon. Wea.
   Rev., 98, 175-212.

———————— , and R.F. Strickler, 1964: Thermal equilibrium of the atmos-
   sphere with a convective adjustment. J. Atmos. Sci., 21, 361-385.

Matsuno, T., 1970: Vertical propagation of stationary planetary waves
   in the winter northern hemisphere. J. Atmos. Sci., 27, 871-883.

———————— , 1971: A dynamic model of the stratospheric sudden warming,
   J. Atmos. Sci., 28, 1479-1494.

———————— , and I. Hirota, 1966: On the dynamic stability of polar vor-
   tex in wintertime. J. Meteor. Soc. Japan, 44, 122-128..

McIntyre, M.E., 1970: Baroclinic instability of Murray's continuous
   model of the polar night jet. Unpublished manuscript.

Miller, A.J., 1966: Vertical motion atlas for the lower stratosphere during 1958(IGY). Rep. No. 16, Plan. Circ. Proj., M.I.T., 35 pp.

Mintz, Y., 1968: Very long-term global integration of the primitive equations of atmospheric motion: An experiment in climate simulation. Meteor. Monographs, 8, 30, 20-36.

Miyakoda, K., 1963: Some characteristic features of winter circulations in the troposphere and lower stratosphere. Tech. Rep. No. 14, NSF (GP471) Dept. of Geophys. Sci., University of Chicago, 93 pp.

——————————, R.F. Strickler and G.D. Hembree, 1970: Numerical simulation of the breakdown of a polar-night vortex in the stratosphere. J. Atmos. Sci., 27, 139-154.

—————————— , R.F. Strickler, C.J. Nappo, P.L. Baker and G.D. Hembree, 1971: The effect of horizontal grid resolution in an atmospheric circulation model. J. Atmos. Sci., 28, 481-499.

Muench, H.S., 1965: On the dynamics of the wintertime stratospheric circulation. J. Atmos. Sci., 22, 349-360.

Murakami, T., 1965: Energy cycle of the stratospheric warming in early 1958. J. Meteor. Soc. Japan, 43, 262-283.

——————————, 1967: Vertical transfer of energy due to stationary disturbances induced by topography and diabatic heat sources and sinks. J. Meteor. Soc. Japan, 45, 205-230.

Murgatroyd, R.J., 1970: The structure and dynamics of the stratosphere. The global circulation of the atmosphere, pp. 159-195. Royal Meteor. Soc. London, 257 pp. The Salisbury Press.

—————————— , and R.M. Goody, 1958: Sources and sinks of energy from 30 to 90 km. Quart. J. Royal Meteor. Soc., 84, 225-234.

—————————— , F.K. Hare, B.W. Boville, S. Teweles and A. Kochanski, 1965: The circulation in the stratosphere, mesosphere and lower thermosphere. W.M.O. Tech. Note No. 70, Geneva, 206 pp.

Murray, F.W., 1960: Dynamic stability in the stratosphere. J. Geophys. Res., 65, 3273-3305.

Newell, R.E., 1961: The transport of trace substances in the atmosphere and their implications for the general circulation of the stratosphere. Geof. Pura e Appl., 49, 137-158.

Newell, R.E., 1965: The energy and momentum budget of the atmosphere above the tropopause. Proc. of the Sixth Int. Space Sci. Symp., Argentina. R.V. Garcia and T.F. Malone, Spartan Books, Washington, D.C. 106-126.

—————— , 1968: The general circulation of the atmosphere above 60 km. Meteor. Monographs, 9, 31, 98-113. Amer. Meteor. Soc., Boston, Mass.

—————— , D.G. Vincent, T.G. Dopplick, D. Ferruza, J.W. Kidson, 1970: The energy balance of the global atmosphere. The global circulation of the atmosphere, pp 42-90, Royal Meteor. Soc. London, 257 pp. The Salisbury Press.

Newton, C.W., 1971: Mountain torques in the global angular momentum balance. J. Atmos. Sci., 28, 623-628.

Obasi, G.O.P., 1963: Atmospheric momentum and energy calculations for the southern hemisphere during the I.G.Y. Sci. Rep. No. 6. Plan. Circ. Proj. M.I.T., 354 pp.

Oort, A.H., 1964a: On the energetics of the mean and eddy circulation in the lower stratosphere. Tellus, 16, 309-327.

—————— , 1964b: On estimates of the atmospheric energy cycle. Mon. Wea. Rev., 92, 483-493.

Palmer, C.E., 1959: The stratospheric polar vortex on winter. J. Geophys. Res., 64, 749-764.

—————— , and R.C. Taylor, 1960: The vernal breakdown of the stratospheric cyclone over the South Pole. J. Geophys. Res., 65, 3319-3329.

Peng, L., 1965: A simple numerical experiment concerning the general circulation in the lower stratosphere. Pageoph., 61, 191-218.

Perry, J.S., 1967: Long wave energy processes in the 1963 sudden stratospheric warming. J. Atmos. Sci., 24, 539-550.

Phillips, N.A., 1956: The general circulation of the atmosphere: A numerical experiment. Quart. J. Royal Meteor. Soc., 82, 123-164.

—————— , 1963: Geostrophic Motion. Rev. of Geophys., 1, 123-176.

Phillpot, H.R., 1969: Antarctic stratospheric warming reviewed in the light of 1967 observations. Quart. J. Royal Meteor. Soc., 95, 329-348.

Quiroz, R.S., 1969: The warming of the upper stratosphere in February 1966 and the associated structure of the mesosphere. Mon.Wea. Rev., 97, 541-552.

Reed, R.J., J.L. Wolfe and H. Nishimoto, 1963: A spectral analysis of the energetics of the stratospheric sudden warming of early 1957. J. Atmos. Sci., 20, 256-275.

Richards, M.E., 1967: The energy budget of the stratosphere during 1965. Rep. No. 21, Plan. Circ. Proj., M.I.T., 170 pp.

Saltzman, B., 1965: On the theory of the winter average perturbations in the troposphere and stratosphere. Mon. Wea. Rev., 93, 195-211.

—————— , 1968: Surface boundary effects on the general circulation and macroclimate: A review of the theory of the quasi-stationary perturbations in the atmosphere. Meteor. Monograph No. 30. Amer. Meteor. Soc., 4-19.

—————— , and A. Fleischer, 1960: The exchange of kinetic energy between larger scales of atmospheric motion. Tellus, 12, 372-377.

—————— , and S. Teweles, 1964: Further statistics on the exchange of kinetic energy between harmonic components of the atmospheric flow. Tellus, 16, 432-435.

Sanders, F., 1971: Analytic solutions of the non-linear omega and vorticity equations for a structurally simple model of disturbances in the baroclinic westerlies. Mon. Wea. Rev., 99, 393-409.

Sankar-Rao, M., 1965: Continental elevation influence on the stationary harmonics of the atmospheric motion. Pure and App. Geophys., 60, 141-159.

—————— , and B. Saltzman, 1969: On the steady state theory of global monsoons. Tellus, 21, 308-330.

Scherhag, R., 1952: Die explosionsertigen stratosplarenerwarmungen des spatwinters 1951-52. Ber. Deut. Wetterd. U.S. Zone, 6, 51-63.

Schniff, H.I., 1969: Neutral reactions involving oxygen and nitrogen. Canadian J. of Chem., 47, 1903-1916.

Shen, W.C., G.W. Nicholas and A.D. Belmont, 1968a: Comparison of 15 Tiros VII data with radiosonde temperatures. J. App. Meteor., 7, 284-289.

Shen, W.C., G.W. Nicholas and A.D. Belmont, 1968b: Comments on Julian (1967). J. App. Meteor., 7, 300-302.

Smagorinsky, J., 1953: The dynamic influence of large scale heat sources and sinks on the quasi-stationary mean motions of the atmosphere. Quart. J. Royal Meteor. Soc., 79, 342-366.

Starr, V.P. and R.M. White, 1954: Balance requirements of the general circulation. Final Rep. Part I. Contract No. AF 19-122-153. Gen. Circ. Proj. M.I.T., 186-242.

Teweles, S., 1958: Anomalous warming of the stratosphere over North America in early 1957. Mon. Wea. Rev., 86, 377-396.

_____ , 1963: Spectral aspects of the stratospheric circulation during the IGY. Rep. No. 8. Plan. Gen. Circ. Proj., M.I.T., 191 pp.

_____ , and F. Finger, 1958: An abrupt change in stratospheric circulation beginning in mid-January 1958. Mon. Wea. Rev., 86, 23-28.

U.S. Standard Atmosphere Supplements, 1966: U.S. committee on extension to the standard atmosphere. U.S. Govt. Printing Office, Washington, D.C., 289 pp.

Wexler, H., 1959: Seasonal and other temperature changes in the antarctic atmosphere. Quart. J. Royal Meteor. Soc., 85, 196-208.

Wiin-Nielsen, A., 1971a: On the motion of various vertical modes of transient, very long waves. Part I. Beta-plane approximation. Tellus, 23, 87-98.

_____ , 1971b: _____ . Part II. The spherical case. Tellus, 23, 207-217.

Willett, H.C. and F. Sanders, 1959: Descriptive Meteorology. Academic Press, New York. 355 pp.

BIOGRAPHICAL SKETCH

Kevin Edward Trenberth was born in Christchurch, New Zealand, in November, 1944. His early years were spent in Christchurch, and he attended Linwood High School from 1958 to 1962. The following three years he studied at the University of Canterbury, in Christchurch, and he graduated in 1966 with a B.Sc degree with first class honours in Applied Mathematics.

After graduation he joined the staff of the New Zealand Meteorological Service, in Wellington, where he worked for brief periods in the fields of air pollution, forecasting and instrumentation. In 1968 he was awarded a New Zealand Research fellowship and was accepted for graduate study at Massachusetts Institute of Technology, beginning in September 1968.

Shortly thereafter he met and on March 21, 1970, he married Gail N. Thompson.